

**A STUDY ON HYDROXYAPATITE CONCENTRATION
IN FIBROUS SCAFFOLDS AND ITS EFFECT ON RAT
BONE MARROW STEM CELL PROLIFERATION**

HARIS BIN AKRAM

**FACULTY OF ENGINEERING
UNIVERSITY OF MALAYA
KUALA LUMPUR**

2014

**A STUDY ON HYDROXYAPATITE CONCENTRATION
IN FIBROUS SCAFFOLDS AND ITS EFFECT ON RAT
BONE MARROW STEM CELL PROLIFERATION**

HARIS BIN AKRAM

**THESIS SUBMITTED IN PARTIAL FULFILMENT OF
THE REQUIREMENT FOR DEGREE OF MASTER OF
ENGINEERING SCIENCE**

**FACULTY OF ENGINEERING
UNIVERSITY OF MALAYA
KUALA LUMPUR**

2014

UNIVERSITI MALAYA

ORIGINAL LITERARY WORK DECLARATION

Name of Candidate: *Haris Bin Akram* (I.C/Passport No: *F4219653*)

Registration/Matric No: *KGA 100011*

Name of Degree: *Master of Engineering Science*

Title of Project Paper/Research Report/Dissertation/Thesis (“this Work”):

A STUDY ON HYDROXYAPATITE CONCENTRATION IN FIBROUS SCAFFOLDS AND ITS EFFECT ON RAT BONE MARROW STEM CELL PROLIFERATION

Field of Study: Tissue Engineering

I do solemnly and sincerely declare that:

- (1) I am the sole author/writer of this Work;
- (2) This Work is original;
- (3) Any use of any work in which copyright exists was done by way of fair dealing and for permitted purposes and any excerpt or extract from, or reference to or reproduction of any copyright work has been disclosed expressly and sufficiently and the title of the Work and its authorship have been acknowledged in this Work;
- (4) I do not have any actual knowledge nor do I ought reasonably to know that the making of this work constitutes an infringement of any copyright work;
- (5) I hereby assign all and every rights in the copyright to this Work to the University of Malaya (“UM”), who henceforth shall be owner of the copyright in this Work and that any reproduction or use in any form or by any means whatsoever is prohibited without the written consent of UM having been first had and obtained;
- (6) I am fully aware that if in the course of making this Work I have infringed any copyright whether intentionally or otherwise, I may be subject to legal action or any other action as may be determined by UM.

Candidate’s Signature

Date

Subscribed and solemnly declared before,

Witness’s Signature

Date

Name:

Designation:

ABSTRACT

Composite scaffolds of polycaprolactone (PCL) and bovine derived hydroxyapatite (HA) were produced by blending HA into PCL solution followed by electrospinning. This study mainly focused on studying the materials morphology, characteristics and interactions between the materials and cells. Six groups of scaffolds based on the weight ratio of HA in proportion to PCL were prepared (0%, 10%, 20%, 30%, 40% and 50%). The scaffolds were studied by infra-red spectroscopy (FTIR), 3D confocal laser microscopy and field emission scanning electron microscopy (FESEM) in order to determine the chemical and thermal properties as well as imaging the scaffold to cell interactions. Bone Marrow Stem Cell (BMSC) proliferation assays were carried out on Days 1, 7 and 14 using Resazurin, Deoxyribonucleic Acid (DNA) and Alkaline Phosphatase (ALP) measurements. DNA levels were used to identify cell presence and possible proliferation. ALP levels were used to indicate possible stem cell differentiation to osteoblasts. It was observed that with increasing amounts of HA in the PCL scaffold, the quantity and quality of cell attachment increased. Our study shows that the electrospun nanofibres of PCL incorporated with micro particles of HA could provide a scaffold that could be applied successfully in bone tissue engineering.

ABSTRAK

Perencah komposit polycaprolactone (PCL) dan bovine hydroxyapatite (HA) telah dihasilkan dengan menggabungkan HA ke dalam larutan PCL diikuti dengan elektroputaran. Enam kumpulan perencah berdasarkan nisbah berat HA berkadar dengan PCL telah disediakan (0%, 10%, 20%, 30%, 40% dan 50%). Perencah telah dikaji dengan spektroskopi inframerah (FTIR) , mikroskopi sefokus laser 3D dan pelepasan bidang elektron imbasan mikroskopi (FESEM) untuk menentukan sifat kimia, sifat haba dan juga pengimejan perencah interaksi sel. Ujian percambahan sel-sel stem sum-sum tulang (BMSC) telah dijalankan pada Hari 1, 7 dan 14 menggunakan Resazurin, Asid Deoksiribonuklik (DNA) dan Alkali Phosphatase (ALP) sebagai ukuran. Kehadiran DNA telah digunakan untuk mengenal pasti adanya sel dan perkembangannya. Tahap ALP telah digunakan untuk menunjukkan kemungkinan pembezaan sel-sel stem kepada osteoblas. Diperhatikan bahawa dengan peningkatan jumlah HA dalam perencah PCL, kuantiti dan kualiti lampiran sel meningkat. Kajian kami menunjukkan bahawa nanofiber PCL elektroputar digabungkan dengan partikel mikro HA, boleh menyediakan satu perencah yang boleh digunakan dengan jayanya dalam kejuruteraan tisu tulang.

ACKNOWLEDGEMENTS

All praise is due to Allah, the Almighty, the All-Wise, the All Knowing, the Most Just. Without His help I wouldn't have been able to start let alone finish this work. Then I would like to thank my supervisors, Dr Belinda Murphy and Puan Norita Mohd Zain, their patience, constant advice and guidance and encouragement, especially when it came to cell infections was instrumental in finishing this thesis. My family, for having to endure, countless hours of me complaining of my lab work and cells. Thank you Mummy, Baji, Asma and Yasir. My family in the lab, Kama, Chee Tat, Eng Kuan, Wee Hong, Illida, Iklil, Adli and especially Ali and Yasir, who helped me in my lab work and who also reminded me of the finish line, which at times seemed very far away. A supervisor who provided me with the funding necessary for this work and my Masters, Prof Wan Abu Bakar Wan Abas, without his patience and funds, this work would never have been finished.

TABLE OF CONTENTS

| | |
|--|------|
| ORIGINAL LITERARY WORK DECLARATION | ii |
| ABSTRACT | iii |
| ABSTRAK | iv |
| ACKNOWLEDGEMENTS | v |
| TABLE OF CONTENTS | vi |
| LIST OF FIGURES | xi |
| LIST OF TABLES | xiii |
| LIST OF ABBREVIATIONS | xiv |
| | |
| CHAPTER 1: INTRODUCTION | 2 |
| 1.1 A Brief Overview of Tissue Engineering: History and Definition | 2 |
| 1.1.1 Bone tissue engineering | 4 |
| 1.1.1.1 Anatomy and physiology of bone | 4 |
| 1.1.1.2 Bone fracture and repair | 6 |
| 1.2 Electrospinning | 7 |
| 1.3 Bone Marrow Stem Cells | 8 |
| 1.4 Cell Studies and Existing Electrospun Scaffolds | 9 |
| 1.5 Objectives | 11 |
| | |
| CHAPTER 2: LITERATURE REVIEW | 13 |
| 2.1 Introduction | 13 |
| 2.2 Hydroxyapatite (HA) | 13 |
| 2.2.1 Hydroxyapatite preparation | 13 |
| 2.2.2 Hydroxyapatite sources | 15 |

| | | |
|-------|---|-----------|
| 2.2.3 | Hydroxyapatite in Tissue Engineering | 16 |
| 2.3 | Polycaprolactone (PCL) | 17 |
| 2.3.1 | Properties and characteristics of Polycaprolactone | 17 |
| 2.3.2 | Polycaprolactone in Tissue Engineering | 18 |
| 2.4 | PCL and HA Blends Used in Bone Tissue Engineering | 20 |
| 2.5 | Electrospinning and Its Applications in Tissue Engineering | 21 |
| 2.6 | Stem Cells | 23 |
| 2.6.1 | Isolation and applications of stem cells | 23 |
| 2.6.2 | Characterisation of stem cells | 24 |
| 2.7 | The Effect of Scaffold Material on Stem Cell Differentiation | 25 |
| 2.8 | Cellular Assay Measurements and Protocols | 25 |
| 2.8.1 | Alamar Blue Assay | 26 |
| 2.8.2 | Deoxyribonucleic Acid (DNA) Assay | 26 |
| 2.8.3 | Alkaline Phosphatase (ALP) Activity | 26 |
| | CHAPTER 3: MATERIALS AND METHODS | 28 |
| 3.1 | Introduction | 28 |
| 3.2 | Preparation of Primary Culture Medium | 29 |
| 3.2.1 | Isolation and culture of Rat Derived Bone Marrow Stem Cells (BMSC) | 30 |
| 3.2.2 | Cell seeding and incubation period | 32 |
| 3.3 | Bovine Hydroxyapatite (BHA) Production | 34 |
| 3.4 | Polycaprolactone (PCL) and Bovine Hydroxyapatite (BHA) Scaffold Production | 35 |
| 3.4.1 | Solution preparation | 35 |
| 3.4.2 | Electrospinning | 35 |

| | | |
|---------|--|-----------|
| 3.5 | Bovine Powder Characterisation | 38 |
| 3.6 | Composite Scaffold Characterisation | 41 |
| 3.6.1 | Chemical characterisation | 41 |
| 3.6.2 | Physical characterisation | 41 |
| 3.6.2.1 | Scaffold roughness and thickness | 41 |
| 3.6.2.2 | Surface hydrophilicity | 42 |
| 3.6.2.3 | Fibre diameter | 42 |
| 3.7 | Stem Cells Characterisation | 43 |
| 3.7.1 | Bone Marrow Stem Cell characterisation | 43 |
| 3.7.1.1 | Adherence to plastic with fibroblastic features | 43 |
| 3.7.1.2 | Multilineage differentiation potential | 43 |
| 3.8 | Cell and Scaffold Interactions | 52 |
| 3.9 | Biochemical Assays | 52 |
| 3.10 | Cell Proliferation Assay | 53 |
| 3.11 | Protein and DNA Extraction | 53 |
| 3.12 | Alkaline Phosphatase (ALP) Assay Measurement | 54 |
| 3.13 | Deoxyribonucleic Acid (DNA) Assay Measurement | 55 |
| 3.14 | Statistical Analysis | 56 |
| | CHAPTER 4: RESULTS | 58 |
| 4.1 | Introduction | 58 |
| 4.2 | Bovine Hydroxyapatite (BHA) Characterisation | 58 |
| 4.2.1 | X-Ray Diffraction (XRD) of BHA | 58 |
| 4.2.2 | Fourier-Transform Infra Red Spectroscopy (FTIR) of BHA | 59 |
| 4.3 | Composite Scaffold Characterisation | 60 |
| 4.3.1 | Fourier-Transform Infra Red Spectroscopy (FTIR) of composite | |

| | |
|---|-----------|
| scaffolds | 60 |
| 4.3.2 Electrospun scaffold profile | 61 |
| 4.3.2.1 3-D Confocal roughness profile of electrospun scaffolds | 61 |
| 4.3.2.2 Roughness profile of scaffolds | 62 |
| 4.3.2.3 Surface hydrophilicity | 63 |
| 4.3.2.4 Fibre diameter | 64 |
| 4.4 Stem Cells Characterisation | 67 |
| 4.4.1 Adherence to plastic with fibroblastic features | 67 |
| 4.4.2 Multilineage differentiation of potential | 67 |
| 4.4.2.1 Chondrogenic differentiation | 67 |
| 4.4.2.2 Osteogenic differentiation | 68 |
| 4.4.2.3 Immunofluorescence staining of mesenchymal markers | 69 |
| 4.4.3 Cluster differentiation (CD) markers | 69 |
| 4.5 Cell and Scaffold Interactions | 71 |
| 4.6 Biochemical Assays | 73 |
| 4.6.1 Cell Proliferation Assay | 73 |
| 4.6.2 Alkaline Phosphatase (ALP) Assay | 75 |
| 4.6.3 Deoxyribonucleic (DNA) Assay | 76 |
| CHAPTER 5: DISCUSSION AND CONCLUSION | 79 |
| 5.1 Introduction | 79 |
| 5.2 Bovine Hydroxyapatite Characterisation | 79 |
| 5.3 Scaffold Characterisation | 80 |
| 5.4 Effect of Increasing Hydroxyapatite Concentration on the Scaffold Material | 80 |

| | | |
|-------|---|-----------|
| 5.4.1 | 3D Roughness profile of scaffold | 80 |
| 5.4.2 | Hydrophilicity properties | 81 |
| 5.5 | Stem Cells Characterisation | 82 |
| 5.6 | Field Emission Scanning Electron Microscopy (FESEM) Images | 82 |
| 5.7 | Biochemical Assays | 83 |
| 5.7.1 | Cell Proliferation Assay | 83 |
| 5.7.2 | Alkaline Phosphatase (ALP) Assay | 83 |
| 5.7.3 | Deoxyribonucleic Acid (DNA) Assay | 84 |
| 5.8 | Conclusion and Future Work | 85 |
| | REFERENCES | 86 |

LIST OF FIGURES

| | | |
|----------------|--|----|
| Figure 1.1 | Principles of tissue engineering | 4 |
| Figure 1.2 | Compact and Spongy Bone | 5 |
| Figure 1.3 | Repair of bone | 6 |
| Figure 1.4 | An electrospinning experimental layout | 7 |
| Figure 3.1 | Flow chart of methodology involved in the study | 29 |
| Figure 3.2 | Isolation and culture of Bone Marrow Derived Stem Cells | 31 |
| Figure 3.3 | Counting live and dead cells in a haemocytometer | 33 |
| Figure 3.4 | Bovine Hydroxyapatite production | 34 |
| Figure 3.5(i) | Electrospinning machine setup | 36 |
| Figure 3.5(ii) | Schematic diagram of electrospinning set-up | 36 |
| Figure 3.6 | (A) Glass cover slips stuck on the aluminium sheet to prevent sticking of the electrospun sheet on the aluminium sheet; (B) Schematic representation of cover slips on aluminium sheet | 37 |
| Figure 3.7 | Electrospun sheet is cut into 1 cm by 1 cm squares and placed in a 24 well plate for sterilization by alcohol and then UV radiation | 37 |
| Figure 3.8 | Flowchart depicting a 3-colour combo sample preparation | 49 |
| Figure 3.9 | Expected result of the 3-colour based experiment of BMSC | 51 |
| Figure 4.1 | XRD profile of BHA (pre and post sintering) | 58 |
| Figure 4.2 | FTIR spectra for BHA. The figure shows the pre-sintered and post-sintered peaks of bone powder and BHA isolated from femur, tibia and metatarsus. | 59 |
| Figure 4.3 | FTIR spectra of PCLHA composite scaffolds | 60 |
| Figure 4.4 | 3-D Confocal images of scaffolds | 61 |
| Figure 4.5 | Roughness profile of scaffolds | 62 |

| | | |
|-------------|---|----|
| Figure 4.6 | Contact angle measurements of scaffolds with different BHA concentrations | 63 |
| Figure 4.7 | Cells attached on plastic (T-75 flask) – scale bar 200 μm | 67 |
| Figure 4.8 | Chondrogenic staining – scale bar 200 μm | 68 |
| Figure 4.9 | Alizarin staining. 1000x magnification | 68 |
| Figure 4.10 | Immunofluorescence staining for α -SMA and vimentin | 69 |
| Figure 4.11 | This shows the total distribution of the cells. As can be seen, gates are formed in order to confine the marker testing to a certain area | 70 |
| Figure 4.12 | In the above image, two distinct populations can be observed. These populations exhibit CD90-, CD31- and CD45+ markers | 70 |
| Figure 4.13 | As shown above it can be observed that the BMSCs exhibit positivity and negativity for CD90+, CD31- and CD45- markers | 71 |
| Figure 4.14 | Cell metabolic activity over 2 weeks of cells seeded on all scaffolds | 74 |
| Figure 4.15 | Alkaline Phosphatase measurement over 2 weeks | 75 |
| Figure 4.16 | DNA Assay of seeded scaffolds over 2 weeks [n=16]. (All error bars shown are Standard Error of Mean) | 76 |

LIST OF TABLES

| | | |
|-----------|---|----|
| Table 2.1 | Properties of PCL | 18 |
| Table 3.1 | Sample distribution for Flow Cytometry | 50 |
| Table 4.1 | Contact angle and surface roughness measurements of scaffolds | 64 |
| Table 4.2 | Fibre thickness graph. All FESEM images were taken at 1000x magnification. The average diameter distribution is shown on the right of the individual image. | 65 |
| Table 4.3 | FESEM images over days 1, 7 and 14. All FESEM images were taken at 2000x magnification and scale bar 50 μm . | 72 |

LIST OF ABBREVIATIONS

| | |
|-------|--|
| PCL | Polycaprolactone |
| HA | Hydroxyapatite |
| BHA | Bovine Hydroxyapatite |
| ECM | Extracellular Matrix |
| BMSC | Bone Marrow Stem Cells |
| CD | Cluster Differentiation |
| ALP | Alkaline Phosphatase |
| FESEM | Field Emission Scanning Electron Microscope |
| SEM | Scanning Electron Microscope |
| HSC | Hematopoietic Stem Cells |
| PCLHA | Polycaprolactone Hydroxyapatite Electrospun Polymer Scaffold |
| Tris | tris(hydroxymethyl)aminomethane) |
| PBS | Phosphate Buffer Saline solution |
| PLGA | poly(lactic- <i>co</i> -glycolic) acid |
| IgG | Immunoglobulin G |
| FITC | Fluorescein isothiocyanate |
| PE | R-Phycoerythrin |
| PerCP | Peridinin |
| RPM | Revolutions per minute |
| OD | Optical Difference |
| FACS | Fluorescence-activated cell sorting |
| XRD | X-Ray Diffraction |
| FTIR | Fourier Transform Infrared Spectroscopy |
| TEM | Transmission Electron Microscopy |

CHAPTER 1: INTRODUCTION

CHAPTER 1: INTRODUCTION

1.1 A Brief Overview of Tissue Engineering: History and Definition

Tissue engineering is a relatively new field, first comprehensively defined by Robert Langer from the Massachusetts Institute of Technology in 1988. The most cited publication in the history of tissue engineering regards the birth of this field, and was published by Langer and Vancini (1993) in *Science*. In it they described their definition of tissue engineering, which has come to be regarded as a more-or-less universal definition. They define tissue engineering as “an interdisciplinary field that applies the principles of engineering and life sciences toward the development of biological substitutes that restore, maintain, or improve tissue function or a whole organ”. It’s definition continues to morph from the original form, and the most current definition is the use of a combination of cells, engineering and materials, methods, and suitable biochemical and physio-chemical factors to improve or replace biological functions (Barnes and Harris, 2008). The terms “regenerative medicine” and “tissue engineering” are very closely linked, however they differ in that regenerative medicine generally involves the use of stem cells and tissue engineering may or may not involve the use of cells (Riazi *et al.*, 2009).

Tissue engineering mostly deals with resolving health-related issues that affect organs and their tissues. These include, but are not limited to, diseases of the bone, cartilage, blood vessels, bladder, skin and muscles. The use of biomaterials in trying to solve tissue engineering related issues are growing and has been well documented in many journals, with one journal (*Biomaterials*) being exclusively dedicated to advances and innovation in the use of biomaterials.

A lot of hope rests on tissue engineering, particularly for its potential in combating problems related to organ damage, replacement, and return of functionality. Chaignaud *et al.* (1997), defined tissue-engineering technology as that which combines the study of engineering, cell and molecular biology, materials science, and surgery, toward the development of biological substitutes that restore, maintain, and improve the function of damaged tissues and organs.

According to a definition provided by the National Institute of Health (USA), the pillars of tissue engineering are found in its therapeutic and diagnostic applications. These applications try to maximize the use of both cells and materials. In diagnostic applications of tissue engineering, in-vitro cultured tissues, cells or both are used for assessing drug toxicity, pathogenicity and effectiveness. As far as therapeutic applications are concerned, tissue engineering deals with the use of:

- 1) **Biomaterials:** including novel biomaterials that are designed to direct the organization, growth, and differentiation of cells in the process of forming functional tissues by providing both physical and chemical cues.
- 2) **Cells:** including enabling methodologies for the proliferation and differentiation of cells, acquiring the appropriate source of cells such as autologous cells, allogeneic cells, xenogeneic cells, stem cells, or genetically engineered cells, and the use of immunological-manipulation.
- 3) **Biomolecules:** including angiogenic factors, growth factors, differentiation factors and bone morphogenic proteins.
- 4) **Engineering Design Aspects:** including 2-d cell expansion, 3-d tissue growth, bioreactors, vascularization, cell and tissue storage, and shipping (biological packaging).
- 5) **Biomechanical Aspects of Design:** including properties of native tissues, identification of minimum properties required of engineered tissues, mechanical signals regulating engineered tissues, and the efficacy and safety of engineered tissues.

6) **Informatics** to support tissue engineering: gene and protein sequencing, gene expression analysis, protein expression and interaction analysis, quantitative cellular image analysis, quantitative tissue analysis, in silico tissue and cell modelling, digital tissue manufacturing, automated quality assurance systems, data mining tools, and clinical informatics interfaces.

Figure 1.1 explains the process of tissue engineering.

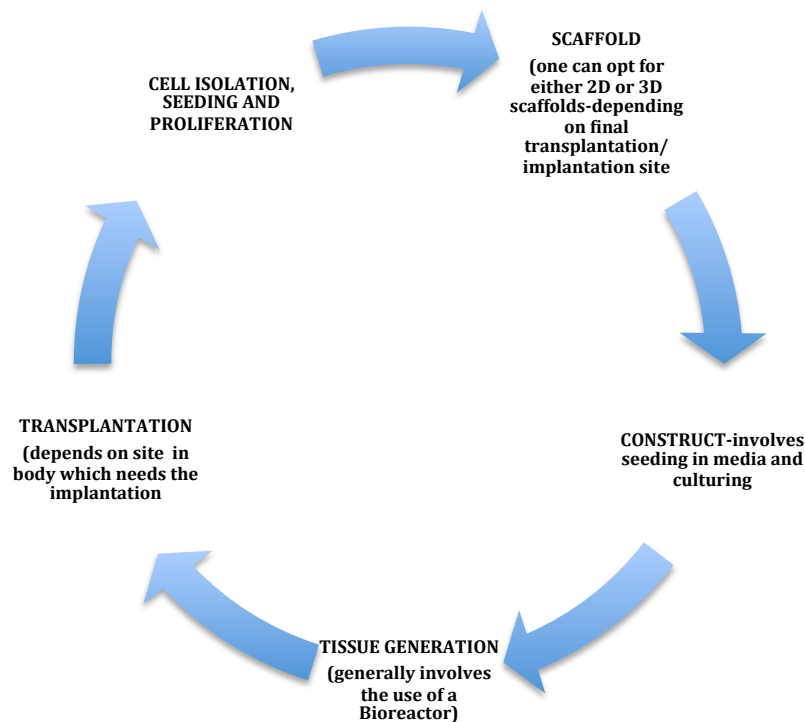


Figure 1.1: Principles of tissue engineering (redrawn based on A.K. Saxena, 2010)

1.1.1 Bone tissue engineering

1.1.1.1 Anatomy and physiology of bone

Bones form an integral part of the body and have an anatomic structure that consists of very dense connective tissue. Forming the skeleton of the human body, they are found in various sizes and shapes. Mineralized bone tissue, also known as osseous tissue, forms a rigid 3-dimensional structure that helps maintain the structure of the bone. Bone tissue has two

main classifications; it is either compact or spongy. The dense layer that forms the exterior of the bone is the compact layer and the spongy layer is the layer that has a lot of pores in between, the bone trabeculae forms a network inside the bone (Figure 1.2). The classification of bone itself is performed based on the shape and size of the bone; e.g. long bones (e.g. tibia, femur), short bones (e.g. carpals), flat bones (e.g. skull), and irregular bones (e.g. vertebra). A long bone has a shaft called diaphysis, with two enlarged ends called epiphysis. The flared portion between the diaphysis and epiphysis is called metaphysis. The inner portion of the bone is a large cavity that is filled with bone marrow, called marrow or medullary cavity.

Compact Bone & Spongy (Cancellous Bone)

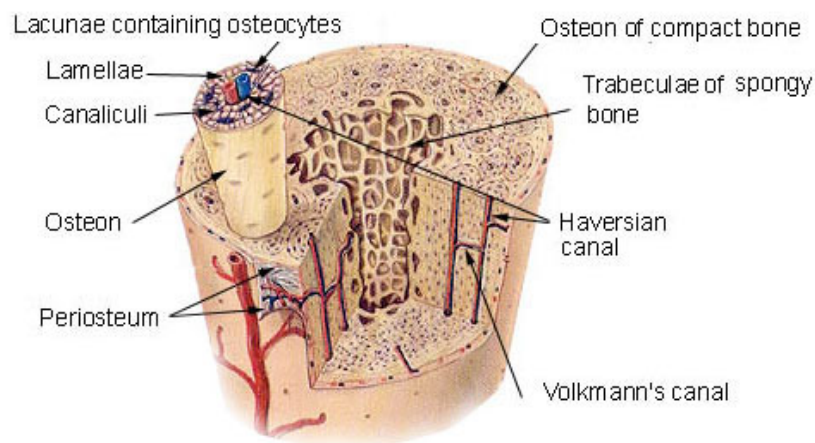


Figure 1.2: Compact and Spongy Bone (picture obtained from National Cancer Institute, United States).

The surface of the bone is enveloped by periosteum. The periosteum consists of an outer fibrous layer that resembles other dense connective tissue, and an inner cellular layer containing osteoprogenitor cells or periosteal cells. The periosteal cells are capable of differentiating into osteoblasts under appropriate stimulus. The endosteum is the lining tissue of both the compact bone facing the marrow cavity and the trabeculae of spongy bone within the cavity. This endosteum consists of fibroblastic flattened cells or called endosteal cells, cells capable of differentiating into osteoblasts under appropriate stimulus (Ross *et al.*, 1995).

1.1.1.2 Bone fracture and repair

When bone fractures, an initial response, which is similar to any injury, occurs - tissue destruction and haemorrhage. This is followed by a neutrophil invasion (which results in acute inflammation) macrophage debridement, fibroblast and capillary proliferation and growth, tissue granulation and finally cartilage or callus formation at the site of the injury. Meanwhile, osteoprogenitor cells of the periosteum proliferate and differentiate into osteoblasts and begin to deposit new bone matrix on the outer surface of the bone some distance from the fracture. These cells progress toward the fracture site until new bone forms as a bony sheath over the fibrocartiliginous callus (Figure 1.3).

This newly formed bone will then invade the callus and lay down new bone matrix within the callus, gradually replacing the callus, described as endochondral ossification. Similarly, in the marrow cavity, endosteal proliferation and differentiation give rise to medullary bone growth from the both ends of the fracture toward the centre, where unite and spongy bone is then formed. This spongy bone is gradually replaced by compact bone, and the bony callus is removed and remodelled by the action of osteoclasts. In healthy individuals, this process usually takes from six to twelve weeks, depending on the severity of the break and the particular bone that is broken (Ross *et al.*, 1995; Chin, 2006).

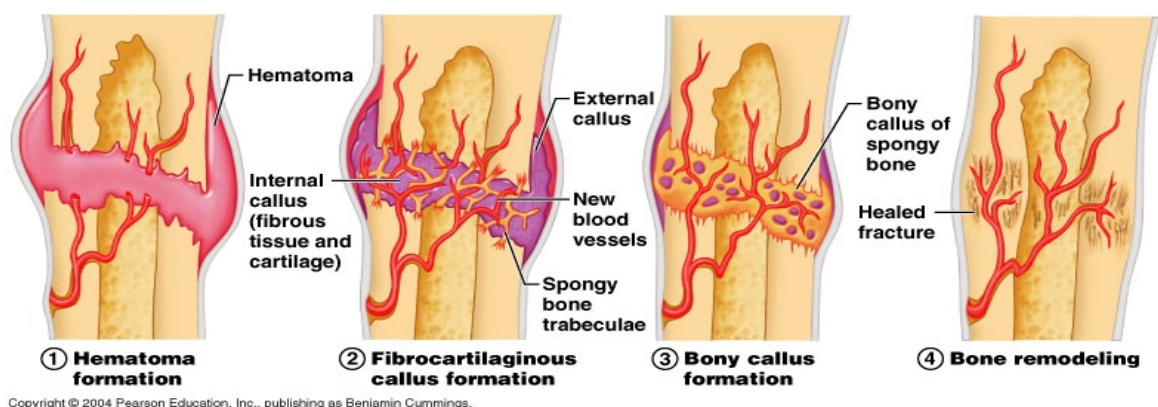


Figure 1.3: Repair of bone (reproduced from Essentials of Human anatomy and Physiology, edited by Elaine N. Marieb, 2008)

1.2 Electrospinning

The earliest record of electrospinning was in the 16th century when William Gilbert described the behaviour of magnetic and electrostatic phenomena. It basically involves creating electrospun fibres on a nano scale that can be spun into sheets and used for a variety of purposes. The properties of electrospinning contain the features of electro spraying and conventional solution dry spinning of fibres. The process does not require the use of coagulation chemistry or high temperatures to produce solid threads from the solution. This makes the process particularly suited to the production of fibres using large and complex molecules (Ziabicki, 1976).

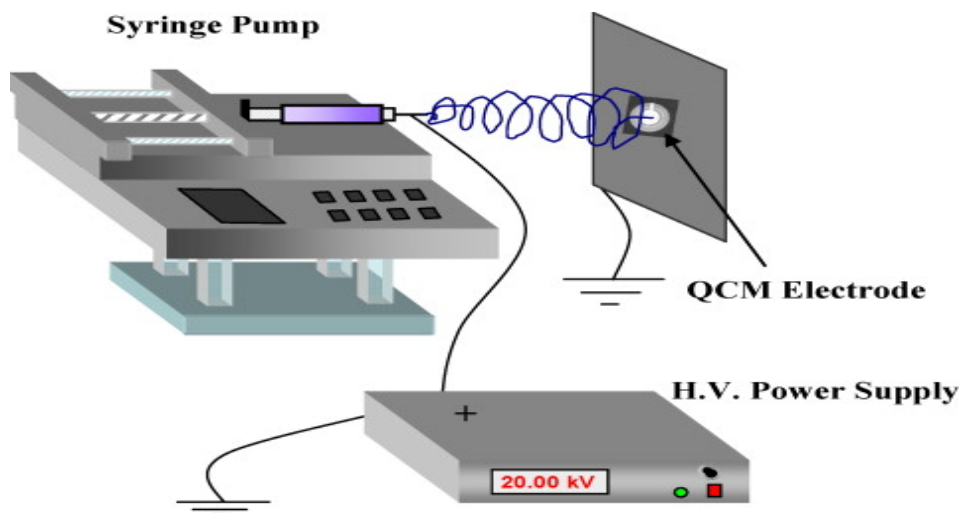


Figure 1.4: An electrospinning experimental layout (reproduced from Sun *et al.*, 2012)

One attractive feature of electrospinning is the relative simplicity and cost effective nature of the setup; the typical electrospinning setup consists of a syringe pump, a high voltage source, and a collector (Figure 1.4). In the process of fabricating an electrospun polymer, the polymer solution is held at a needle tip by surface tension. The application of an electric field using the high-voltage source causes charge to be induced within the polymer, resulting in charge repulsion within the solution. This electrostatic force opposes the surface tension; ultimately, the charge repulsion overcomes the surface tension, causing the initiation of a jet

As this jet travels, the solvent evaporates and an appropriate collector (often an aluminium sheet) can be used to capture the polymer fibre (Pham *et al.*, 2006) and by sequential layering, a sheet is formed.

Parameters that control the process of electrospinning are solution properties, controlled variables, and ambient parameters. The solution properties include the viscosity, conductivity, surface tension, polymer molecular weight, dipole moment, and dielectric constant. The effects of the solution properties can be difficult to isolate since varying one parameter can generally affect the other solution properties (e.g. changing the conductivity can also change the viscosity). Controlled variables include the flow rate, electric field strength, distance between tip and collector, needle tip design, and collector composition and geometry. Ambient parameters include temperature, humidity, and air velocity (Doshi and Reneker, 1995). All these parameters have to be looked at carefully prior to electrospinning a solution blend.

1.3 Bone Marrow Stem Cells

There are two kinds of stem cells found in bone marrow, namely the Hematopoietic Stem Cells (HSCs) and the Mesenchymal Stem Cells (MSCs). HSCs are capable of differentiating into several lineages of hematopoietic cells, such as neutrophils, eosinophils, monocytes, T-lymphocytes, B-lymphocytes, erythrocytes and platelets. MSCs found in bone marrow are cells that are capable of differentiating into several types of connective tissues. Mesenchymal Stem Cells (MSCs), also known as Marrow Stromal Cells (Adel and Mao, 2004), are defined as self-renewable, multipotent progenitor cells with the ability to differentiate into several distinct mesenchymal lineages, such as bone, cartilage, muscle, tendon, ligament and fat tissue (Caplan, 1991; Pittenger *et al.*, 1999). In addition to differentiation into their

natural derivatives, MSCs have the potential to differentiate into other types of tissue-forming cells. These include hepatic (Petersen *et al.*, 1999; Shu *et al.*, 2004), renal (Poulsom *et al.*, 2003), pancreatic (Chen *et al.*, 2004), pulmonary (Wu Min and Yu-Quan, 2004), cardiac (Orlic *et al.*, 2001), and neural cells (Croft and Przyborski, 2004; Suon *et al.*, 2004).

Bone marrow-derived fibroblastic colonies were first successfully isolated from guinea pigs as described by Friedenstein *et al.* (1970), based on the adherence of marrow-derived fibroblastic cells to the plastic substrate of the cell culture plate and a concomitant lack of adherence of marrow-derived hematopoietic cells. These fibroblastic cells were found to be able to become osteocytes when implanted into recipient animals (Friedenstein *et al.*, 1966).

Bone marrow consists of 0.001% to 0.01% mesenchymal stem cells, but the high proliferation rate of these isolated mesenchymal stem cells enables them to be expanded over one billion-fold in culture (Haynesworth *et al.*, 1992). However, the marrow-derived MSCs obtained by this technique are heterogeneous, which likely contain a variety of cells including fibroblasts, osteoblasts or osteoprogenitor cells, adipose cells, reticular cells, macrophages, endothelial and a fraction of hematopoietic stem cells (Seshi *et al.*, 2000). Consequently, this has led to the investigation of the use of primary cultures of bone marrow-derived MSCs which enables one to culture more homogenous cell populations.

1.4 Cell Studies and Existing Electrospun Scaffolds

There is a constant innovation and research in the field of tissue engineering with regards to the production of scaffolds that are biocompatible, biodegradable and encourage the growth, proliferation and in some cases the differentiation of cells. Electrospun scaffolds are taking centre stage as more and more compounds are being mixed and their effects are being

studied. Polycaprolactone (PCL), a common polymer, is being used as a base solvent to which other materials, both organic and inorganic are being added to. PCL/gelatin nanofibrous scaffolds were seeded with fibroblasts and were tested for dermal reconstitution and wound healing (Chong *et al.*, 2007). This combination was found to be highly effective in encouraging cell growth, adhesion and proliferation. Electrospun PCL/gelatin constructs were also used in nerve tissue engineering and were found to enhance the nerve differentiation potential and proliferation when compared to pure electrospun PCL constructs (Ghasemi-Mobarakeh *et al.*, 2008). PCL has also been used with synthetic hydroxyapatite (HA) in an electrospun form with osteoblasts, however, in a 1:1 ratio of HA and PCL (Venugopal *et al.*, 2008). The study compared mixtures of HA, Gelatin and Polycaprolactone. Venugopal *et al.* (2008), observed that the addition of HA to a PCL scaffold resulted in an increase in osteoblast proliferation over 6 days, and an increase in the amount of alkaline phosphatase produced over 10 days.

The gap that has been identified in existing research is that whilst many studies have been performed using electrospun PCL and hydroxyapatite, there are not any studies performed on optimizing the concentration or ratio of Polycaprolactone to hydroxyapatite, or further observations identifying the optimal concentration of hydroxyapatite in terms of causing cell differentiation, in particular, differentiation from mesenchymal stem cells to osteoblasts.

1.5 Objectives

- 1) To study the synthesis and characterize characterization of a biomaterial produced from bovine hydroxyapatite (BHA) and Polycaprolactone (PCL).
- 2) Studying the effect of increasing BHA concentration in an electrospun PCL scaffold with regards to material morphology, characterisation, and cellular growth and interactions with the biomaterial produced.
- 3) Studying the effect of increasing BHA concentration in an electrospun PCL scaffold on mesenchymal cell differentiation.
- 4) Identifying the optimal BHA concentration in an electrospun PCL scaffold with regards to mesenchymal cellular differentiation to osteoblasts.

CHAPTER 2: LITERATURE REVIEW

CHAPTER 2: LITERATURE REVIEW

2.1 Introduction

This chapter will thoroughly discuss the existing sources of previously carried out similar experiments and will analyze the different segments involved in this research as well as discuss the reason for the successes and failures of the previous experimental setup. Looking at the overall picture, this thesis shall delve into research dealing with hydroxyapatite, polymer electrospinning, the effects of materials on the cell culture and the reasons for the different assays chosen. Additionally, there will be a discussion on the different biochemical assays present and the reasons behind their choice coupled with previous experimental work on those tests.

2.2. Hydroxyapatite (HA)

2.2.1 Hydroxyapatite preparation

Hydroxyapatite has many uses and has been well documented on its exceptional osteoconductive and bioactive properties. These attractive properties are present because of the similarity of hydroxyapatite with regards to its chemical and biological composition as well as its crystallographic composition to the mineral portions of hard tissue, e.g. bones and related tissues (Herliansyah, 2009 and Suchanek, 1998).

There are many ways to produce hydroxyapatite and these include, but are not limited to, production of hydroxyapatite from inorganic synthesis, which would use the wet chemical method in aqueous solutions (Pramanik, 2005 and Kivrak, 1998). This method would involve making hydroxyapatite by using the inorganic oxides of calcium and phosphorus with additional additives and mixed in a ball mill for 16 hours followed by drying and then

shaping the dried hydroxyapatite into pellets and sintering them at 1250 °C. This was done until the stoichiometric ratio of Ca/P of 1.6 was obtained, so as to confirm that the material formed was hydroxyapatite. Another method of producing hydroxyapatite from inorganic synthesis is the sol-gel method. This method has been used by Balamurugan (2002) and Layrolle (1998), and is used to make hydroxyapatite by mixing calcium acetate dissolved in ethandiol and a phosphorus precursor solution (which contains refluxed phosphorus pentoxide). These solutions were mixed with specific molar ratios which according to the authors (Balamurugan, 2002) ensured that the stoichiometric ratio of hydroxyapatite (Ca/P: 1.67) was adhered to.

Another method employed to produce hydroxyapatite is the hydrothermal method. This method (Majubala *et al.*, 2000) involved the use of corals which were washed, dried and heated until 900 °C for 2 hours. The resultant powder was then mixed with diammonium hydrogen orthophosphate and water, with the solution under hydrothermal conditions for some hours to form hydroxyapatite.

Another method to produce hydroxyapatite is the thermal deposition method. This was employed by Gross and Berndt (1997) to produce hydroxyapatite. Briefly what they did was, since they were creating hydroxyapatite coating, they sprayed spherical hydroxyapatite powder using a spray torch and then heat the powder up to 1400 °C and then run characterisation tests on the powder. Additionally as Tadic and Epple (2003) have shown, one can also produce hydroxyapatite by using the continuous precipitation method. The above mentioned are the more common chemical synthesis methods of hydroxyapatite.

2.2.2 Hydroxyapatite sources

Hydroxyapatite can be synthesized by extracting it from different sources. These sources include, but are not limited to, hydroxyapatite extracted from corals (Murugan and Rao, 2002), egg shells (Sasikumar and Vijayaraghavan, 2006), cuttlefish shells (Rocha *et al.*, 2005 and Rocha *et al.*, 2005), natural gypsum (Herliansyah *et al.*, 2006), natural calcite (Herliansyah *et al.*, 2007) and bovine bone (Ooi *et al.*, 2007; Herliansyah *et al.*, 2006 and Ruksudjarit *et al.*, 2007).

In particular, the focus will be on the extraction of hydroxyapatite from bovine bones, as this has been identified in previous studies (Ooi *et al.*, 2007; Herliansyah *et al.*, 2007) as being an easily available and pure source of hydroxyapatite. From Ooi *et al.* (2007), the means of extracting bovine hydroxyapatite was by using bovine bones, which was cut into various rectangular samples, defatted and annealed in an electric furnace under nine different temperatures which ranged from 400 °C to 1200 °C and they used a heating rate of 5 °C per minute with a 2 hour holding time. They then tested produced powder by X-ray Diffraction (XRD) and Fourier Transform Infrared (FTIR) spectroscopy and found that the best temperature for sintering bone powder to obtain bovine hydroxyapatite was above 700 °C as there were no secondary phases present in the bone matrix. Although they recommended the hydroxyapatite produced for clinical application, but they did not carry out any cellular studies on the produced scaffold.

Herliansyah *et al.* (2006), defatted the bones by ensuring that the impurities were shaved and removed from the bones and then sun dried them for 3 days. The dried bone pieces were then cut into cubic pieces using a hacksaw and calcined at 5 temperatures ranging from

700 °C to 1100 °C, by increasing the temperature at a rate of 5 °C per minute and holding it for 2 hours to remove all organic matters.

2.2.3 Hydroxyapatite in Tissue Engineering

Hydroxyapatite has been featured in tissue engineering as a pure scaffold itself and also as an additive to various polymers and other compounds and has then been tested on different types of cells (Kirkpatrick *et al.*, 1998).

A porous scaffold of HA was made and seeded with mesenchymal stem cells and observed that the cells proliferate within the scaffolds interconnected pores which aided bone tissue engineering by allowing the introduction and proliferation of bone cells and osteotropic agents into the scaffold. Their scaffold, which they named the IP-CHA (interconnected porous hydroxyapatite), when used in animal experiments showed superior osteoconduction, with a large portion of the pores being filled with newly formed bone (Yoshikawa and Myoui, 2005).

Marra *et al.* (1999) made a hydroxyapatite scaffold composite using a polymer blend of PCL and HA as well as poly(lactic-*co*-glycolic) acid (PLGA) and HA. The method that they used for preparing the scaffolds was the particulate leaching technique which involved dissolving the polymers in chloroform which was used as a solvent and then suspending both sodium chloride (NaCL) and different concentrations of HA in the solution and then mixing the solution with distilled water.

By performing biodegradability, histological, Scanning Electron Microscopy (SEM) and Transmission Electron Spectroscopy (TEM) analyses, they discovered that there was no

significant difference in terms of biodegradability between the different concentrations of HA. The SEM results showed cell growth on the surface of the seeded scaffolds at 2 and 4 weeks. TEM displayed thick and confluent layers of cells on the surface of the scaffold. Histologically, what was observed was that there was a positive stain for collagen and this was found more on the surface of the scaffold. It can be inferred from the experiment by Marra *et al.* (1999), that the vast majority of stem cells seeded on a scaffold containing HA and PCL generally tend to stay on the surface, so a thick 3-D scaffold should not be used, otherwise, it may hamper the migration and proliferation of cells.

2.3 Polycaprolactone (PCL)

2.3.1 Properties and characteristics of Polycaprolactone

Poly(ϵ -caprolactone) is normally made from ϵ -caprolactone via ring opening polymerization. Poly(ϵ -caprolactone) is generally semi-crystalline, with a melting point of 59 – 64 °C, glass-transition temperature of -60 °C (Middleton and Tipton, 2000). Various copolymers based on ϵ -caprolactone have been synthesized, such as ϵ -caprolactone with DL-lactide (Kohn and Langer, 1996; Goupil, 1996; Lewis and Fabisial, 1997), and ϵ -caprolactone with glycolide (Schindler *et al.*, 1977), yielding materials with more rapid degradation rates, and lower stiffness compared to pure polyglycolic acid (PGA), respectively.

Since PCL is an aliphatic polyester which is composed of hexanoate repeats, its physical, thermal and mechanical properties depend on two key factors, which are firstly, its molecular weight and secondly, its degree of crystallinity (Labet and Thielemans, 2009). At ambient temperature, it is also known to be soluble in a variety of solvents, which include but are not limited to, chloroform, dichloromethane, carbon tetrachloride and benzene. It is also insoluble in alcohols, petroleum ether, diethyl ether and water (Sinha *et al.*, 2004).

PCL has many properties and characteristics that make using it as an additive in compounds very attractive. These include biodegradability, which is conditional on the molecular weight, crystallinity and the environment which the PCL is in (Chen *et al.*, 2000; Peñ a *et al.*, 2006; Lam *et al.*, 2000). The dependence of molecular weight and the PCL properties are displayed in Table 2.1 below. It is miscible with many other polymers like poly(vinyl chloride), poly(styrene–acrylonitrile) and other polycarbonates. It has also been proven to be mechanically compatible with other polymers and naturally occurring compounds such as polyethylene, poly vinyl acetate and rubber.

Table 2.1: Properties of PCL (Labet and Thielemans, 2009)

| Properties | Range |
|---|-------------|
| Number average molecular weight ($M_n/\text{g mol}^{-1}$) | 530–630 000 |
| Density ($\rho/\text{g cm}^{-3}$) | 1.071–1.200 |
| Glass transition temperature ($T_g/^\circ\text{C}$) | (–65)–(–60) |
| Melting temperature ($T_m/^\circ\text{C}$) | 56–65 |
| Decomposition temperature ($/^\circ\text{C}$) | 350 |
| Inherent viscosity ($\eta_{\text{inh}}/\text{cm}^3 \text{ g}^{-1}$) | 100–130 |
| Intrinsic viscosity ($\eta/\text{cm}^3 \text{ g}^{-1}$) | 0.9 |
| Tensile strength (σ/MPa) | 4–785 |
| Young modulus (E/GPa) | 0.21–0.44 |
| Elongation at break ($\epsilon/\%$) | 20–1000 |

2.3.2 Polycaprolactone in Tissue Engineering

Polycaprolactone has been used extensively with many other compounds and materials to produce scaffolds for tissue engineering (Agrawal and Ray, 2001). There has been extensive work done using PCL for bone tissue engineering. This is due to its physical and chemical properties, which make it ideal for use as a scaffold.

Williams *et al.* (2004), did a study using PCL scaffolds made using SLS (Selective laser sintering), seeded with bone morphogenetic protein-7 transduced fibroblasts in order to test

the mechanical properties of PCL in relation to bone tissue engineering. They discovered that the PCL when synthesized using SLS, supported bone regeneration, in particular, aiding the cortex of the bone which surrounds the marrow space to form. Judging by the data obtained, they concluded that the scaffolds would be able to withstand early functional loading and using the SLS, it would be able to fit the desired anatomical position in the bone. However, the use of the SLS method had some limitations, which were also pointed out by Williams and her colleagues that included particle size. Basically, if the particles were very large, then they increased the granularity of the edges and layers of the SLS produced scaffold and if the PCL particle size was very small, then the spreading properties and flow of the produced scaffold was highly limited.

Shin *et al.* (2004), seeded rat osteoblasts on an electrospun PCL scaffold and cultured them for 4 weeks and then subsequently transplanted those seeded scaffolds in-vivo into rats. They observed that cell and extracellular matrix production were present throughout the scaffolds, also detected was mineralization and collagen type I. It was interesting to note that Shin *et al.*, considered the electrospun PCL scaffold as a 3-D structure because large, interconnected voids were present between the fibres. They mentioned that normal mesenchymal stem cells (MSC) seeded on PCL can produce alkaline phosphatase (ALP). However, it is generally considered negligible when compared to the amount produced by osteoblasts.

There has been some encouraging research in using PCL as a bone patch to repair holes in the skull (Tan, 2004). Basically, Tan and his team used fused deposition modelling (FDM) in creating the 3-D PCL scaffolds required for this clinical application. FDM works by creating objects by extruding the PCL using an extrusion head by working on all the three axis' (x, y and z) of a 3-D object.

2.4 PCL and HA Blends Used in Bone Tissue Engineering.

Bone tissue regeneration is taking on an important role, in order to restore skeletal function with focus on orthopaedics. In most clinical situations, where orthopaedic surgery is required, there are limitations with regards to sources of bone graft materials. Generally, graft materials include autologous bone (from the patient), allogeneic bone (from a donor), and demineralized bone matrices, as well as a wide range of synthetic biomaterials such as metals, ceramics, polymers, and composites (Meijer *et al.*, 2007). These limitations create a demand for materials that can be used in bone tissue engineering and electrospinning appears to fill the void.

PCL has been used commonly as a synthetic biodegradable polymer for tissue engineering, however its use in tissue engineering is limited because of its inadequate mechanical strength and low bioactivity. A study was done using halloysite nanoclay (NC) as an inorganic filler material with PCL to prepare PCL/NC fibrous scaffolds via electrospinning (Nitya *et al.*, 2012). The PCL/NC electrospun scaffold was found to be mechanically superior to the pure PCL electrospun scaffolds. It was also noted that the PCL/NC scaffolds has more protein adsorption and increased mineralization when incubated in simulated body fluid. The in-vitro results showed that the human mesenchymal stem cells (hMSCs) seeded on the PCL/NC scaffolds were viable and could proliferate faster than in PCL scaffolds as confirmed by fluorescence and scanning electron microscopic observations. An increase in ALP activity displayed osteogenic differentiation of hMSCs on the nanoclay embedded scaffolds.

Professor Ramakrishna's research team (Venugopal *et al.*, 2007) in the National University of Singapore, did a study of PCL and HA using a 2% to 2% ratio of PCL and HA by

electrospinning the two. The only concentration used for HA was the 1:1 ratio with PCL. They discovered that after seeding osteoblasts for 6 days, there was some migration of the osteoblasts inside the nanofibrous scaffold and this was then translated into an increase in cell proliferation (measured by the MTT assay) over a 6 day period. ALP activity increased as well and was measured over time periods of 5 and 10 days. Their limitation in the experiment was however that only 1 concentration of HA was blended with the PCL and that besides FTIR, there was no further characterisation of the scaffold. Additionally, the HA used was obtained using synthetic techniques.

Deepika *et al.* (2009) also used a co-polymer containing polycaprolactone and poly-lactic acid, mixed with hydroxyapatite. The purpose of creating this blend was to investigate whether the spraying of HA particles onto nanofibres was better than blending the HA particles with nanofibres. Their investigations showed that the electrospaying of HA particles helped to attain a rough surface, which aided in increased cell proliferation and attachment. It also aided in improved mechanical properties. Once again, osteoblasts were used in this study to observe the attachment of cells to the scaffold.

Wei and Ma (2004) used another method that was used to create scaffolds. They employed thermally induced phase separation technique to create a nano-hydroxyapatite/polymer composite scaffold. The addition of HA increased the protein adsorption capacity of the scaffold and increased the mechanical properties.

2.5 Electrospinning and its Applications in Tissue Engineering

There has been recent interest in the use of electrospinning as a technology to fabricate scaffolds in tissue engineering due to a realization that electrospun scaffolds are highly

adaptable to different tissues, adding different additives and amounts can control the texture and thickness of the scaffold. The biodegradability of electrospun scaffolds is also controllable by blending different materials together, both natural and synthetic. Due to the nature of the fibre arrangement, one can even control the biological response of the scaffold. This added with the possibility of adding protein, DNA and RNA to the mix makes for a very exciting technology to be used in the fabrication of scaffolds (Sill and Recum, 2008).

Electrospinning in tissue engineering takes into consideration various factors that need to be considered which include, but are not limited to the type of material being spun, the orientation of the fibre and the porosity of the scaffold that will be determined. The material of choice for electrospinning must be biocompatible and must take into consideration the final application for which the electrospun scaffold will be used for. For example, scaffolds required for bone tissue engineering need to be rougher in texture than those required for skin applications.

Fibre orientation plays a big role in the type of tissue the electrospun scaffold needs to be utilized for. There is either aligned or random fibre orientation. Schnell *et al.* (2007), studied the effect of using aligned nanofibrous scaffolds, made from PCL and collagen/PCL, to control axonal outgrowth and glial cell migration in peripheral nerve regeneration. It was discovered that while both scaffolds facilitated oriented outgrowth of axons and glial cell migration, the collagen/PCL blend has given superior guidance to axons.

By incorporating chitosan in PCL nanofibres, and seeding them with osteoblasts derived from mice, a group of researchers (Yang *et al.*, 2009), found that SEM imaging showed that the whole construct surface was covered by cells and newly covered Extracellular Matrix (ECM). Additionally, the formation of integral tissue in the constructs without the

PCL/Chitosan nanofibres meant that the use of electrospun scaffolds in tissue formation aided immensely in creating a structure that will degrade over time leaving a proper fully formed tissue in place.

The use of electrospinning in tissue engineering has also been explored in the area of heart tissue engineering (Zong *et al.*, 2005). Cardiomyocytes were seeded on electrospun scaffolds made from non-woven poly(lactide) and poly(glycolide)-based (PLGA) scaffolds. In this experiment, the in-vitro studies showed a dose response effect of the PLGA concentration in the degradation rate together with a change in the pH value. In the SEM evaluation, it was noted that the fine fibre network of the matrix made it possible for the cardiomyocytes to crawl underneath fibre and thus, creating possible layers of tissue. By the use of confocal microscopy on the scaffolds, they deduced that the cardiomyocytes had a preference for hydrophobic surfaces.

Ekaputra *et al.* (2009), fabricated electrospun PCL/Collagen fibre and seeded pig Bone Marrow Mesenchymal cells (pBMMCs) on these fibre. Their immunohistochemistry showed that the osteogenic differentiation markers were stronger when cultured with the collagen co-polymer as opposed to the pure PCL alone. However, the scaffolds had to be osteogenically induced by adding osteogenic cell sheets around the PCL/Collagen scaffolds and this in turn, aided the osteogenic differentiation as well.

2.6 Stem Cells

2.6.1 Isolation and applications of stem cells

Mature MSC possess differentiation potential into cells of bone, cartilage, adipose, muscle, tendon, ligament and marrow. These cells have been found in a variety of tissues which

include, but are not limited to, bone marrow, adipose tissue, synovium, dental pulp, cord blood and umbilical cord (Pittenger *et al.*, 1999; Zuk *et al.*, 2001; Sudo *et al.*, 2007, Caplan *et al.*, 2007). With specific regard to bone tissue engineering, the primary source of cells has been the bone marrow mesenchymal stem cells. The main reason is because these cells have proven over time that they are capable of bone and cartilage formation (Friedenstein *et al.*, 1987).

Bone Marrow Stem cells are normally isolated based on their growth potential and their adherence to plastic. The aspirate can originate from rats, rabbits or humans. Irrespective of the source, generally all stem cells are seeded and passaged (also known as culture expanded) prior to testing. In passaging, the population doubles and can continue, as some research has shown up to 50 passages (Bianco *et al.*, 2001).

2.6.2 Characterisation of stem cells

In the characterisation of MSC, there are certain criteria that needs to be followed. These criteria have been set by the International Society for Cellular Therapy and these criteria include that MSCs must be adherent to plastic when maintained in culture (Dominici *et al.*, 2006). Secondly, the MSCs must be positive for the surface antigens CD105, CD73 and CD90. Additionally, the MSCs must be lacking in markers for monocytes, macrophages and B cells, as well as the expression of the haematopoietic antigens CD45(-) and CD34(-). For characterisation purposes, it is necessary to have a combination of some negative markers as well as at least one positive marker. Last but not least, the MSCs must have the potential to differentiate into osteoblasts, adipocytes and or chondrocytes under standard in vitro differentiating conditions (Rosenbaum *et al.*, 2008).

2.7 The Effect of Scaffold Material on Stem Cell Differentiation

The type of material that stem cells are seeded on can possibly impact the type of cell it forms. In light of bone tissue engineering, more and more researchers are moving towards materials that are osteoconductive, osteoinductive and are capable of osteointegration. This reasoning was brought about because it was established that cells are highly sensitive to their surroundings and environment (Stevens and Stevens, 2008). The reaction of the cells to the texture of the material, especially with regards to groves, ridges, wells and other features at both the micron and nanoscale level is now established (Stevens and George, 2005).

Example, the use of hydroxyapatite to create a rougher surface which can induce cell differentiation was investigated by Deligianni and colleagues (2000). They used synthetic HA which was moulded into discs and these were then seeded with MSC and were observed for cell attachment, proliferation and differentiation. It was found that the addition of the HA increased the cell proliferation, adhesion and detachment strength. As far as the cellular differentiation was concerned, there has been ALP activity recorded, however it was not statistically significant when it was compared with the positive control.

2.8 Cellular Assay Measurements and Protocols

Cellular measurements are important as they are used as a method of quantitative measurement. This adds a depth to the study that qualitative measurements are unable to provide. In addition they provide an overall picture to the experimental set up which allows for in-depth analysis of the different environments that the material and cells have been exposed to.

2.8.1 Alamar Blue Assay

The Resazurin dye or better known as the Alamar Blue assay, is a blue dye, which remains so until it is reduced to its pink form, as a result of metabolic activity. It can be measured by both absorbance and fluorescence.

2.8.2 Deoxyribonucleic Acid (DNA) Assay

The DNA assay that was carried out was the Hoescht 33258 stain. It is part of the Hoescht family which is composed of 3 main stains. The Hoescht 33258 stain works off the basis of excitation spectra which is what is then used to pick up the DNA amount. It is a fluorescent dye which works by binding to the AT-rich part of the DNA which then allows it to quantify and detect DNA by graphing it logarithmically between the fluorescence reading and the AT base pairs.

2.8.3 Alkaline Phosphatase (ALP) Activity

ALP is an enzyme that is released by osteoblasts and has thus been characterized as an osteoblast marker. An increase in the level of this enzyme is reflective of an increase in the activity of osteoblasts.

CHAPTER 3: MATERIALS AND METHODS

CHAPTER 3: MATERIALS AND METHODS

3.1 Introduction

This chapter covers the various methodologies used for the extraction and cultivation of the stem cells used in the experiments to the production, and for the characterisation and isolation of the various materials used. The fabrication process of the materials and the various parameters used will also be discussed. The different biochemical assays utilized in measuring the performance of the cells with the various materials tested will also be discussed and elaborated upon. The overall methodology of the study is illustrated in Figure 3.1.

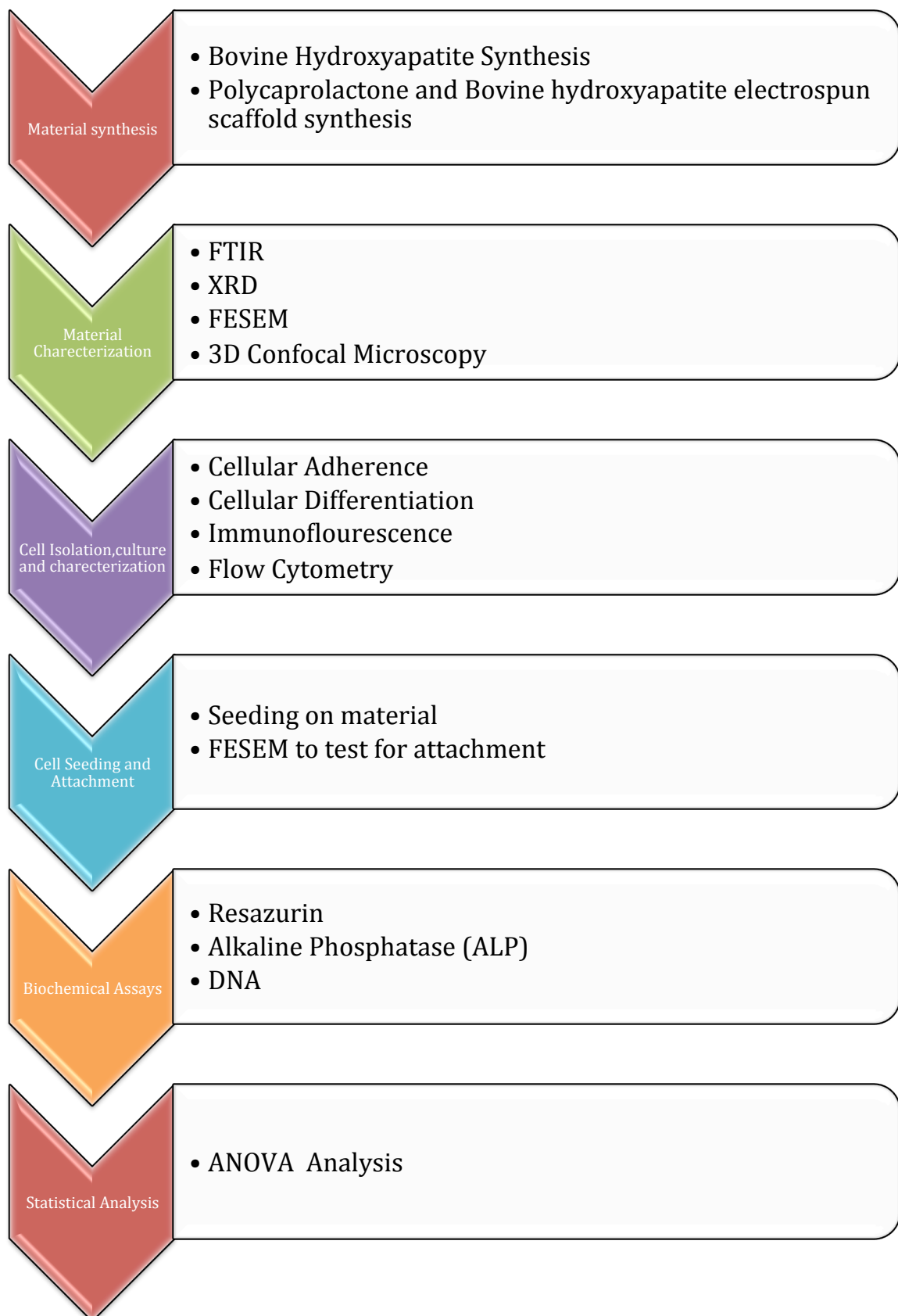
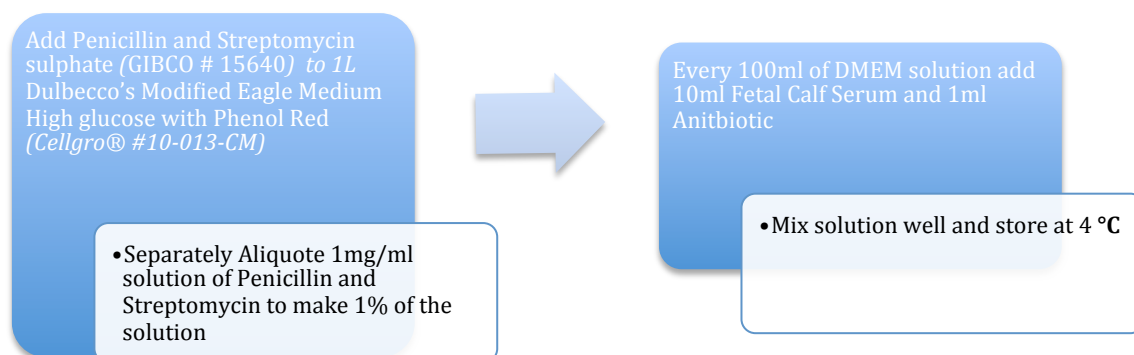


Figure 3.1: Flow chart of methodology involved in the study

3.2 Preparation of Primary Culture Medium

For the culture of bone marrow stromal cells, Dulbecco's Modified Eagle Medium (DMEM) containing 10% foetal calf serum (FCS), 100 units/ml penicillin and 100 units/ml streptomycin was used. The flowchart below shows the preparation of the culture medium.



3.2.1 Isolation and culture of Rat Derived Bone Marrow Stem Cells (BMSC)

In this study, BMSCs were obtained from young adult (5-6 weeks old, male, 150-170 grams) Sprague Dawley rats supplied by the Animal house, Faculty of Medicine, University of Malaya. The BMSC isolation protocols were approved by the Animal Ethics Committee [Ethics number: BM/10/11/2008/KBM(R)], Faculty of Medicine, University of Malaya.

BMSC isolation and culture protocols described by Maniopoulos C. *et al.* (1988), were employed for this study with some minor modifications. All of the steps are illustrated in Figure 3.2. Basically, following spinal dislocation and immersion of whole animal in 70% alcohol solution for 5 minutes, femurs and tibias of Sprague Dawley rats were aseptically excised inside a laminar hood. Soft tissues attached to the excised bones was cleaned off and

washed in culture medium (prepared previously Sec 3.2). The diagram below shows how the cells were isolated and cultured. Upon reaching confluence, the cells were then passaged, and all cells were cultured until passage 2-3, and seeded on the scaffolds when they were at those passages.



Figure 3.2: Isolation and culture of Bone Marrow Derived Stem Cells. A: Sprague Dawley Rat is the source of the cells (5-6 weeks old); B: Cleansing of rat's femur and tibia of any flesh; C: Cleaned bone is washed briefly in a solution containing a high concentration of antibiotics; D: The two metaphyseal ends of the bone are cut and the bone marrow is flushed out; E: Cell clumps are broken by repeated pipetting; F: Cell suspension is transferred to tube for centrifugation at 1500 RPM for 5 minutes; G: Cell pellet is re-suspended by repeated pipetting; H: Cells are seeded onto a T-75 flask; I: Cells are cultured in 5% CO₂ incubator at 37 °C for 4 days.

3.2.2 Cell seeding and incubation period

The cells were then counted using a haemocytometer (described below) and were seeded on sterilized scaffolds at a density of 20,000 cells per cm^2 inside 24 well plates and were labelled accordingly.

The seeded scaffolds were then placed into the incubator for 2 hours. These scaffolds were then taken out and placed inside the sterile biosafety cabinet and the culture medium was added (this was done gently and from the sides so as to minimize the impact of adding culture medium to the cells which could result in cells being detached from the scaffold). Culture medium was changed regularly twice a week. The seeded scaffolds were cultured for time periods of 1, 7 and 14 days. At these time points, biochemical assays as well as SEM tests were carried out (described in Sections 3.6 and 3.7)

A haemocytometer is a graduated counting chamber that can be observed under a microscope and is used to determine the concentration or number of cells in a suspension. In this experiment, a common *Neubauer* type chamber was used. The slide was divided into 4 large squares in which the total number of cells were counted and processed according to the formula described below.

A haemacytometer was used by first preparing a homogenous suspension of cells. It is an instrument used for counting the blood cells in a measured volume using a counting chamber of uniform depth that is covered by a ruled cover glass (Miller-Keane, 2003). This is normally done by pipetting cells post trypsinization. 20 μl was taken out of the cell suspension in the culture medium and then pipetted into a 1ml micro centrifuge tube. To this tube, 20 μl of Typan blue (caution: Trypan blue is a mutagen and must be handled with

care) was then added. The mixture was then pipetted thoroughly and 20 μl was then pipetted out under the glass cover slip and into the haemocytometer, where the number of live and dead cells were counted. The live cells shine brightly and the dead cells are stained with trypan blue. The total number of cells in the 4 squares (each square is 1 mm^2) were counted and then processed according to the following formula to get the total number of cells per ml (Figure 3.3).

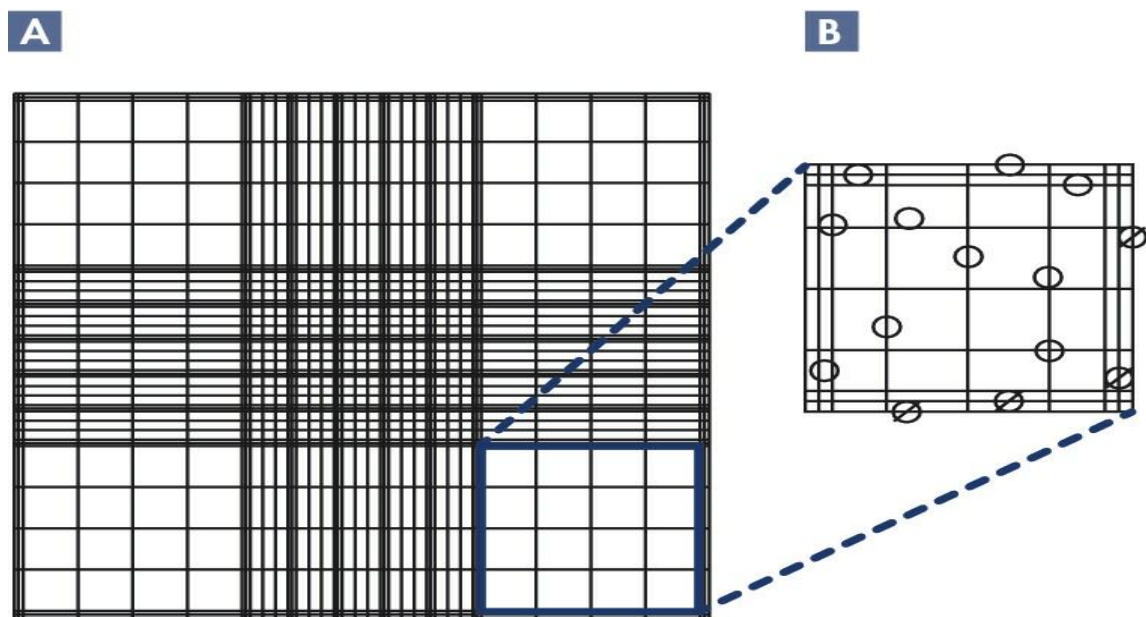


Figure 3.3: Counting live and dead cells in a haemocytometer. (A) One chamber of a haemocytometer slide under 10x objective and 10x ocular. The chamber is divided into 9 major squares. (B) Detailed view of one of the 9 major squares. Only cells that overlap the top and left borders of squares should be counted to avoid overestimating the cell concentration. O: cells that should be counted; Ø: cells that should be ignored (Image courtesy of qiagen.com)

Formula for measuring the number of cells/ml:-

$$\frac{[(\text{Total number of cells counted in } 4\text{mm}^2) \div 4] \times 10000}{\text{Dilution (ml of suspension)}}$$

Dilution (ml of suspension)

3.3 Bovine Hydroxyapatite (BHA) Production

Bovine bones (femur, tibia and metatarsus) were obtained from the local abattoir and then cleaned from macroscopic impurities and substances, including the ligaments and tissues. The bones were then defatted by boiling (100°C) in distilled water for 3 hours, and dried in an oven at 70°C for 7 days in order to remove as much water content from the bones as possible. The purpose of defatting was to reduce soot formation during the heating process in the furnace. The dried bones were then ground into powder using a Schein Orthopaedic machine (T2002 ULTRA). The powdered bone was then sieved to between $25\text{-}40\ \mu\text{m}$. The sieved powder was then heated in a furnace to 1100°C at a heating rate of $10^{\circ}\text{C}/\text{min}$ to obtain pure BHA (Herliansyah *et al.*, 2006; 2009).



Figure 3.4: Bovine Hydroxyapatite production. A: Raw bovine bones are defatted; B: Dried Defatted Bone; C: Dried bone is then ground into powder; D: Bone powder is obtained; E: Powder is then sieved between $25\text{-}40\ \mu\text{m}$; F: Sieved powder is then heated to 1100°C in a furnace.

3.4 Polycaprolactone (PCL) and Bovine Hydroxyapatite (BHA) Scaffold Production

3.4.1 Solution preparation

PCL ($M_n = 80,000 \text{ g mol}^{-1}$) was purchased from Sigma-Aldrich, USA. Chloroform and dimethylformamide (DMF), which were used as solvents for all the experiments, were purchased from Merck and Friendemann Schmidt, respectively.

Solution blending of PCL and BHA was carried out in weight compositional ratios of 100:0, 90:10, 80:20, 70:30, 60:40 and 50:50 respectively. PCL was first dissolved in a mixed solvent consisting of 9 parts chloroform and 1 part DMF using a magnetic stirrer at 50°C for 3 hours. After obtaining a homogenous solution, BHA was added and stirring continued for another 20 hours. In order to agitate and break possible random agglomerations of BHA, the solution was sonicated for 1 hour.

3.4.2 Electrospinning

The electrospinning set-up consisted of a syringe pump (Longer Pump, China), a 20 ml Terumo syringe, a needle (Terumo needle, $0.91 \times 30 \text{ mm}$), a transformer (capable of generating voltage up to 24 kv) and a high voltage capacitor (Maxwell Laboratories Inc. USA, capacitance $0.22 \mu\text{F}$, Voltage: 50 kV). The high voltage produced by the transformer was passed through a rectifier and a half-rectified DC current was obtained. The capacitor was used to decrease ripples and produce a more stable half-rectified DC wave. A piece of aluminium foil placed horizontally 18 cm from the needle tip was used as collector. The electrospinning was carried out while the syringe needle was positively charged at 12 kv and the syringe pump feeding rate was set at 3 ml/h. The set-up was placed inside a tailor made transparent acrylic box. Some small holes were created in the walls of the box as outlets for

the evaporated solvent. A hygrometer (Hana Instruments, Romania) was used to monitor the humidity and temperature changes during the electrospinning process. The relative humidity varied from 60% to 75% during the spinning time and temperature changed in the range of 28 ± 2 °C. The resultant electrospun sheets were placed inside a vacuum oven at 40 °C for 24 hours to remove any possible residual solvent.



Figure 3.5: (i) Electrospinning machine setup which includes A: Box with minimal airflow for electrospun sheet; B: Syringe Pump; C: Aluminium sheet onto which electrospun scaffold was formed.

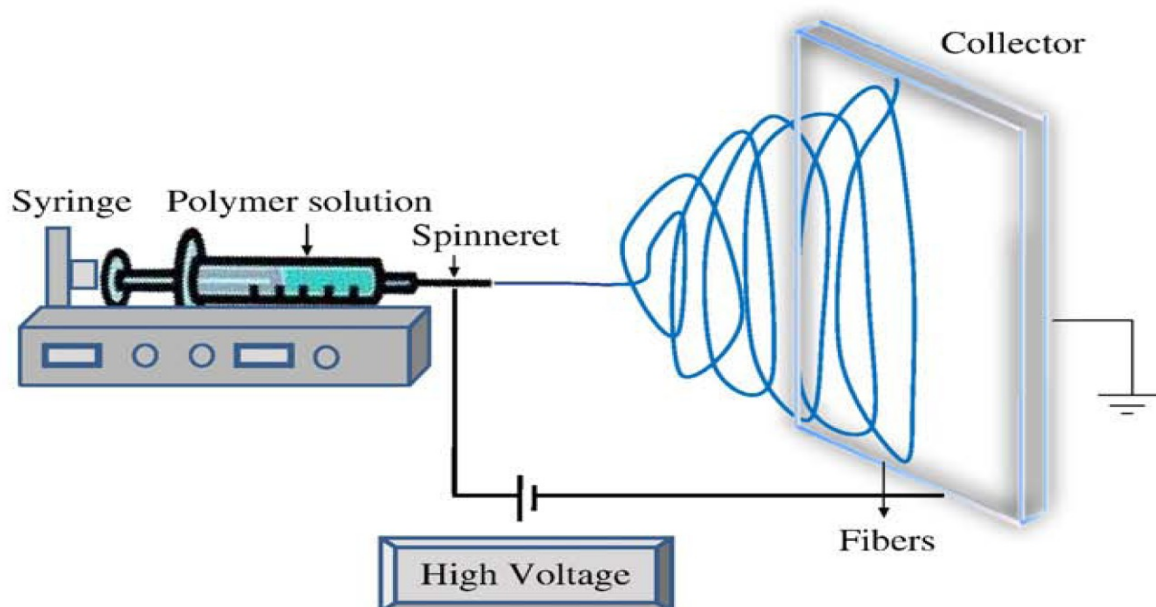


Figure 3.5: (ii) Schematic diagram of electrospinning set-up (reproduced from Zhu and Chen, 2013)

For the electrospinning process, glass cover slips measuring 20 mm by 20 mm were stuck on the aluminium foil (Figure 3.6) (Venugopal *et al.*, 2007). This was done mainly for two reasons, primarily to ease the peeling off of the scaffold sheet from the aluminium foil after it is electrospun as the sheet has a tendency to stick on the aluminium foil, which can cause a difference in the thickness of the sheet; secondarily, because having a rougher surface aids in the culture of cells.



Figure 3.6: (A) Glass cover slips stuck on the aluminium sheet to prevent sticking of the electrospun sheet on the aluminium sheet. (B) Schematic representation of cover slips on aluminium sheet.

The resultant scaffold sheet was cut into 1 cm by 1 cm squares (Figure 3.7) and sterilized by soaking the scaffolds in 70% ethanol at 4 °C overnight, then draining the alcohol and exposing the sample to Ultraviolet light for 3 hours (Tan *et al.*, 2008). The reason they were soaked in alcohol was to disinfect the scaffold of any possible contamination. The scaffolds were then subjected to UV irradiation to remove any possible bacterial infection.

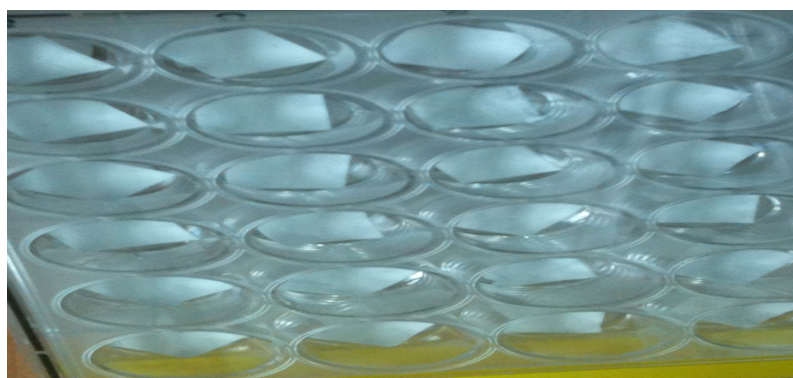


Figure 3.7: Electrospun sheet is cut into 1cm by 1cm squares and placed in a 24 well plate for sterilization by alcohol and then UV radiation.

3.5 Bovine Powder Characterisation

The Bovine Hydroxyapatite powder was characterized by using two main methods:-

1) Fourier Transform Infrared Spectrometer (FTIR):

Infrared (IR) spectrometer is used to see the vibrations of bonds (stretches and/or bends) of atoms present in a compound, thus providing evidence of the functional groups present in that particular compound. It measures the frequencies of IR light (wavelength: 0.76 to 1000 μm) absorbed by a compound (Pavia *et al.*, 2001). Fourier Transform Infrared spectrometer (FTIR) is the most modern infrared spectrometer (compared to conventional dispersive-type instrument) that uses an interferometer to measure a spectrum.

The major advantages of using an FTIR spectrometer as opposed to using a dispersive instrument are (Wade, 2003):

- (a) It has the sensitivity required to measure all frequencies simultaneously, rather than scanning through the individual frequencies.
- (b) Less energy is needed from the source.
- (c) Less time is needed for a scan (typically 1 to 2 seconds).
- (d) Several scans can be completed in a few seconds and averaged to improve the signal.
- (e) Resolution and accuracy are improved as a laser beam is used alongside the IR beam to control the speed of the moving mirror and to time the collection of data points.

A computer-interfaced FTIR spectrometer operates in a single-beam mode, but the spectrum obtained is identical to that from a traditional double-beam dispersive instrument. A “background” spectrum subtraction method is employed. First, an interferogram of the “background” (which consists of the infrared-active atmospheric gases, CO₂ and water

vapour) is obtained and subjected to a Fourier transform which yields the spectrum of the background. Then, the spectra of both the compound and the background are obtained. The computer software automatically subtracts the spectrum of the background from the sample spectrum, yielding the spectrum of the compound being analysed. Commonly, a spectrum of a compound of interest is a plot of transmittance percentage (%) versus wave numbers (cm^{-1}).

2) X-Ray Diffraction (XRD)

XRD is a way to ascertain the arrangement of atoms inside a crystal which has been exposed to a beam of X-Rays. Once the beam strikes the crystal, the beam splits in various directions based on the constituents of the crystal. Based on the intensities and angles created by this splitting of the light beam, one can produce a 3-D picture of the density of electrons present in the crystal. This then aids in determining the position of the atoms in the crystals, the chemical bonds present in between them, the order in which they are arranged, and additional information regarding the interactions between the atoms in the crystal (Dutrow and Clark, 2013).

In XRD, a crystal is mounted on a goniometer and turned whilst being exposed to X-Rays. This exposure produces a diffraction pattern of regularly spaced spots known as reflections. These reflections are in actuality 2D pictures, which are then converted into 3D pictures using the mathematical formula of *Fourier Transform*, which is then added to known chemical data of the sample. There is a possibility of error occurring if the crystals are not uniform enough in their internal structure.

The main principles of XRD are based on some factors. The factors relevant to this thesis are:

- (a) Atomic Form Factors: This works on the concept of Bohr's atomic model. The electron density of the atoms will be associated with different distance vectors. These vectors are then in turn associated with variation in phase shifts. The smearing of the electron density exhibits a decrease of coherency and reduction in the scattered intensity. This then enables us to determine the phase shift of the crystal, hence reducing the number of possibilities.
- (b) Structure factor: Using the Bragg and Laue equations, it was found that there is only one atom per unit cell. The scattered intensity is then scaled with the square of the atom charge coupled with the interference function. The more complex a structure, the increase in the total charge distribution of the cell.
- (c) Multiplicity: this deals with the number of specific planes that may cause reflections at the same position.
- (d) Adsorption factor: This is where the X-Rays suffer from a reduction in their intensity, which is caused by their absorption.

The results are then compared with the JCPDMS database. This is a database for inorganic compounds, which is then used to identify and match the peaks of the obtained graph with one that exists in the database. In this experiment, the obtained peak was matched to the peaks of hydroxyapatite available in the database. A Scan speed of 7° per minute and a step scan of 0.02° were used for this experiment.

The non-sintered and sintered BHA powder was used, and a comparison was made and shown in the results. The HA powder was placed inside the Bruker AXS for XRD. Once the characterisation was done, the sintered BHA was sieved between 20-45 μm . This was done so as to ensure that the particle size of the HA was optimum for cell culture (Quia et al., 2006).

3.6 Composite Scaffold Characterisation

The scaffolds were characterized in two ways. This was both physical and chemical.

3.6.1 Chemical characterisation

Chemical characterisation was accomplished by using Fourier Transform Infra Red (FTIR) Spectroscopy in order to analyze the chemical bonds in between the polymers and hydroxyapatite scaffolds. All the produced scaffolds were analysed using a *Fourier Transform Infrared Spectroscopy (FTIR-ATR)* (Perkin Elmer Spectrum 400) powered by ATR technique. The spectra were collected at room temperature between 4000 and 400 cm^{-1} at a resolution of $\pm 2 \text{ cm}^{-1}$.

3.6.2 Physical characterisation

Physical characterisation, was accomplished by using 3-D Confocal Laser Microscopy (OLYMPUS: LEXT OLS4000) which was carried out on the scaffolds in order to determine the thickness and roughness profiles of the scaffolds. This also included observing the surface hydrophilicity as well as fibre diameter of the different scaffolds as explained below.

3.6.2.1 Scaffold roughness and thickness

Scaffold roughness was observed by obtaining two different readings from the same machine i.e the 3-D Confocal Laser Microscopy (OLYMPUS: LEXT OLS4000). The machine allows us to determine the thickness and roughness profiles of the scaffolds. The procedure for obtaining this result was basically to use a standard cut piece of the polymer to

be tested and then place it under the microscope's camera and set the software to scan the polymer's layers after which it constructs an image based on the different planes of the polymer which are determined by the contours of the polymer. The image also enables it to determine the roughness by analyzing the planes and categorizing the polymer with less contours, as smoother and with more contours, as rougher by measuring the length and depth of the contours.

3.6.2.2 Surface hydrophilicity

The scaffold surface hydrophilicity was assessed using the Contact Angle Analyser (DataPhysics OCA35 machine). This was done by placing the polymer under the camera lens of the DataPhysics OCA 35 machine (after making sure that the lens were set at a standard magnification for all the samples) and dropping water on the polymer. This is then subjected to a video recording by the system and analysed using the SCA20 software.

3.6.2.3 Fibre diameter

The diameter of the fibres were measured using the FESEM (FEI Quanta FEG 250). Basically, once the image was taken, it was exported into Adobe Photoshop and using the measurement tool, 100 points of the fibre diameter were identified, measured and the length noted. These values were then analysed and plotted in Microsoft Excel to obtain standard deviation values and a graph depicting surface roughness (Figure 4.5)

3.7 Stem Cells Characterisation

3.7.1 Bone Marrow Stem Cell characterisation

The isolated bone marrow stem cells were characterized in this experiment in four ways. The characterisation was carried out as previously described (Blanc and Rinde, 2007). The characteristics were identified as the ability to form fibroblastic colonies, adherence to plastic, tri-lineage differentiation capability (to Osteo, Adipo and Chondrogenic), expansion potential, MSCs stain negative by flow cytometry for haematopoietic markers; Cluster Differentiation marker 34, Cluster Differentiation marker 45 and Cluster Differentiation marker 14 and positive for Cluster Differentiation marker 73, Cluster Differentiation marker 90 and Cluster Differentiation marker 105. In addition the regeneration and maintenance of a tissue compartment, multipotency and staining positively for mesenchymal markers are the characteristics of mesenchymal stem cells. The experiments that were carried out for characterisation of the isolated stem cells are listed as below: -

3.7.1.1 Adherence to plastic with fibroblastic features

This was carried out by observing the attachment of the cells to the bottom of the T-75 flasks via phase contrast microscope (Nikon Eclipse TS100) as shown in Section 4.6.1 This was also used to observe the expansion potential and the fibroblastic colonies that were formed.

3.7.1.2 Multi lineage differentiation potential

BMSCs are able to differentiate into several specific mature cells under certain growth factors. Induction of BMSCs differentiation into osteoblast, adipocytes and chondrocytes

can prove the multipotent ability of BMSCs. At a minimum, it is advisable to differentiate the BMSCs into at least two lineages. StemPro® Chondrogenesis Kit (A1007101, Gibco) and StemPro® Osteogenesis Kit (A1007201, Gibco) were used to induce chondrogenesis and osteogenesis, respectively.

3.7.1.3 Chondrogenic differentiation:

BMSCs were isolated and expanded with primary medium. The BMSCs were then passaged when cultures reach 60 – 80% confluency. BMSCs of passage between 2 to 6 were used in the chondrogenesis assay. BMSCs were harvested and seeded in 6-well plates at a cell density of 100 viable cells/5 µl medium droplet for 20 droplets per well. BMSCs were then left to attach to the culture surface in a CO₂ incubator for 2 hours before adding with Chondrogenesis Differentiation Medium. To confirm chondrogenic differentiation, Safranin O staining was performed. In order to perform Safranin O staining, the medium was aspirated carefully from the well. The cells were then rinsed with distilled PBS. The cells were fixed by 10% Formalin for 5 – 10 minutes followed by rinsing with water. The fixed cells were put in 1.5% Safranin O for 40 minutes and followed by rinsing in distilled water for 3 times. The well was flooded with 0.02% alcoholic fast green for 30 seconds followed by 1% acetic acid 3 seconds. Then the well was rinsed quickly with distilled water. The well was then flooded with 95% ethanol for 1 minute. The cells were dehydrated in 2 changes of 100% ethanol with 1 minute each. The cells were then observed under an inverted microscope.

3.7.1.4 Osteogenic differentiation:

BMSCs were isolated and expanded with primary medium. The BMSCs were then passaged when cultures reach 60 – 80% confluency. BMSCs of passage between 2 to 6 were used for

this osteogenesis assay. BMSCs were harvested and seeded in 6-well plates at a cell density of 3×10^3 to 5×10^5 viable cells/cm². BMSCs were expanded in primary medium for 2 to 4 days (to near or complete confluency) before being changed with Osteogenesis Differentiation Medium.

Alizarin Red S staining was performed on BMSCs after the cells were incubated with Osteogenesis Differentiation Medium for 21 days. Alizarin Red S Solution was prepared by dissolving 2g Alizarin Red S powder in 100 ml distilled water. The medium was aspirated carefully from the well containing the cells exposed to the osteogenic differentiation medium. The cells were then fixed by incubating in ice cold 70% ethanol for 1 hour at room temperature. The alcohol was aspirated carefully and rinsed twice (5 – 10 minutes each) with water. The water was then aspirated and excess Alizarin Red Solution was added to cover the wells. The well plate was incubated at room temperature for 30 minutes. After 30 minutes, Alizarin Red Solution was removed and the wells were washed for 4 times with 1 ml water and aspirated after each wash. One to one and a half millilitre water was added to each well to prevent the cells from dying. The cells were then observed under an inverted microscope (NIKON TS 100) at non-fluorescent lighting conditions i.e normal white light.

3.7.1.5 Immunofluorescence staining for Mesenchymal markers

Mesenchymal markers are used to identify various antibodies that indicate the presence of various cells, for eg. the mesenchymal markers vimentin, Twist, Snail, Slug and Sip1 are used to detect tumour cells in breast cancer patients (Kallergi et al., 2011). The markers CD44, CD105/endoglin, CD106/VCAM-1, collagen-IV, fibronectin, actin and DAPI nuclear staining can be detected by immunofluorescence staining and are used either collectively or individually to positively identify mesenchymal stem cells, the number used is dependent on

the additional tests (eg. Flow Cytometry marker identification) being carried out (Schieker et al., 2007).

This was done following the procedure outlined in the lab manual prepared by Holmberg et al., from the Morimoto Laboratory, Northwestern University (Jolly C. et al., 1997 and Kim et al., 2002). The fixation solution (was made fresh in the hood). This was made by adding 4.3 ml (4%) of 37% Formaldehyde (*Acros Organics*) to 35.7 ml of 1X PBS (*Gibco*). To this was then added 40 ml of 0.1 M Tris (*Acros Organics*). The detergent solution was made by adding 0.75 g (0.5%) of Saponin (*Sigma*) to 0.75 ml (0.5%) Triton X-100 (*Fisher Scientific*). Later, they were added to 150 ml of 1X PBS. The blocking solution was made by adding 1 ml of FBS (*Gibco*) (10%), 0.03 ml of Triton X-100 (0.3%) and 8.97 ml of 1X PBS together. Washing solution was made by adding 6 ml of FBS (2%), 0.90 ml of Triton X-100 (0.3%) and 293 ml of 1X PBS together. A few drops of mounting (Antifade) Solution which is also known as D.P.X. Mountant (*R&M Chemicals*) was also used.

After preparation of the solutions, 0.5 to 1.0 ml of cell suspension/well was added into the 4-well chamber slides (*Nunc*) for 24 hours. The wells were then covered with a lid and incubated for 24 hours. The chamber slides were retrieved and the culture medium was then pipetted out. The plastic well and the rubber linings were removed, by using a given separator and forceps. The slides were then washed with 1X PBS in a coplin jar at room temperature for less than 3 minutes. The 1X PBS was removed and 40 ml of fixation solution was then added in the hood. They were then incubated at room temperature for 10 minutes. A clean coplin jar was then added with 0.1 M Tris. The slides were then transferred to the 0.1 M Tris and incubate at room temperature for 5 minutes.¹

¹ Slides can be stored in 1X PBS/0.01% NaN₃ after this step.

The 0.1 M Tris was then removed and washed with 1X PBS for 3 minutes. The same goes to the 1X PBS and then the slides were washed 3 x 5 minutes in a detergent solution at room temperature. The samples were then placed in a clean coplin jar with 1X PBS. The slides were transferred to the 1X PBS and wash for 3 minutes. They were then removed from 1X PBS and 200 µl/slide of blocking solution was added. It was then covered with 22 x 60 mm cover glass, and incubated at 37 °C for 45 minutes to 1 hour. The primary antibody was then diluted with the washing solution, and stored on ice or at 4 °C. The cover glass was removed and 15 µl of the diluted primary antibody was added to each well. The slides had new cover glass placed over them, and were then incubated at 37 °C for 1 to 1.5 hours. The washing solution was pre-warmed and placed inside a clean coplin jar in a 45 °C water bath. The cover glass was removed and washed for 3 x 5 minutes in 45 °C washing solution at room temperature. The secondary antibody was then diluted with the washing solution.

Each well was then exposed to 15 µl of the diluted secondary antibody. The well was then covered with a new cover glass, and incubated at 37 °C for 1 hour. The slides were then placed in a coplin jar with aluminium foil to protect them from light as the antibodies are light sensitive. The cover glass was then removed and washed three times for 5 minutes, each time, in 45 °C washing solution at room temperature in the covered jar. Then DAPI staining is carried out by adding 15 µl of DAPI (1 µg/ml in 1X PBS), covered with a new cover glass and incubated at room temperature for 2 minutes. Then, the DAPI stained slides were washed twice for 3 minutes each with 1X PBS. Shake off the excess liquid from the slides. 5 µl of mounting solution is then added to each well, which is then covered with a cover glass and sealed with nail polish. The samples were then stored in a slide container at 4 °C prior to viewing under the Nikon TS 100 inverted microscope. The Nikon Eclipse TS100 is an inverted microscope with different filters used in the imaging process. The filters that were used were the NCB11, ND8 and GIF (green interference).

3.7.1.6 Cluster Differentiation (CD) markers.

Mouse anti rat antibodies with their fluorescent probes Cluster Differentiation 31-PE, Cluster differentiation 45-FITC, and Cluster differentiation 90-PerCP respectively were used. If these cells were BMSCs, they would yield negative for Cluster Differentiation 31 and Cluster Differentiation 45 and would be positive for the Cluster Differentiation 90 marker.

The samples (newly isolated cells, P1) were incubated (5% CO₂, 37 °C). The cells were trypsinised at >80% confluence. They were then neutralized with 5 mL medium and the samples were filtered by using a cell strainer of mesh size 70 microns followed by 40 microns. The filtered samples were then centrifuged for 5 minutes at 1000 RPM and the pellet was then resuspended with enough 1X PBS to adjust to the final concentration of approximately 10 million cells/mL, of which 4 ml was used in this experiment. One sample was prepared with all 3-colour combos and another three control samples that has a single colour each as described below.

Staining (Direct² and Live³ Method)

² direct staining does not involve secondary antibodies.

³ live method is employed, therefore fixation and permeabilization steps are omitted as they are only for intracellular staining.

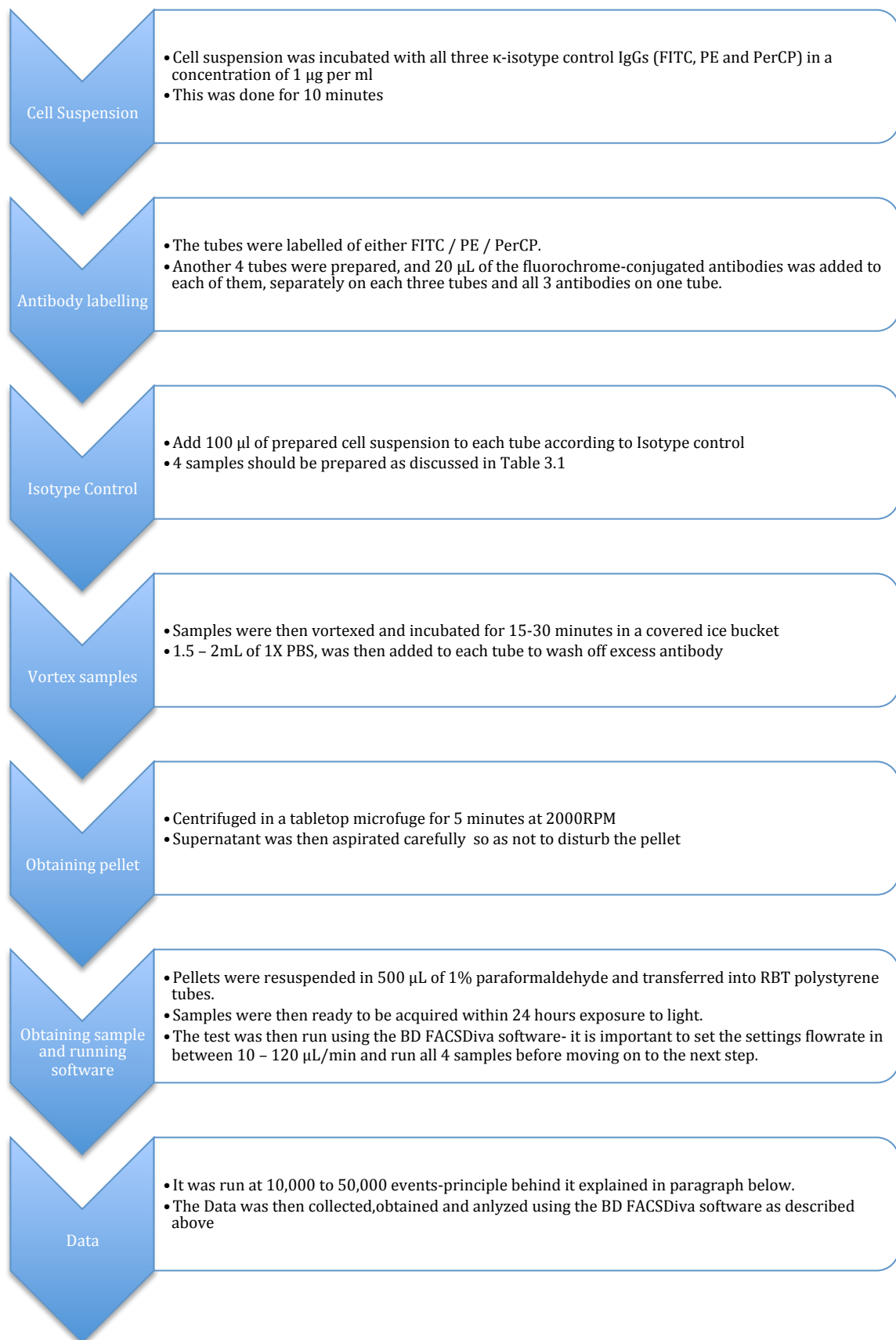


Figure 3.8: Flowchart depicting a 3 colour combo sample preparation.

Table 3.1: Sample distribution for Flow Cytometry

| Sample | Isotype Control | Fluorochrome-Conjugated Antibodies |
|---------------|------------------------|---|
| Test Sample | FITC + PE + PerCP | FITC + PE + PerCP |
| FITC Control | FITC | FITC |
| PE Control | PE | PE |
| PerCP Control | PerCP | PerCP |

The BD FACS Canto II works on the principle of a fluidic system. In the fluidics system, the sample travels up the sample injection tube, and hydrodynamic focusing within the flow cell forces particles into a single-file stream where laser light intercepts the stream at the sample interrogation point. This design permits particles to flow through the centre of the flow cell and by doing so, read the different events present and then characterise them based on the tandem dye conjugates.

3.7.1.7 Data analysis

The BD FACS Diva software then collected the data related to voltage output. The voltage output was, in turn, translated in either its height or area to obtain the cell distribution, not width. This distribution can be viewed in all four samples or separately. The software can also isolate and observe dual population relationships, according to the need. The study acquired the dot plot data of side scatter vs. forward scatter for all four samples. This shows the distribution of cells according to the complexity vs. size (The steps are all in Uppercase, followed by the explanation of the steps). GATING: From the dot plot, the study drew a box

to gate the region of interest, excluding cell debris and any unwanted distribution. In case of BMSC, the cells may range from 10 to 40 microns. This was done for all 4 samples. SCALING: Next, at Cell count vs. Fluorescent histogram; the curve was fixed to log scale to get a proper fit of both the negative and positive population. COMPENSATION: Using the data from the single colour controls, two colour dot plots of each colour combination were drawn and the following pairs compensated:

- i) FITC-%PE ii) PE-%FITC iii) PerCP-%FITC
- iv) FITC-%PerCP v) PE-%PerCP vi) PerCP-%PE

The data plot was set on bioexponential scaling before compensating, in case of a value that may pile up on the axis and lead to error.

After compensation, a Side scatter vs Forward scatter plot of CD90 was selected. Following this, the gate was set to the 10 to 40 micron region and a log scale histogram created from it. This reveals any positive and negative peaks of CD90 (Since it is hypothesized that CD90 is positive, there should not be any peak on the negative side). To look at CD45 and CD31 antigens within CD90 positive, the CD90 positive peak was gated, and a dot plot of CD45 x CD 31 was created from it. The CD45 x CD31 dot plot was divided into 4 distinct quadrants such as in Figure 3.9. These quadrants translate as follows:

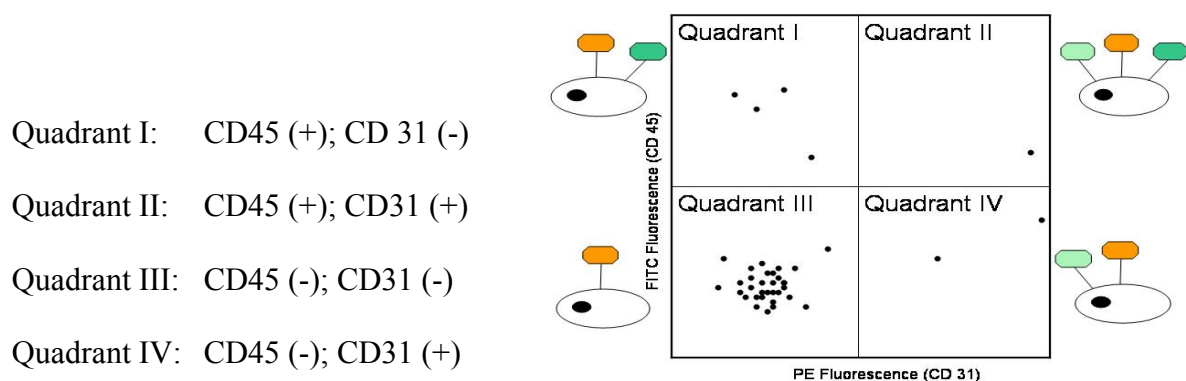


Figure 3.9: Expected result of the 3-colour based experiment of BMSC

3.8 Cell and Scaffold Interactions

FESEM was carried out on the scaffolds pre and post seeding. Post seeding, the time points were Day 1, 7 and 14. Since the FESEM used was the FEI Quanta FEG 250, no sample preparation was required as the samples were observed in a low vacuum.

The FESEM images were used to:

- 1) Observe and measure Fibre diameter. This measurement was done at 100 points on the image and the measurements were then processed in MS Excel.
- 2) Calculate the porosity using the Image J software
- 3) Observe cell attachment and morphology to the scaffolds on various days.

3.9 Biochemical Assays

There were three main biochemical assays carried out on the scaffolds, they were all quantitative and were measurements of the proliferation of the cells as well as the type of cells that were proliferating. The three tests were: -

- 1) Resazurin (also known as Alamar Blue) cell proliferation assay. Used to measure the metabolic activity of cells.
- 2) Alkaline Phosphatase (ALP) Assay, this assay is a measurement of the amount of alkaline phosphatase enzyme produced, which is an indicator of the amount of osteoblastic activity present in the cells
- 3) Deoxyribonucleic Acid (DNA) Assay, this assay measures the amount of DNA present in the cells, and aids in giving a general idea of the number of cells (both live and dead).

3.10 Cell Proliferation Assay

The resazurin test was carried out by initially creating a resazurin solution. This was done by using resazurin powder obtained from Sigma Aldrich, which was reconstituted by adding 14 mg of Resazurin into 100 ml of culture medium DMEM-LG without Phenol Red: SIGMA-D9521. This was done following the manufacturer's instructions. All the samples and controls (24-well plate) were then washed gently three times with pre-warmed PBS prior to the Resazurin test. After the washing, 500 μ l of medium (without Phenol Red) was added to each well. 50 μ L of Resazurin solution (14 mg/100 ml phenol red-free medium) was added subsequently. The well plate was incubated for 4 hours. 10 minutes before the incubation time ended, the plates were covered with aluminium foil and placed onto the plate shaker and shook gently for 10 minutes. After shaking, the plate was transferred into the laminar flow hood. 100 μ L from each well (24-well plate) was transferred to a 96-well plate in triplicates while still lights were off.

- 1) The absorbance was measured at 690 nm and 600 nm using a FLUOstar OPTIMA BMG LABTECH micro-plate reader.
- 2) The absorbance reading was then taken to be the metabolic activity of the cells (Fidalgo et al, 2010).

3.11 Protein and DNA Extraction

In order to obtain the protein and DNA from the cells to measure Alkaline Phosphatase Activity, the method previously described was followed (Zhao. et al., 2009). Briefly, the seeded scaffolds were washed twice in PBS after the Resazurin assay and placed inside 1.5 ml micro-centrifuge tubes and frozen at -80 °C until the samples were processed further. The samples were then subjected to physical force and were frozen and thawed 3 times. The

thawed samples were then sonicated on ice and centrifuged at 12,000 RPM for 10 minutes. The supernatant obtained was then used to carry out protein and DNA testing.

3.12 Alkaline Phosphatase (ALP) Assay Measurement

Alkaline Phosphatase is determined by measuring the rate of hydrolysis of various phosphate esters under specific conditions. One of these esters is Nitrophenyl Phosphate (pNPP) and was introduced as a substrate by Fujita in 1939. Following that, Bowers and McComb reported an endpoint procedure in 1946. In 1974, the Committee on Enzymes of the Scandinavian Society of Clinical Chemistry and Clinical Physiology adopted a modification of the procedure as the recommended procedure. The method that has been followed in this thesis is based on the above mentioned methods with some addition by the methods followed by Wilkinson et al., 1969.

50 µl of the supernatant obtained was then added to 200 µl of pNPP solution (SIGMA ALDRICH: N1591) in a 96-well plate (TPP Corporation). This was then incubated at room temperature for 30 minutes. The reaction was then stopped by adding 50 µl of 3 M sodium hydroxide (NaOH) to the solution. The solution was then read at 405 nm absorbance. All absorbance readings were carried out using a BMG Labtech FluoStar Optima. The absorbance reading that were obtained were then processed using the following formula (this was done in order to change the absorbance to International Units)

$$(IU/L) = \frac{Abs./Min \times 1000 \times 0.3}{18.75 \times 1 \times 0.050} = Abs./min \times 2187$$

Where Abs./min = Average absorbance change per minute (in this experiment, the samples were incubated for 30 minutes)

1000 = Conversion of IU/ml to IU/L, 0.30 = Total reaction volume (ml), 18.75 = Millimolar absorbivity of Nitrophenol, 0.050 = Sample Volume (ml), 1 = Light Path in cm.

3.13 DNA Assay Measurement

In order to measure the DNA assay, first a DNA Standard solution has to be prepared. This is done by using calf thymus DNA (D1501) obtained from Sigma Aldrich. The DNA standard solution is then prepared by dissolving 50mg of calf thymus DNA overnight at 0-4 ° C in 50 ml sterile PBS without sonication or stirring. In order to test for the purity of the DNA, the Optical Density was read in the ratio of OD₂₆₀/OD₂₈₀. This was done in order to make sure that the DNA is fully dissolved (the OD ratio should be above 1.8). OD₂₆₀ is caused by constituents of DNA and OD₂₈₀ is caused by contamination of DNA. The DNA strands were then pipetted around 40 times with a sterile glass Pasteur Pipette to shear the DNA, which was then filtered through a 0.45 um syringe filter. The precise DNA concentration by the OD₂₆₀ reading was determined from a 1:20 dilution (a 50 ug/ml solution has an OD₂₆₀ reading of 1.00). The aliquots were then stored at 4 °C.

DNA measurement for samples was done by adding 2 mg Hoescht 33258, which was added into each ml of dH₂O to make Hoescht stock solution, which was stored in 4 °C in a light tight bottle. Prior to use, the stock solution was diluted 10000x to 0.1 µg/ml in TEN buffer. Serial dilutions were made of the DNA standard at 25, 12.5, 6.25, 3.125, 1.5625 and 0.78125 µg/ml. The original concentration was 50 µg/ml in 100 µl diluted in PBE. In a 96-well plate, 10 µl PBE was added as a blank and a triplicate was made of this. The samples were added in the remaining wells. 200 µl of working solution was then added to each well prior to reading. The reading was done using fluorescence at 355 nm excitation, and 460 nm emission using a BMG Labtech FluoStar Optima, which automatically calibrates the readings to the prepared standard.

3.14 Statistical Analysis

Using SPSS ver.18, a normal distribution of amount of Resazurin, ALP and DNA was verified by Skewness and Kurtosis methods (sample is normal if value of Skewness and Kurtosis is in the range of -1.96 to +1.96). When results from different runs for the static or a certain frequency of stimulation show normal distribution, the amount of Resazurin, ALP and DNA can be averaged to give a representative value for each of the frequencies tested, as for the static controls.

A test of significance for the difference in the results between each group of samples can be done if each sample group is normally distributed. A one-way analysis of variance (ANOVA) was used to compare the groups. A value of $p < 0.05$ was used to indicate statistical significance (Johnson, 2010).

CHAPTER 4: RESULTS

CHAPTER 4: RESULTS

4.1 Introduction

In this chapter, the results obtained are reviewed in a comprehensive manner. At certain points, the figures and tables will be elaborated together with the analysis below the figures and results. Briefly, the results of the characterisation will be seen, and these will form a prelude to the cellular assays and the biochemical tests, which should give us an idea of the relationship between the materials investigated and their effects on cellular growth.

4.2 Bovine Hydroxyapatite (BHA) Characterisation

4.2.1 X-Ray diffraction of BHA

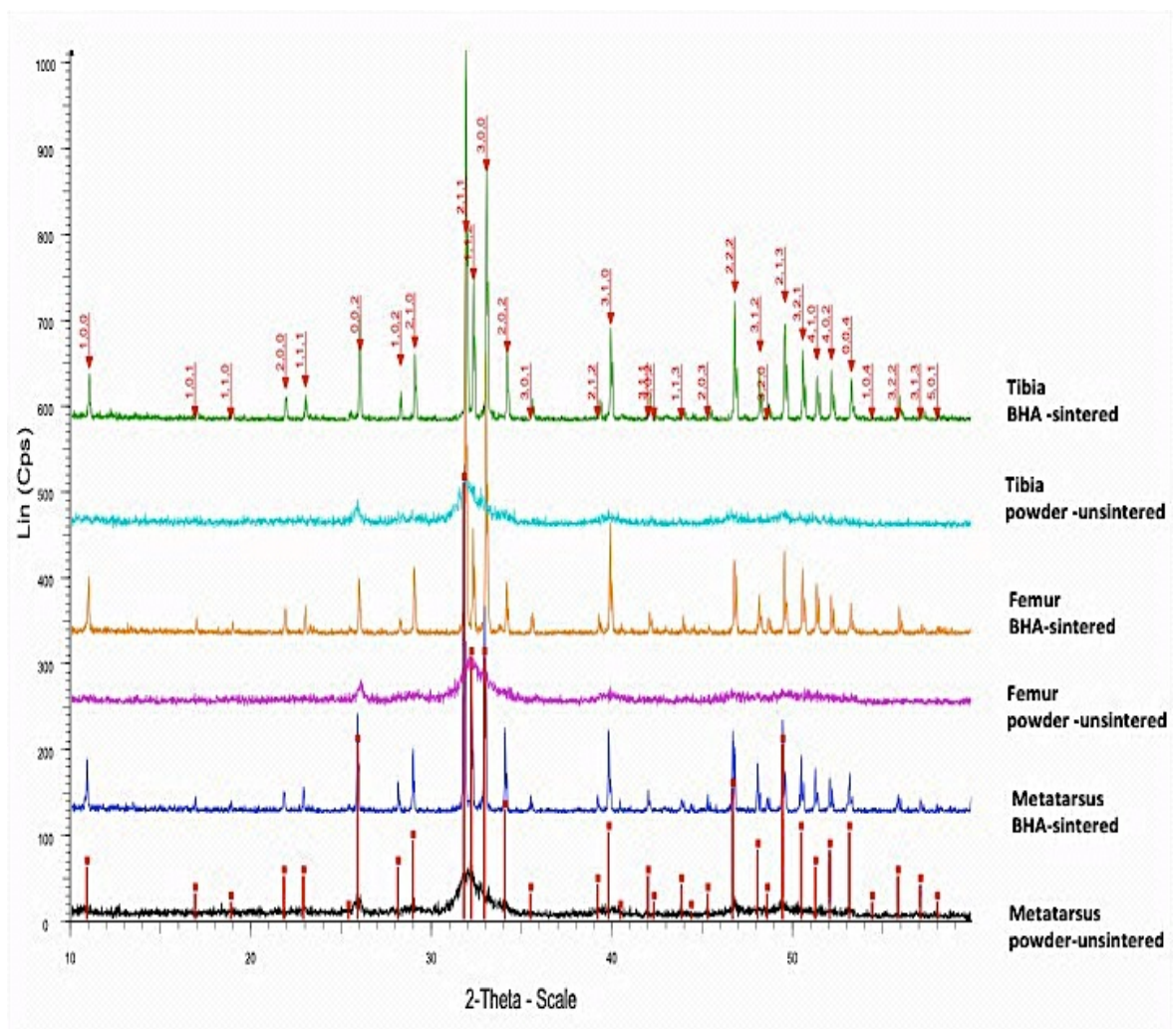


Figure 4.1: XRD profile of BHA (pre and post sintering)

The above figure shows the difference in the sintered and non-sintered XRD profiles from the three parts of the bones. As can be observed from the above figure, the XRD profile for sintered bone powder (i.e. Hydroxyapatite) is the same irrespective of the part of the bone from which it originates. Further, it was noted that in stark contrast to the unsintered bone powder, it shows the presence of many organic substances. In the sintered profile only the inorganic profile of Hydroxyapatite can be seen, hence showing that the sintering gets rid of any other possible compounds which may have affected the cellular assays. All the peaks for the sintered HA are consistent with those of 211, 300 and 202, hence showing the XRD result is consistent with the peaks required for HA.

4.2.2 Fourier-Transform Infra Red Spectroscopy of BHA

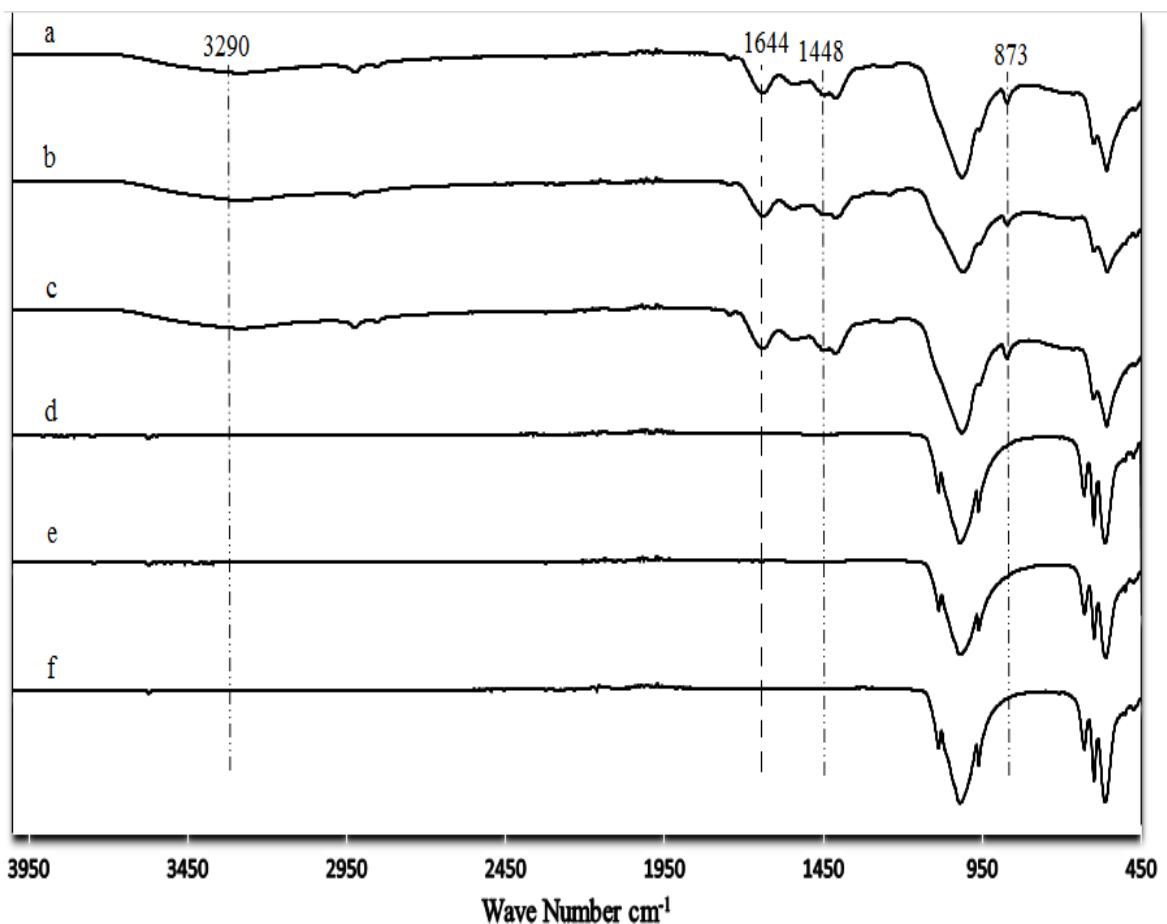


Figure 4.2: FTIR spectra for BHA. The figure shows the pre-sintered and post-sintered peaks of bone powder and BHA isolated from femur, tibia and metatarsus. a) Tibia pre-sintered, b) Metatarsus pre-sintered, c) Femur pre-sintered, d) Tibia post-sintered, e) Metatarsus post-sintered, f) Femur post-sintered

FTIR was carried out to enable us to compare the pre and post sintered BHA powder to observe the structural evolution of the BHA powder. It was also essential to couple it together with the XRD reading to ensure that the BHA produced has the same characteristic peaks of the standard HA. The FTIR was important in determining that all the BHA obtained was the same irrespective of which part of the bone it came from.

4.3 Composite Scaffold Characterisation

4.3.1 Fourier-Transform Infra-Red (FTIR) spectroscopy of composite scaffolds

FTIR for the composite scaffolds was carried out to ensure that the amount of BHA added to the polymer was consistent with the solution blend, as the BHA had a tendency to settle to the bottom of the syringe while electrospinning. It was noted that the increase of HA percentage was in tandem with the increase of HA added. Figure 4.13 shows that the relationship between the increase of BHA powder and the increase in the phosphate group is directly proportional.

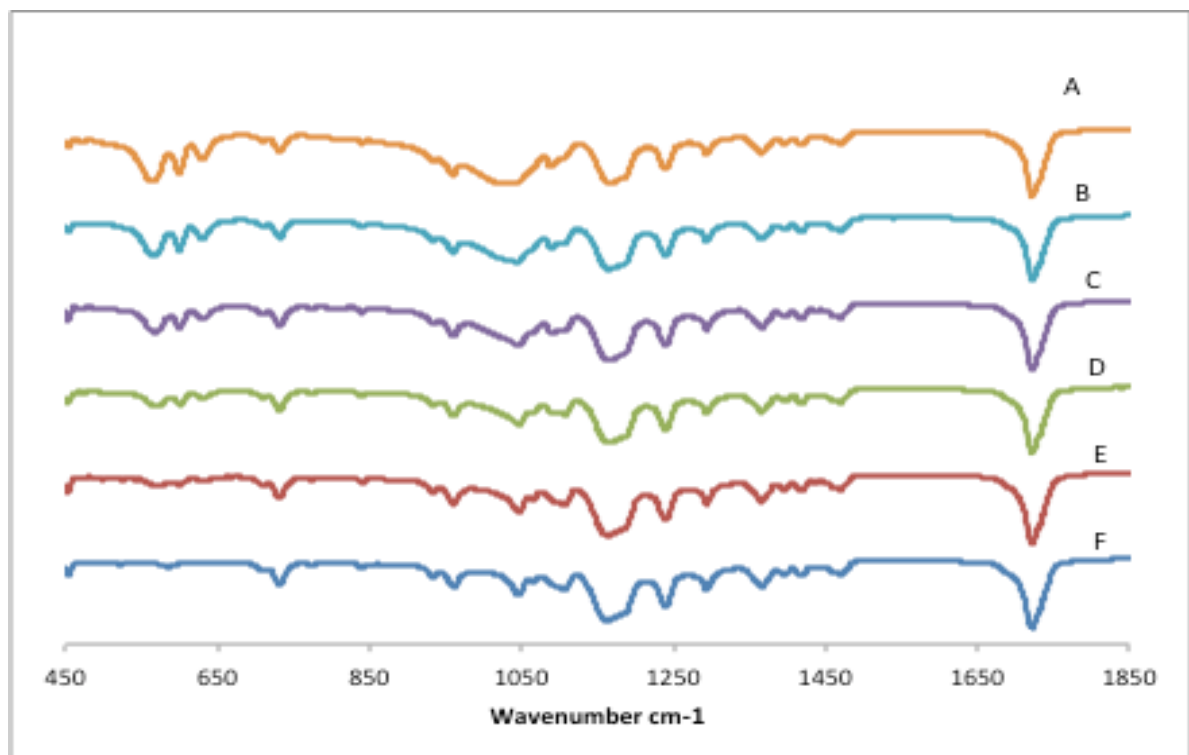


Figure 4.3: FTIR spectra of PCLHA composite scaffolds. A) PCLHA50%, B) PCLHA40%, C) PCLHA30%, D) PCLHA20%, E) PCLHA10% and F) PCL.

4.3.2 Electrospun scaffold profile

4.3.2.1 3-D Confocal roughness profile of electrospun scaffolds

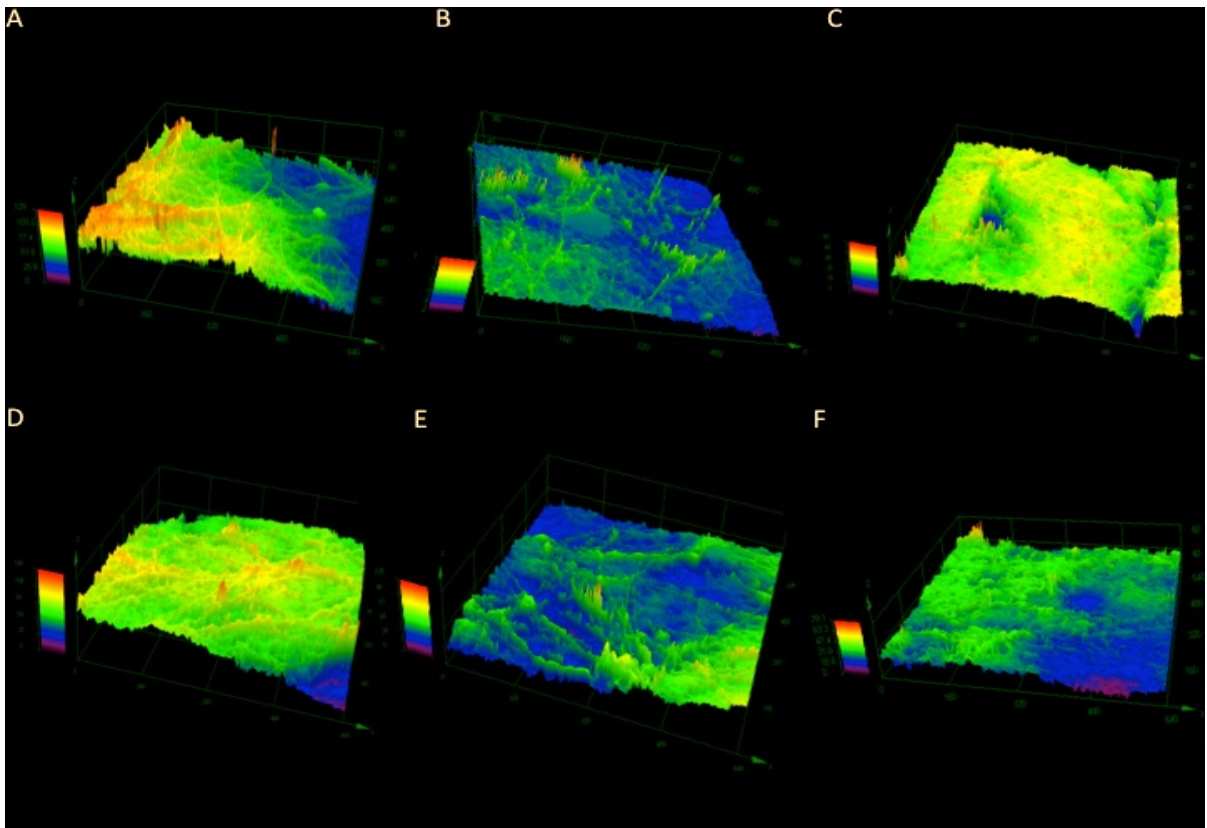


Figure 4.4: 3-D Confocal images of scaffolds. A) PCL, B) PCLHA10%, C) PCLHA20%, D) PCLHA30%, E) PCLHA40% and F) PCLHA50%.

The above figure shows a distribution of the surface roughness of the various scaffolds, showing that the addition of HA in respect to the roughness ratio is highest in PCLHA30%. This result was slightly unexpected, as logically it was expected that PCLHA50% would possess the highest roughness value.

There are a few reasons why this may have occurred; the HA distribution in the scaffold was uneven, a problem faced due to the micron size of the HA, which was difficult to electrospin as the concentration of HA became higher; and, there were more HA particles, which made the electrospun fibres heavier and harder to have an even distribution of HA. This was

manifested by the consistent clogging up of the syringe used in the electrospinning set up and in the uneven texture that was noted in the electrospun scaffolds.

The roughness profile was conducted on a section of the electrospun scaffold. This has been one of the limitations of using this machine as the roughness profile is calculated only on one section of the scaffold as opposed to the whole electrospun sheet.

4.3.2.2 Roughness profile of scaffolds

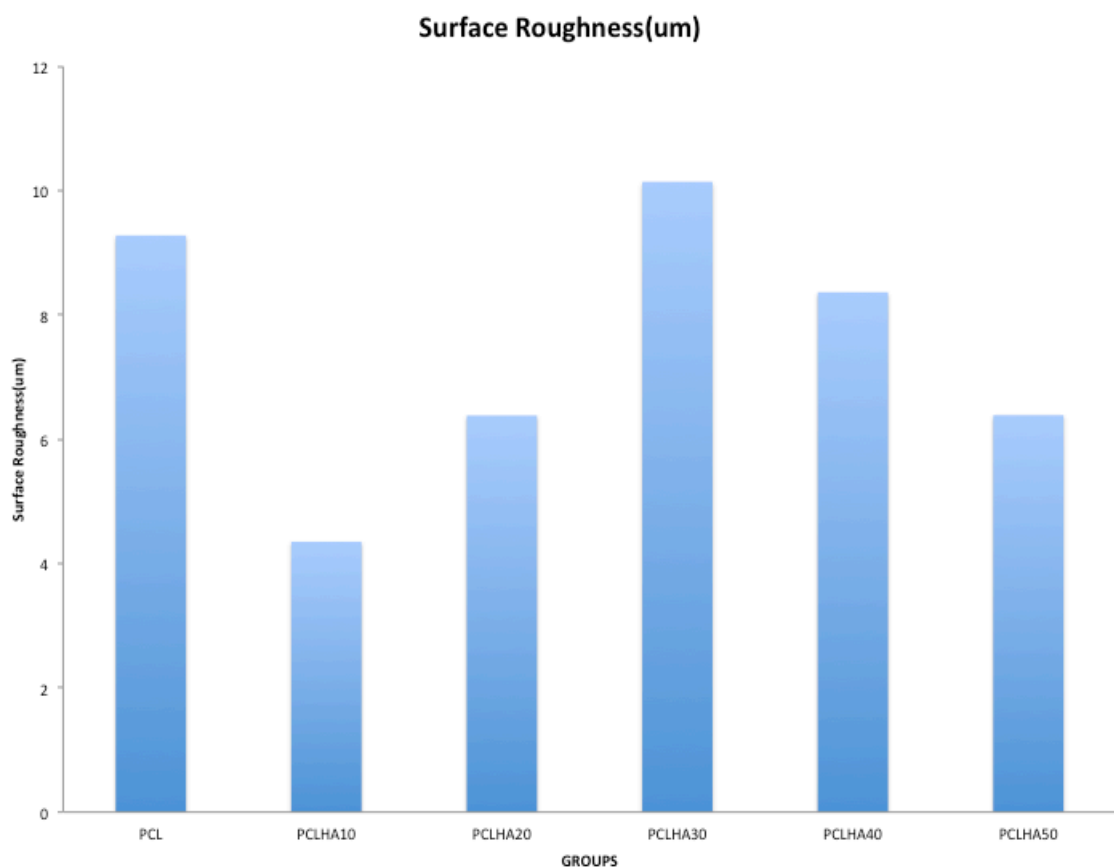


Figure 4.5: Roughness profile of scaffolds

The above graph compliments Figure 4.4 and confirms that the scaffold with the most roughness is PCLHA30%, followed by PCL, then PCLHA40%, PCLHA50%, PCLHA20% and then PCLHA10%.

4.3.2.3 Surface hydrophilicity

The graph below shows the contact angle measurements demonstrating a steady decline in the contact angle along with an increase in the BHA concentrations, exhibiting an inversely proportional relationship between BHA concentration and contact angle. The contact angle is important as it exhibits the extent of hydrophobicity or hydrophilicity of a material. As can be seen in the graph (Figure 4.6) plotted below, the contact angle is the lowest for PCLHA50% which means that it is the most hydrophilic and should be amongst the better scaffolds for cell proliferation. The most hydrophobic is the PCL scaffold, which according to these results should have the least cell growth. This information is additionally displayed in Table 4.1.

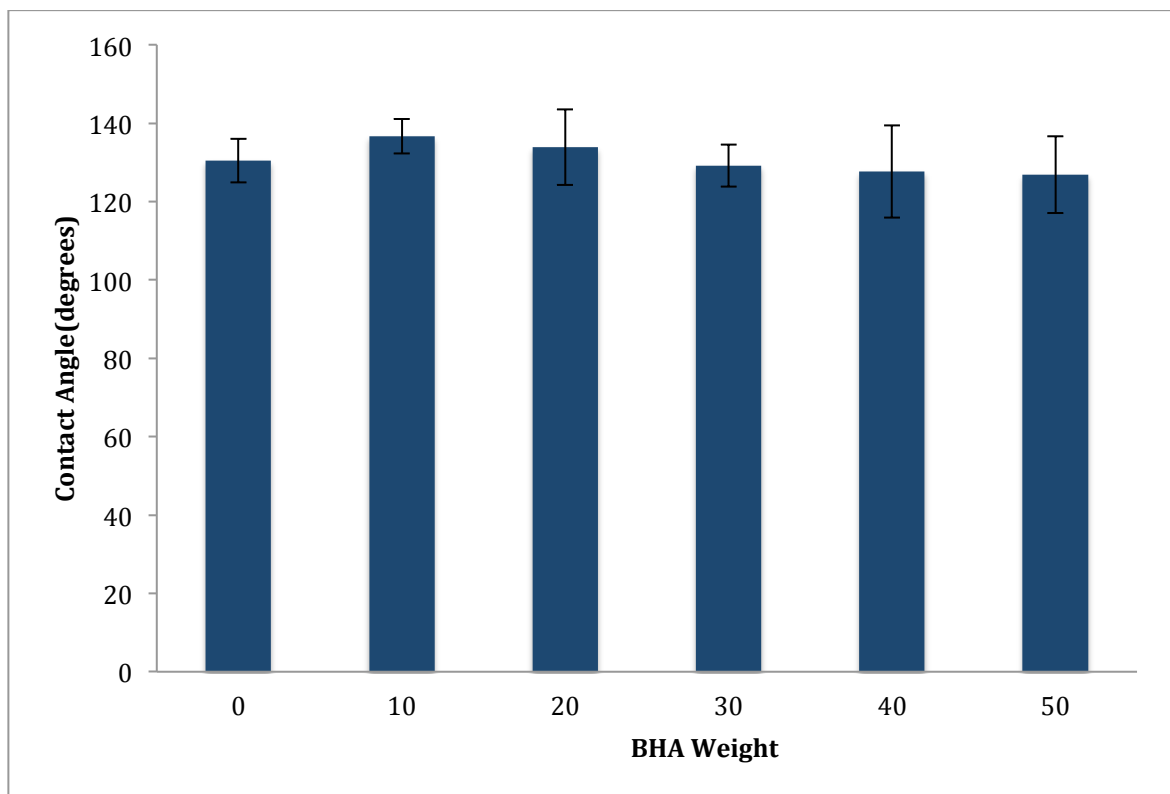


Figure 4.6: Contact angle measurements of scaffolds with different BHA concentrations.

Table 4.1: Contact angle and surface roughness measurements of scaffolds.


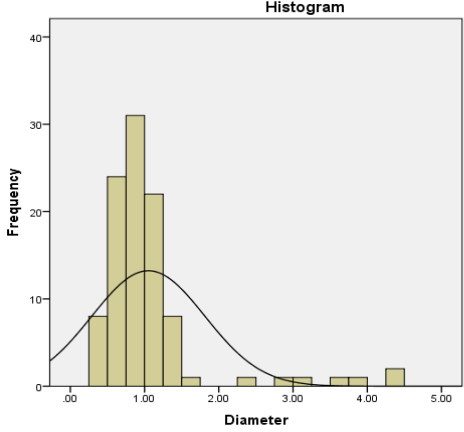

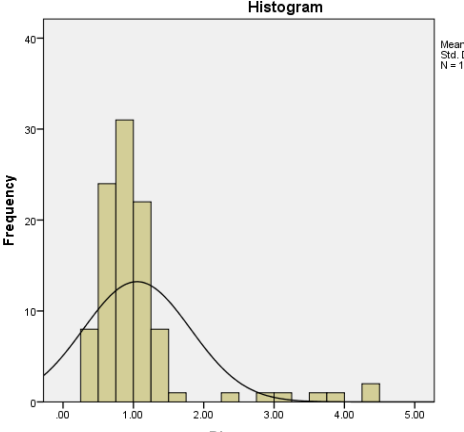

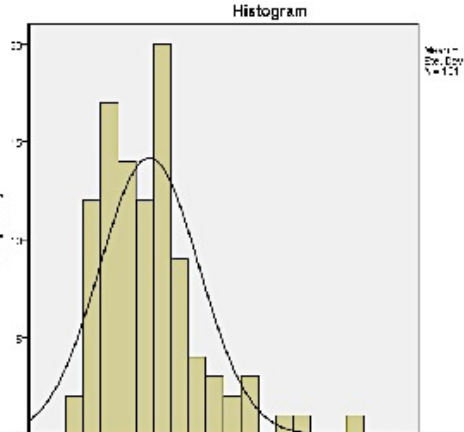
| Sample | Contact Angle | Standard Deviation | Surface Roughness (μm) |
|---------------|----------------------|---------------------------|---|
| PCL | 130.40 | ± 5.54 | 9.28 |
| PCL - HA 10% | 136.66 | ± 4.37 | 4.35 |
| PCL- HA 20% | 133.85 | ± 9.60 | 6.38 |
| PCL - HA 30% | 129.18 | ± 5.36 | 10.14 |
| PCL - HA 40% | 127.66 | ± 11.79 | 8.36 |
| PCL - HA 50% | 126.87 | ± 9.79 | 6.39 |

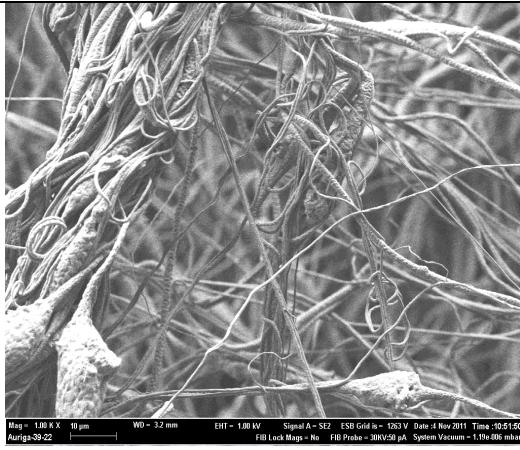
4.3.2.4 Fibre diameter

The FESEM images were taken in order to study the morphology of the scaffold prior to seeding as well as to determine the diameter of the fibres both with and without HA, as well as with the different concentrations of HA. This was essential as whether the cells would be able to seed on the fibres needed to be ascertained or if they would “slip through” the fibres and not be seeded properly.

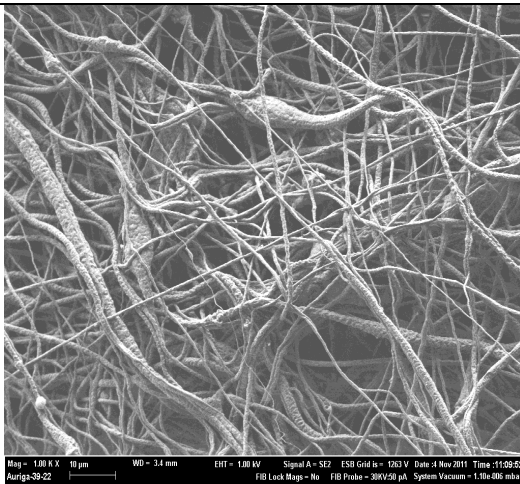
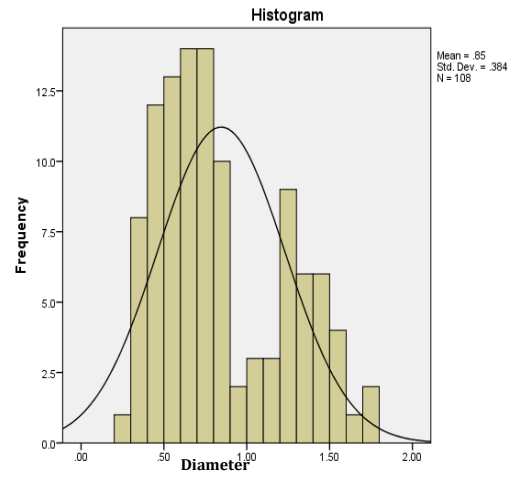
As observed in Table 4.2 the fibres are distributed in an uneven fashion, however in the process, they created different layers, which act as a 3D layer of sorts. There is plenty of gap and support for the cells to attach themselves to and create layers. The fibre diameter is essential as it enables us to observe the difference in fibre thickness across the different HA percentages added. It is a mechanism to test the distribution of the HA, as can be observed, the distribution of HA and fibre diameter appears to be standard.

Table 4.2: Fibre thickness graph. All FESEM images were taken at 1000x magnification. The average diameter distribution is shown on the right of the individual image.

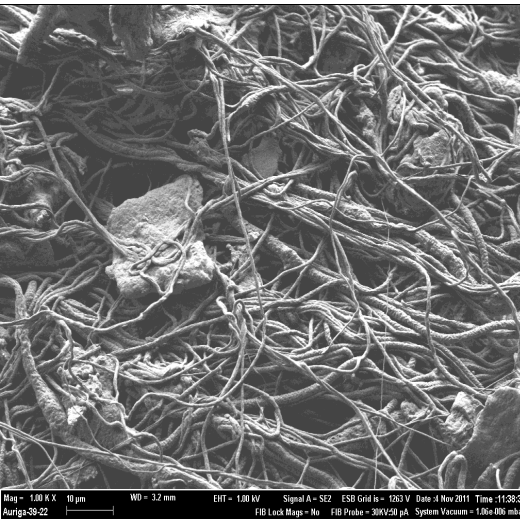
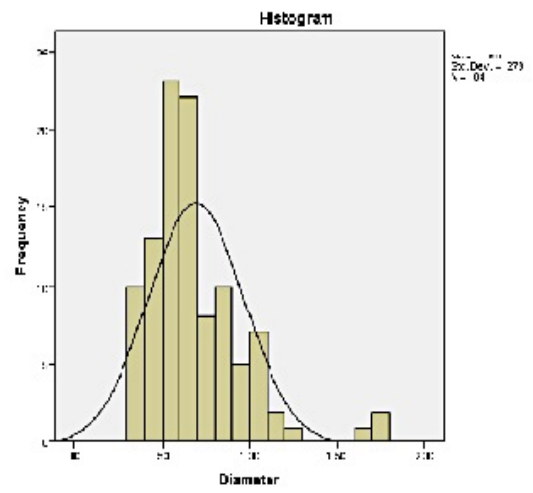
| Scaffold | Fibre Thickness Graph |
|--|---|
|  <p data-bbox="264 757 798 784">Mag = 1.00 K X 10 µm WD = 3.6 mm EHT = 1.00 kV Signal A = SE2 ESB Grid is = 1263 V Date = 1 Nov 2011 Time = 10:07:52 Auriga-39-22 FIB Lock Magn = No FIB Probe = 30KV50 pA System Vacuum = 3.02e-006 mbar</p> <p data-bbox="501 819 564 851" style="text-align: center;">PCL</p> |  <p data-bbox="1114 389 1203 407" style="text-align: center;">Histogram</p> <p data-bbox="1318 425 1404 459">Mean = 1.05 Std. Dev. = .762 N = 101</p> |
|  <p data-bbox="264 1276 798 1303">Mag = 1.00 K X 10 µm WD = 3.0 mm EHT = 1.00 kV Signal A = SE2 ESB Grid is = 1263 V Date = 1 Nov 2011 Time = 10:17:40 Auriga-39-22 FIB Lock Magn = No FIB Probe = 30KV50 pA System Vacuum = 1.06e-006 mbar</p> <p data-bbox="450 1361 619 1393" style="text-align: center;">PCLHA10%</p> |  <p data-bbox="1114 909 1203 927" style="text-align: center;">Histogram</p> <p data-bbox="1318 945 1404 978">Mean = 1.05 Std. Dev. = .762 N = 101</p> |
|  <p data-bbox="264 1814 798 1841">Mag = 1.00 K X 10 µm WD = 3.0 mm EHT = 1.00 kV Signal A = SE2 ESB Grid is = 1263 V Date = 1 Nov 2011 Time = 10:34:32 Auriga-39-22 FIB Lock Magn = No FIB Probe = 30KV50 pA System Vacuum = 3.36e-006 mbar</p> <p data-bbox="450 1921 619 1953" style="text-align: center;">PCLHA20%</p> |  <p data-bbox="1114 1447 1203 1464" style="text-align: center;">Histogram</p> <p data-bbox="1318 1482 1404 1516">Mean = 1.27 Std. Dev. = .355 N = 101</p> |



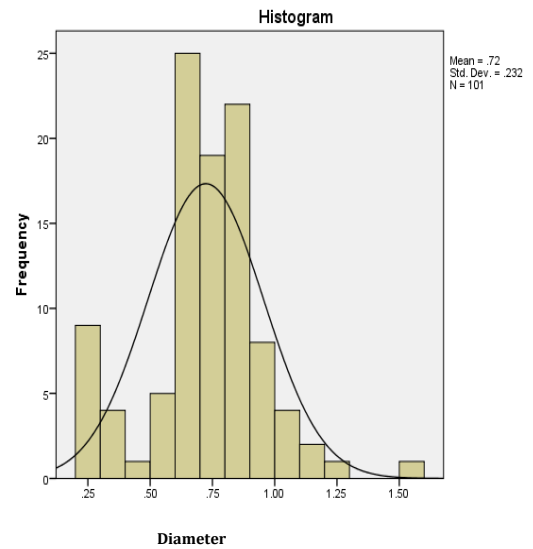
PCLHA30%



PCLHA40%



PCLHA50%



4.4 Stem Cells Characterisation

4.4.1 Adherence to plastic with fibroblastic features

This was done to observe the fibroblastic colony formation during the attachment of the cells to plastic as well as expansion potential of the cells. The bone marrow cells are growing and forming wave like structures showing the fibroblastic nature of the cells as seen in Figure 4.7. MSCs are very similar to fibroblasts in their features, and so form similar colonies of cells, especially on a 2D plane.

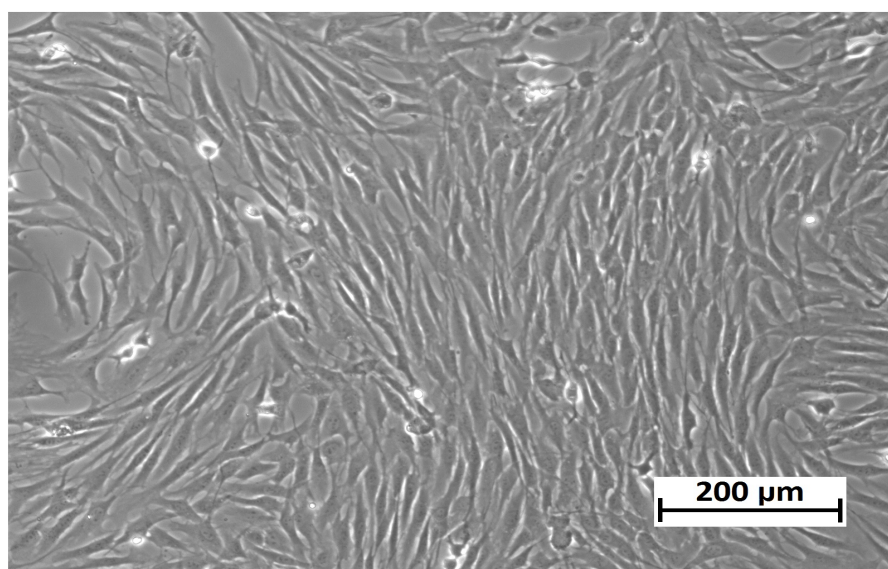


Figure 4.7: Cells attached on plastic (T-75 flask) - scale bar 200 μm

4.4.2 Multilineage differentiation of potential

4.4.2.1 Chondrogenic differentiation

The cells were induced to differentiate into chondrocytes as indicated in Figure 4.8, although the staining was not as clear as the Alizarin stain. The cartilage was stained by Safranin O, producing a yellow-orange colour which is considered stained very mildly as true cartilage would be stained in an orange-red colour. The cytoplasm was stained bluish

green by fast green dye. However, chondrogenesis was proven by production of cartilage, which can be observed in the image below.

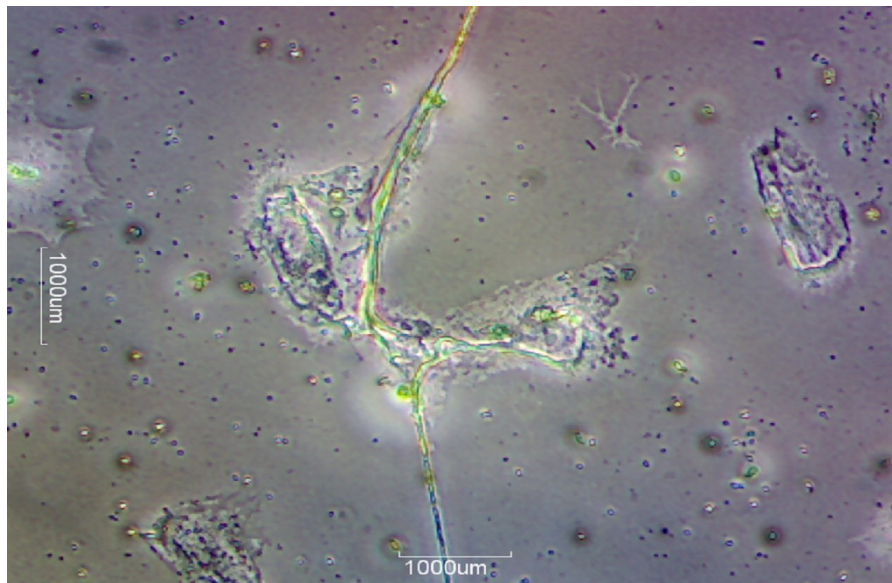


Figure 4.8: Chondrogenic staining– scale bar 1000 μm

4.4.2.2 Osteogenic differentiation

Calcium deposits were stained red by Alizarin Red Solution. It is important to note that the reason calcium stains were used is that they are a precursor to osteoblasts and these stain bright red, making it easy to observe a calcium stain.

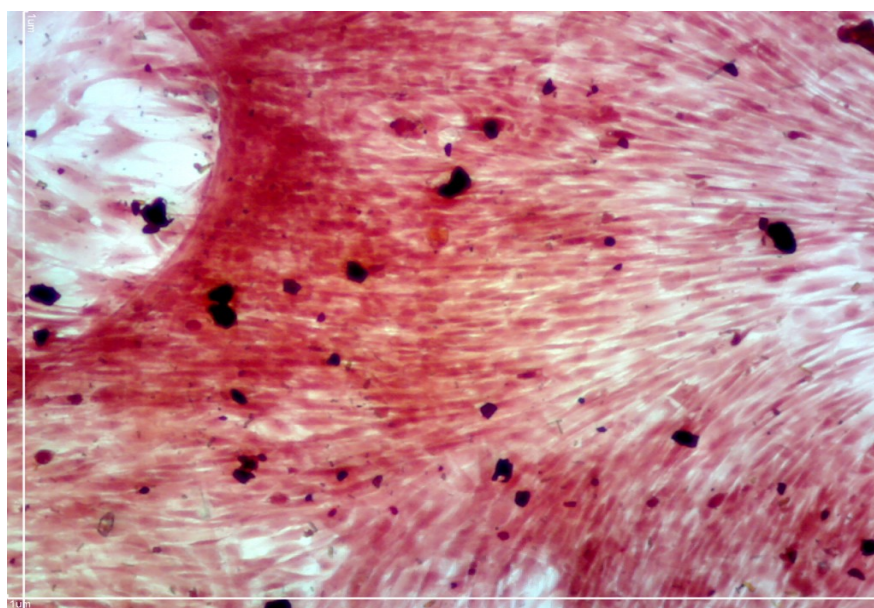


Figure 4.9: Alizarin staining. 1000x magnification.

4.4.2.3 Immunofluorescence staining of Mesenchymal markers

DAPI staining was performed to observe the nuclei as in Figure 4.10. It works by binding to the A-T regions of the DNA. The biggest benefit is that it can pass through an intact cell membrane and thus, is used to stain both live and fixed cells. α -SMA, also known as alpha smooth muscle actin, is generally used as a marker for myofibroblast formation.

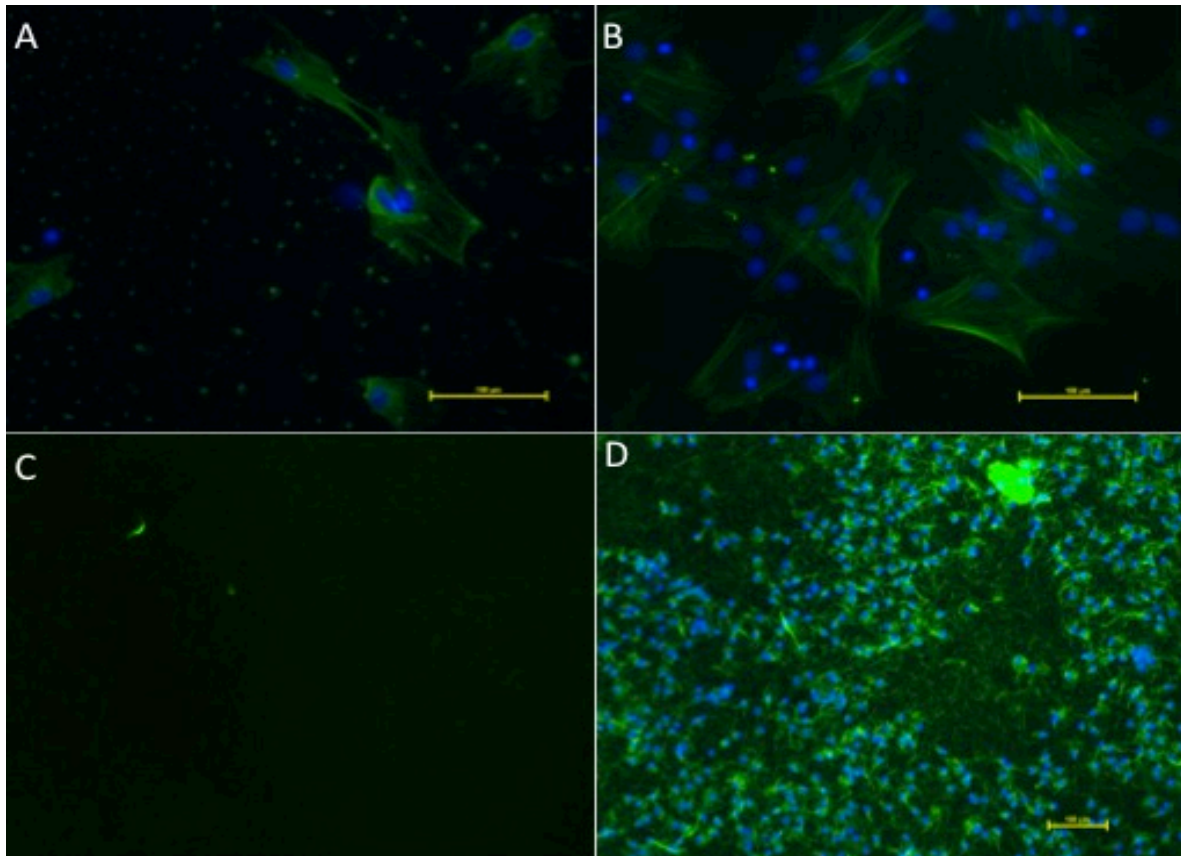


Figure 4.10: Immunofluorescence staining for α -SMA and vimentin. Cultured MSCs express both α -SMA (A) and vimentin (B), and negative control (no cells) that were stained with both antibodies as shown in (C). Cultured MSCs stained with both antibodies express on (D). Nuclei were stained with DAPI. Scale bar 100 μ m.

4.4.3 Cluster Differentiation (CD) markers

Figures 4.11 – 4.13 show images of cells corresponding to the CD markers. 2 negative and 1 positive set of CD markers were coupled with the previous test show that the cells used in this study were BMSCs.

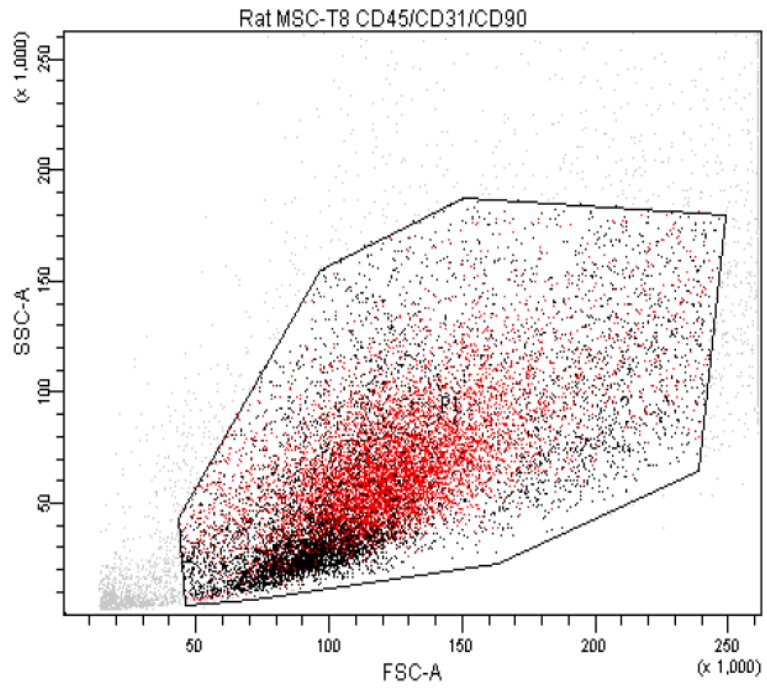


Figure 4.11: This shows the total distribution of the cells. As can be seen, gates are formed in order to confine the marker testing to a certain area.

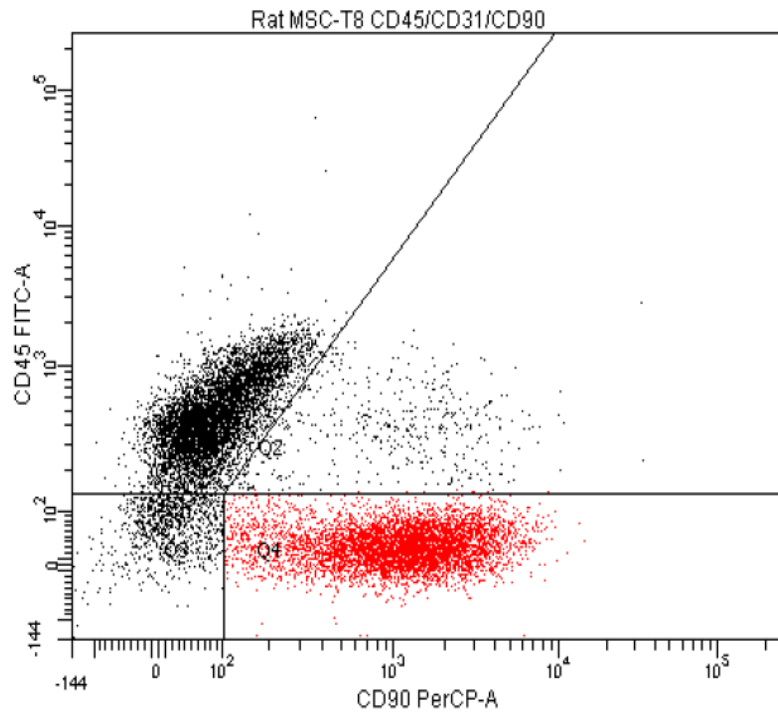


Figure 4.12: In the above image, two distinct populations can be observed. These populations exhibit CD90-, CD31- and CD45+ markers.

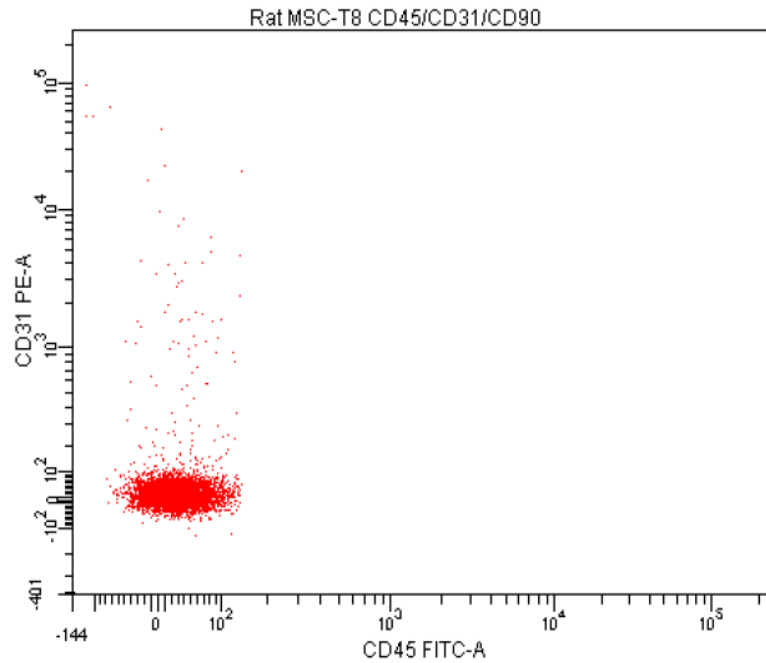
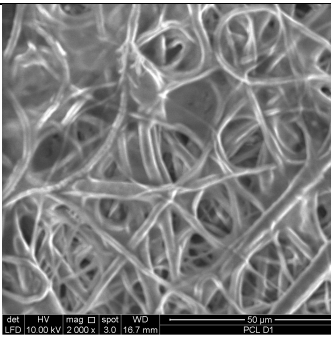
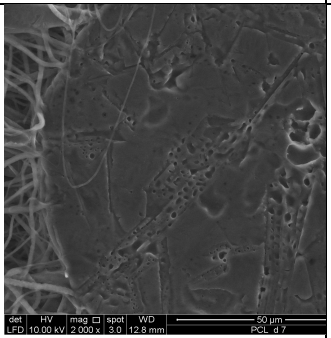
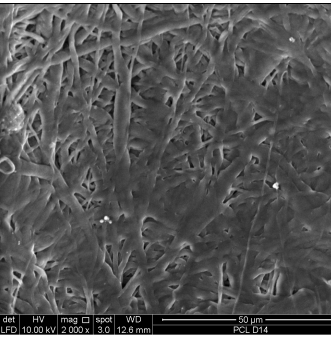
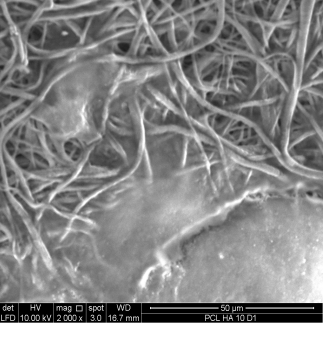
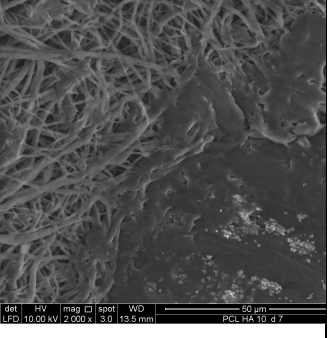
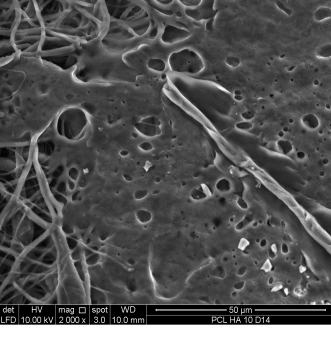
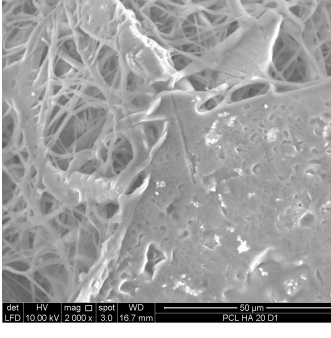
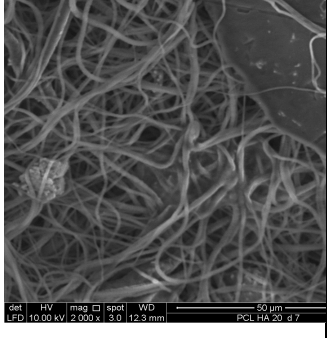
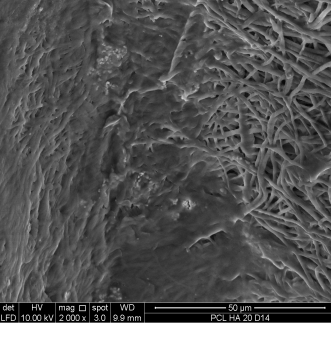
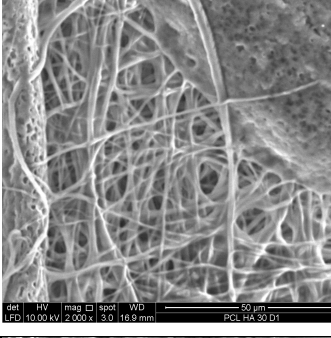
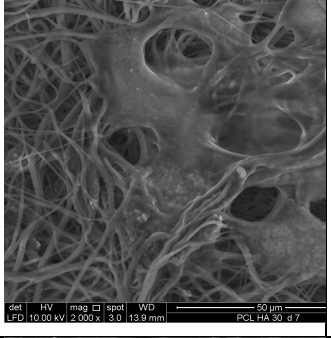
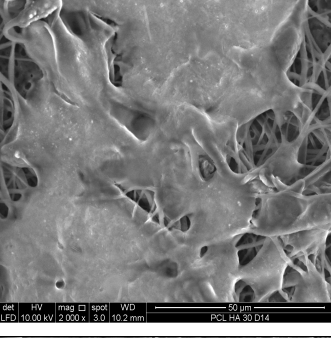
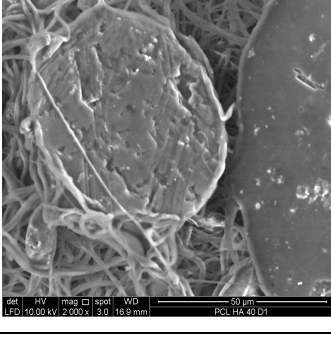
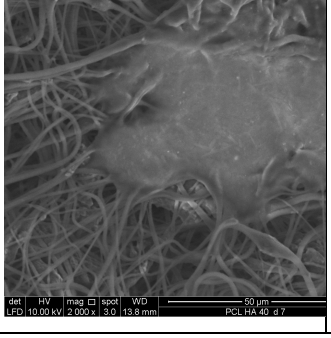
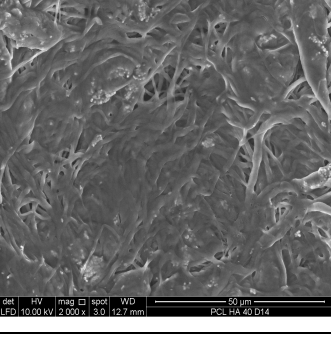
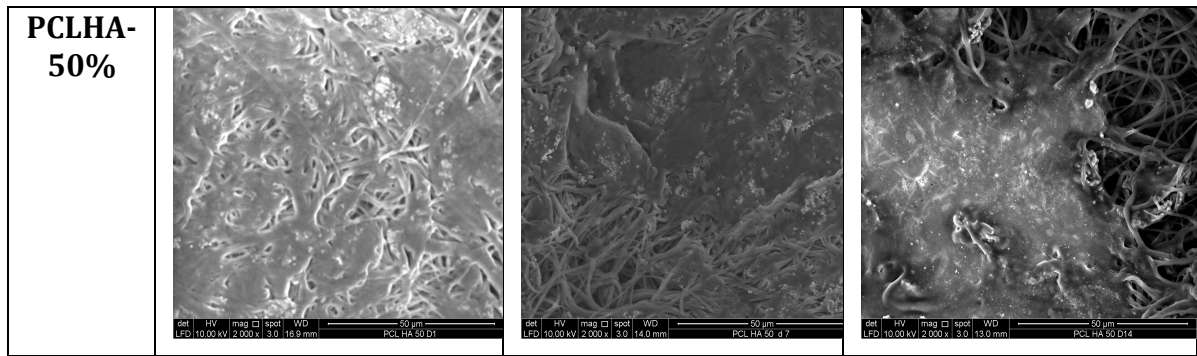


Figure 4.13: As shown above it can be observed that the BMSCs exhibit positivity and negativity for CD90+, CD31- and CD45- markers.

Flow cytometry analysis has shown that the majority of the isolated cell populations are CD31-/CD45-/CD90.Thy1+ (41.1%) and CD31-/CD45+/ CD90.Thy1- (48.3%). A total of 41.1% of the population were phenotypically characteristic of mesenchymal stem cells (MSC) and were negative for endothelial marker CD31 and hematopoietic marker CD45 but positive for CD90.Thy1, which is a general marker for three types of cells: endothelial cells, hematopoietic stem cells and MSCs (32). Because CD31 was negative, it is safe to conclude that the expression of CD90.Thy1 represented MSCs alone. A total of 48.3% of the population were fibrocytes (33,34), which are mesenchymal precursor cells that can differentiate into myofibroblasts and fibroblasts. The presence of fibrocytes agreed with the hypothesis that plated cells may differentiate into the fibroblastic lineage by default. Because the flow cytometry samples were tested after the first passage in T-75 culture flasks, it is possible that some of the MSCs had differentiated into fibrocytes.

Table 4.3: FESEM Images over days 1, 7 and 14. All FESEM images were taken at 2000x magnification and scale bar 50 μ m.

| Scaffold | Day 1 | Day 7 | Day 14 |
|------------------|--|--|---|
| PCL |  det HV mag spot WD LFD 10.00 kV 2.000 x 3.0 16.7 mm 50 μ m PCL D1 |  det HV mag spot WD LFD 10.00 kV 2.000 x 3.0 12.8 mm 50 μ m PCL d 7 |  det HV mag spot WD LFD 10.00 kV 2.000 x 3.0 12.8 mm 50 μ m PCL D14 |
| PCLHA-10% |  det HV mag spot WD LFD 10.00 kV 2.000 x 3.0 16.7 mm 50 μ m PCL HA 10 D1 |  det HV mag spot WD LFD 10.00 kV 2.000 x 3.0 13.5 mm 50 μ m PCL HA 10 d 7 |  det HV mag spot WD LFD 10.00 kV 2.000 x 3.0 10.0 mm 50 μ m PCL HA 10 D14 |
| PCLHA-20% |  det HV mag spot WD LFD 10.00 kV 2.000 x 3.0 16.7 mm 50 μ m PCL HA 20 D1 |  det HV mag spot WD LFD 10.00 kV 2.000 x 3.0 12.3 mm 50 μ m PCL HA 20 d 7 |  det HV mag spot WD LFD 10.00 kV 2.000 x 3.0 9.9 mm 50 μ m PCL HA 20 D14 |
| PCLHA-30% |  det HV mag spot WD LFD 10.00 kV 2.000 x 3.0 16.9 mm 50 μ m PCL HA 30 D1 |  det HV mag spot WD LFD 10.00 kV 2.000 x 3.0 13.9 mm 50 μ m PCL HA 30 d 7 |  det HV mag spot WD LFD 10.00 kV 2.000 x 3.0 10.2 mm 50 μ m PCL HA 30 D14 |
| PCLHA-40% |  det HV mag spot WD LFD 10.00 kV 2.000 x 3.0 16.9 mm 50 μ m PCL HA 40 D1 |  det HV mag spot WD LFD 10.00 kV 2.000 x 3.0 13.8 mm 50 μ m PCL HA 40 d 7 |  det HV mag spot WD LFD 10.00 kV 2.000 x 3.0 12.7 mm 50 μ m PCL HA 40 D14 |



4.5 Cell and Scaffold Interactions

The FESEM images were taken on Days 1, 7, and 14 (Table 4.2) at a magnification of 1000x for a qualitative analysis. This was done so as to observe the cell attachment on the different scaffolds. As can be observed from the table above, the cells were forming layers of hardened material by day 14. On day 7 it is possible to note the cells attaching themselves to the fibres and beginning to fill in the “pores” made in between the fibres. On Day 1, it can be observed that the cells have been seeded the day before just beginning to settle in the scaffold.

4.6 Biochemical Assays

4.6.1 Cell proliferation

As seen in Figure 4.14, the Resazurin reading on Day 1 is very similar, showing that the seeding density was similar on all the scaffolds. There are no significant differences between the different scaffolds on Day 1. Day 7 showed that PCLHA30% was significantly lower ($p < 0.05$) than when compared to Thermanox on Day 7. Day 14 exhibited a sharp increase in PCLHA30%, which was outstripped by PCLHA40%, which exhibited the highest peak. In order of the highest to the lowest metabolic activity on Day 14, the groups are; PCLHA40%, Thermanox, PCLHA50%, PCLHA30%, PCL, PCLHA10% and lastly was PCLHA20%.

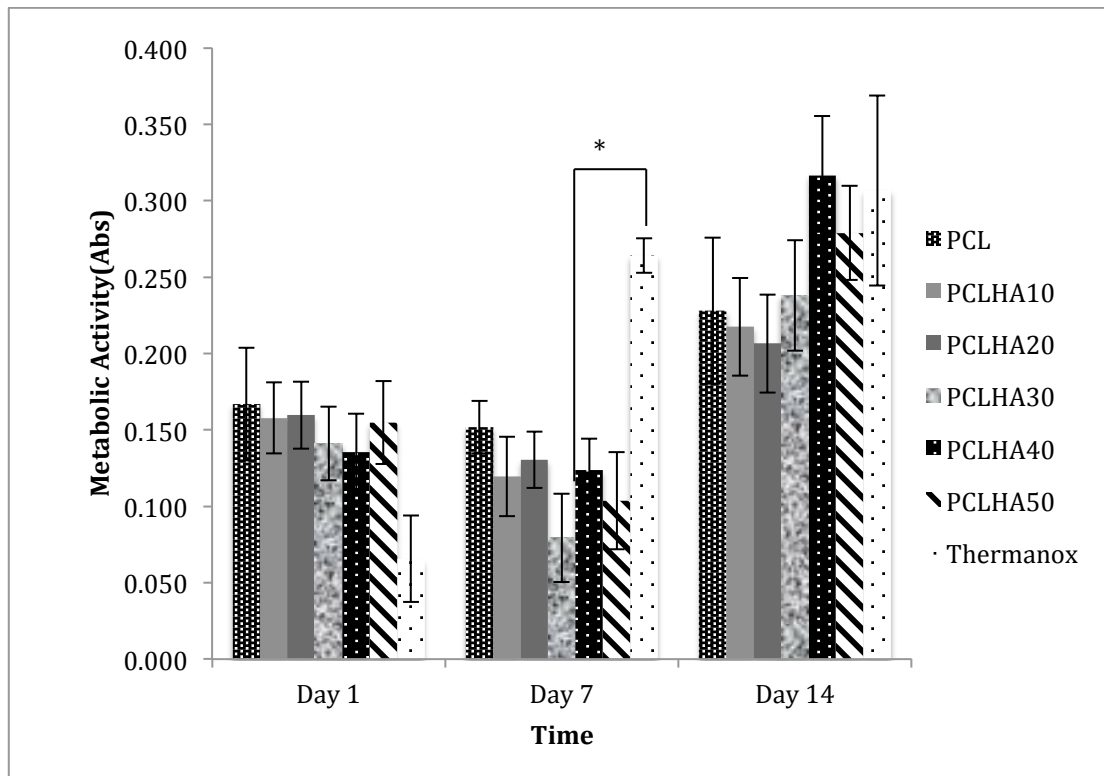


Figure 4.14: Cell metabolic activity over 2 weeks of cells seeded on all scaffolds.

Within the days it was found that on Day 1, all scaffolds except PCL and Thermanox, were significantly lower ($p < 0.05$) when compared against PCLHA40% Day 14. When Day 7 samples were compared to Day 14 samples, it was found that PCL Day 7 was significantly lower than PCLHA40% Day 14. PCLHA10% Day 7 was significantly lower than PCLHA40%, PCLHA50%, Thermanox samples on Day 14. PCLHA20% was significantly lower than PCLHA40% AND Thermanox day 14. PCLHA30% was significantly lower than PCLHA30%, PCLHA40%, PCLHA50% and Thermanox Day 14. PCLHA40% was significantly lower than PCLHA40% and Thermanox Day 14. PCLHA50% was significantly lower than PCLHA40%, PCLHA50% and Thermanox Day 14. On day 14, there was no significant difference between Day 14 samples of PCL, PCLHA10% and PCLHA20% when compared to the rest of the days. PCLHA30% was significantly higher than Thermanox Day 1 and PCLHA30% Day 7. PCLHA40% was significantly higher than

all tested groups on Day 1 and 7. PCLHA50% was significantly higher than Thermanox Day 1, PCLHA10% Day 7, PCLHA30% Day 7 and PCLHA50% Day 7. Thermanox Day 14 was significantly higher than when compared to Day 1, PCLHA 40% and Thermanox, and for all Day 7 scaffolds with the exception of PCL (n=16).

4.6.2 Alkaline Phosphatase (ALP) Assay

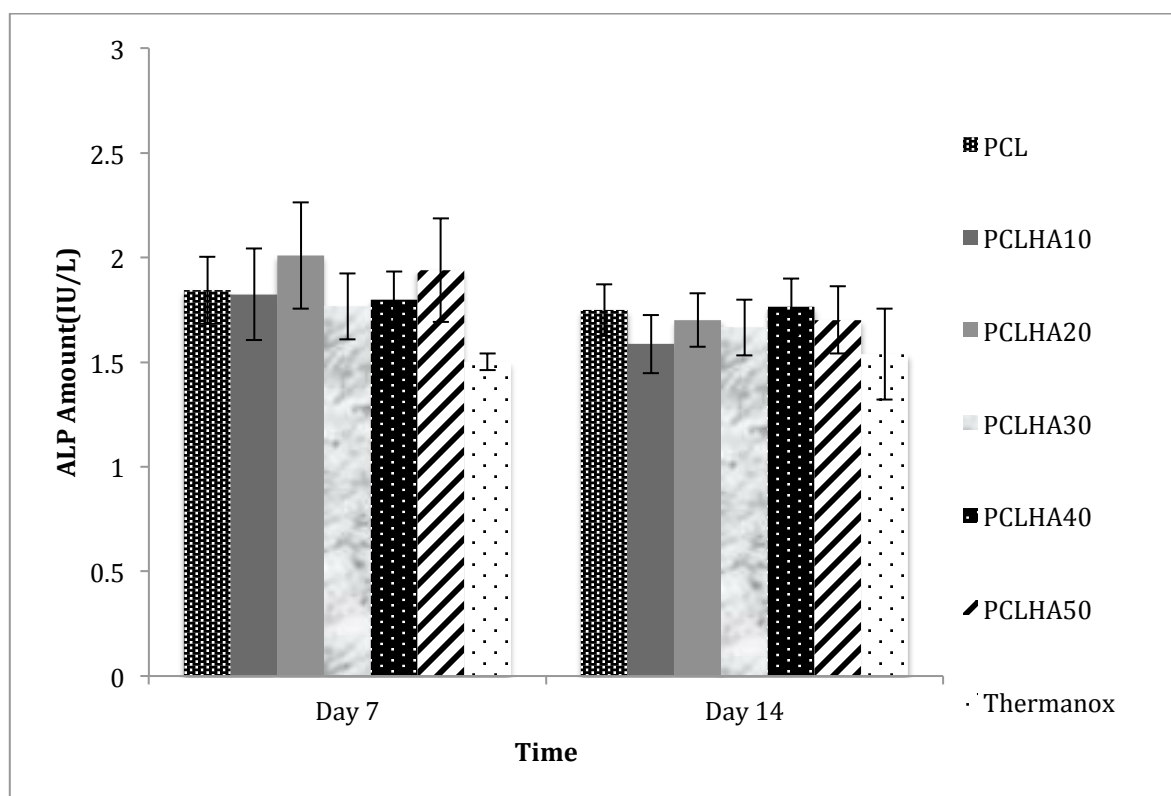


Figure 4.15: Alkaline Phosphatase measurement over 2 weeks.

The figure shows the ALP readings that were recorded across all tested groups, however the reading peaked on Day 7 for PCL-HA(50%). This is probably due to the high HA concentration, which increases the osteoblastic differentiation potential of the material. Interestingly, on day 14 the highest peak recorded was from the PCL-HA (40%) group, which perhaps is an illustration of the cells beginning to adapt more to this concentration. There was no significant difference recorded between all the groups either between days, or within days (n=16).

4.6.3 Deoxyribonucleic Acid (DNA) Assay

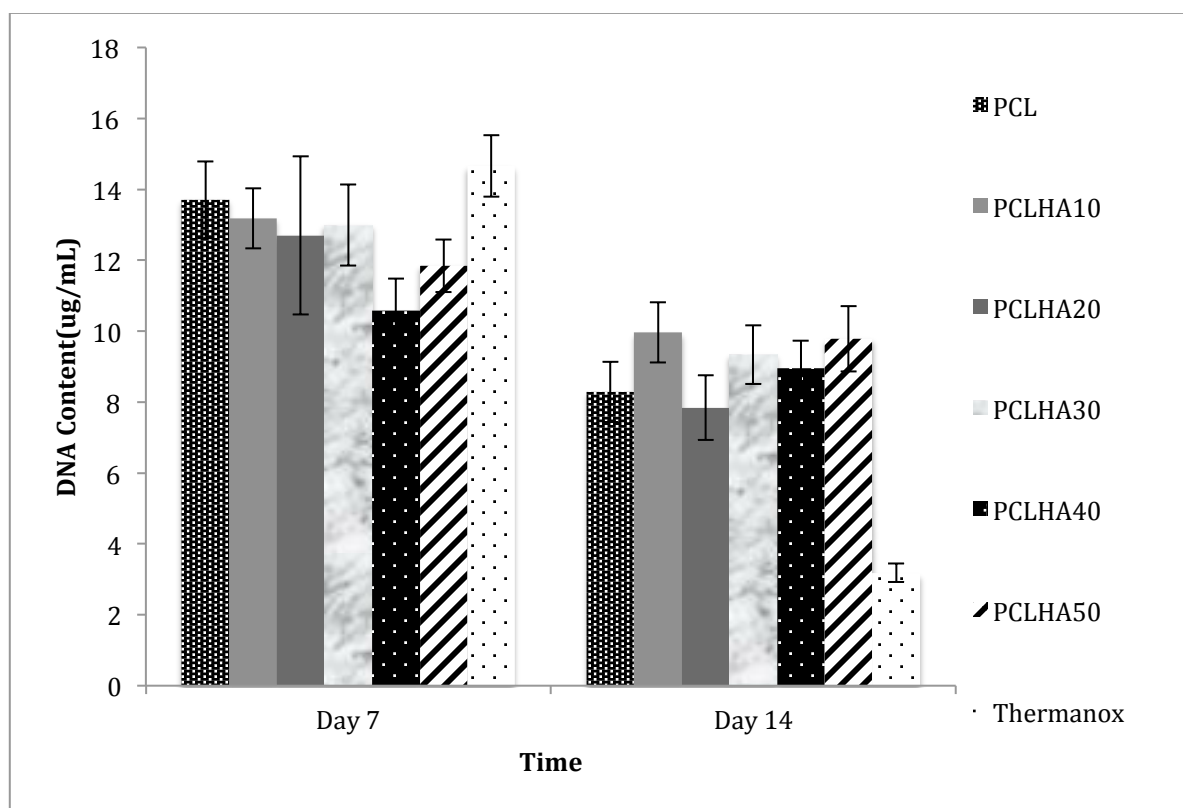


Figure 4.16: DNA Assay of seeded scaffolds over 2 weeks [n=16] (All error bars shown are Standard Error of Mean)

As can be observed from the graph above, on Day 7, the highest DNA amount recorded was for PCL, this was in line with the Resazurin result for Day 7. On Day 7, the PCL scaffold was found to be significantly higher than PCL, PCLHA20% and Thermanox on Day 14. PCLHA10% on Day 7 was significantly higher than PCLHA20% and Thermanox samples on day 14. PCLHA20% Day 7 was significantly higher than Thermanox Day 14. PCLHA30% was not significantly different from any other scaffolds on both the days. PCLHA40% Day 7 was significantly higher than Thermanox Day 14, whereas Thermanox Day 7 found to be insignificant against any group on Day 7. However, Thermanox Day 14 was significantly lower than all Day 7 scaffolds as well as PCLHA10% and PCLHA30% on Day 14. PCLHA20% on Day 14 was significantly lower than PCL, PCLHA10%, PCLHA30% and Thermanox on Day 7. PCLHA30% on Day 14 was

significantly higher than Thermanox Day 14. PCLHA50% on Day 14 was also found to be significantly higher than Thermanox Day 14. These results contrasted with the results of Resazurin for both Days 7 and 14. On day 14, the DNA assay showed that all the scaffolds yielded a lower DNA amount however, on Day 14 for Resazurin, all the scaffolds exhibited an increased metabolic activity rate.

CHAPTER 5: DISCUSSION AND CONCLUSION

CHAPTER 5: DISCUSSION AND CONCLUSION

5.1 Introduction

This chapter focuses on the analysis of the results as well as presenting the conclusion derived from the analysis, with reference to the objectives highlighted in Section 1.6. Parallels will be drawn with existing research and future work potential will be highlighted. In the conclusion section there is discussion with an emphasis on objectives and how those objectives were achieved.

5.2 Bovine Hydroxyapatite Characterisation

Hydroxyapatite has been used extensively in and for cell culture. In contrast, combining biologically-produced micron-sized hydroxyapatite with a polymer has not been carried out previously. The XRD (Figure 4.1) confirmed the hypothesis that irrespective which part of the bovine bone was used, when it was prepared in the manner described previously (Herliansyah et al., 2006; Ooi et al., 2007; Herliansyah et al., 2009), pure hydroxyapatite is obtained from the bovine bone. The unsintered powder's XRD profile exhibits the presence of many impurities which are non-existent in the sintered version, thus resulting in a purer HA product matching the JCPDS (Joint Committee on Powder Diffraction Standards) database for HA, which is discussed later. This result suggests that the bovine model is a stable system. The well-resolved XRD peaks of the sintered BHA powder (Figure 4.1) were within the 2θ range between 20° and 50° . When the XRD peaks of all the sintered BHA were indexed on the basis of hexagonal crystal system of space group $P6_3/m$ with respect to the JCPDS database, the Bragg peaks of sintered BHA powder at $\sim 22, 23, 26, 28, 29, 30-35, 39, 40, 42, 46, 48$ and $49^\circ (2\theta)$ were similar to the characteristic peaks of HA, which means

hydroxyapatite is obtainable from a bovine source which is both natural and easily replenishable. The FTIR (Figure 4.2) of the hydroxyapatite samples, both pre and post sintering, also showed loss of the organic bonds post sintering, thus confirming the XRD for the HA, which confirmed earlier work (Legeros, 2008). There, the band of OH⁻ at 3290 cm⁻¹ was shown to disappear in sintered bovine bones, when compared to unsintered samples. This result suggests a dehydroxylation of sintered samples. Sintering has also caused decomposition of organic matter, with the FTIR spectra showing missing absorption peaks relating to carbonate at 870 to 880 cm⁻¹ and 1300 to 1700 cm⁻¹ in sintered BHA compared to unsintered samples. Overall, the FTIR spectra of BHA is reproducible regardless of which part of the bovine bone is used.

5.3 Scaffold Characterisation

The FTIR (Figure 4.3) that was carried out for the materials post electro spinning showed a clear distinction between the additional bonds created by the addition of the HA. The analysis carried out of the materials post electrospinning showed that the intensities of PO₄⁻³ bands ν_3 (1020 to 1040 cm⁻¹) and ν_4 (560 to 565 cm⁻¹) and -OH (620 to 630 cm⁻¹) peaks increased as the weight % of HA is increased.

5.4 Effect of Increasing Hydroxyapatite Concentration on the Scaffold Material

5.4.1 3D Roughness profile of scaffold

It has been previously reported that surface roughness benefits protein absorption in culture medium, especially with regards to biofilms (Bos et al., 1999). While observing the roughness profile (Fig. 4.4 and Fig 4.5), it was difficult to establish an actual trend in the addition of hydroxyapatite; this was probably due to the size of HA being used. The size of

the hydroxyapatite as compared to previous studies was larger by approximately one thousand times. This was because this study used micron sized HA (25-40 μm) as opposed to nano-sized HA (50~200 nm) (Venugopal et al., 2007). One of the possible limitations that was observed in using this particle size was that, possibly, the HA was not distributed completely homogenously during the electrospinning process. Hence, in the roughness profile, which focused on a small select area of the scaffold, it was observed that it was difficult to establish a relationship between the concentration of the HA and the roughness of the sample. To overcome this limitation, the sample size was increased for the cellular assays to 16 samples per group per test point.

5.4.2 Hydrophilicity properties

The increase of the HA content in the scaffold, reduced the contact angle of the scaffold (Figure 4.6), which in turn was better for cell-material interaction, as it decreased the hydrophobicity of the scaffold. The hydrophobicity has been known to be instrumental in affecting the cell growth and attachment to materials (Webb et al., 1998) and hence a reduction in the contact angle caused by the increase in HA concentration increased the cell attachment potential of the scaffolds.

Both of these results were used to meet the first objective discussed in Chapter 1, section 1.6. This was an observation of the effect of increasing hydroxyapatite concentration on the material morphology and characteristics.

5.5 Stem Cells Characterisation

According to Dominici et al. 2006, the criteria for cells to be classified as stem cells include adherence to plastic (Figure 4.7). The adherence was noticed under the phase contrast microscope, additionally since the cells were adherent and growing and were not washed off with the changing of the medium, adherence to plastic was concluded. Secondly, another characteristic is that they must be able to differentiate into different lineages. This was also proven (Figure 4.8 and 4.9) to be possible for the cells that were isolated and cultured in this experiment. Essentially, the staining of cells post differentiation proved that they can differentiate into different lineages. Thirdly, they should test positive for the presence of mesenchymal markers, including α sma and vimentin. This was also shown to be positive by staining green (Figure 4.10). Lastly, they should test positive and negative for certain markers. The cells used were shown to be positive for CD 90 (a fibroblastic marker) and negative for CD 31 and 45, which are markers for endothelial and haematopoietic cells (Figure 4.11, 4.12 and 4.13). In conclusion, upon looking at all the obtained results and the procedures followed, it was confirmed that the cells used in this study were mesenchymal stem cells derived from the bone marrow of rats.

5.6 FESEM Images

The FESEM images for the non-seeded or empty scaffolds showed that the hydroxyapatite was embedded on and around the PCL fibres (Table 4.2). This then enhanced possible differentiation. As was noticed in the FESEM image obtained for PCLHA40%, there was some calcification that was present after 14 days (Table 4.3).

5.7 Biochemical Assays

5.7.1 Cell Proliferation Assay

The Resazurin profile (Figure 4.15), measures the metabolism of cells by a measurement of the reduction in the resazurin dye (Fidalgo et al., 2010). It showed that the highest increase in cell metabolic activity was in the PCLHA40% group followed by the PCLHA50%, then PCLHA30%. Resazurin showed that over the 14 day period, from day 1 up to 14 days, the PCLHA40% group showed a twofold increase which was quite extraordinary and was possibly due to the lower contact angle of the scaffold. The PCL only scaffold which has been investigated and reported extensively showed a limited increase, which was statistically lower than the PCLHA40% group. This result tackled the second objective (Section 1.6), which was observation of the effect of an increase of HA concentration on cell growth and proliferation.

5.7.2 Alkaline Phosphatase (ALP) Assay

Whilst the PCLHA40% is not the highest tested concentration of HA, it was the second highest one and showed no significant difference in the ALP reading (Figure 4.17). This was probably because the ALP reading was taken on Days 7 and 14, so as to maintain similar testing time to the Resazurin testing time, however, it is believed that if the ALP had been tested until day 28, a significant increase in the activity of the Alkaline phosphatase enzyme would have been expected, which would have been directly proportional to the amount of HA present in the scaffold. This hypothesis can be made based on previous literature which showed that overtime on hydroxyapatite scaffolds caused ALP levels to increase (Qi et al., 2013). This result tackled the third objective (Section 1.6), observation of the effect of an increased HA concentration on cell differentiation.

5.7.3 Deoxyribonucleic Acid (DNA) Assay

The DNA results proved to be difficult to analyse, as they exhibited contrasting results to the Resazurin results measured over Days 7 and 14. They showed a decline in the amount of DNA produced, which contrasted an increase in metabolic activity displayed in the Resazurin results. After careful analysis of the FESEM results together with the remaining results, it was observed that the cells are growing and proliferating, hence the conclusion is that there are two possible reasons for a decrease in the amount of DNA: Firstly, it may be due to the extraction of the DNA which was a method prescribed by Zhou et al. (2009), resulted in a loss of DNA material in the last 2 weeks of their 6 week experiment. Essentially the DNA measurement was dropping 1 μg a week for the last 2 weeks, when compared to this experiment which had a loss of 3 μg a week. Although this losses were greater in proportion to Zhou et al. (2009) the trend was similar. Secondly, looking at literature it has been reported in a study (Karlsson et al., 2003) which observed the seeding of osteoblasts on non-porous alumina that the Alamar blue showed a decline in the amount of cells on Day 14, than when compared to Day 7, however in contrast the DNA content went up on Day 14. Hence, there is a precedence of contrasting results between DNA and Alamar blue assays which has also occurred in this experimental set-up.

5.8 Conclusion and Future Work

An electrospinning device was used to produce fibres within a micro range. Using this system, composites of PCL-BHA scaffolds were produced. This was the first time a biomaterial was made from micron sized naturally derived bovine hydroxyapatite electrospun with Polycaprolactone. It was possible, in addition to producing the biomaterial, to also study the effect of increasing the bovine hydroxyapatite in relation to a reduction in the polycaprolactone concentration. From this, it was possible to conclude that not only does this scaffold support the growth, proliferation and attachment of BMSCs and is hence, biocompatible and noncytotoxic to cells; but also to determine the ideal concentration for further additional tests (discussed in the following paragraphs).

Alkaline phosphate is one of the common bone cell-specific markers used to assess the presence of bone cells, and from our preliminary study, it was shown these scaffolds are osteoinductive based on the presence of alkaline phosphate activity and in a manner which is not yet shown to vary based on the relative proportions.

These results exhibited enormous potential in the differentiation and proliferation potential of PCLHA40%. It is recommended that in the future experiments are repeated, involving cell differentiation analysis, gene expression studies, and investigation of factors like RUNX2, Osteocalcin and ATF-4. The biggest challenge facing any researcher who may wish to carry these in-vitro tests, is the correct and effective methodology for extracting these factors and other proteins for measurement from the scaffold.

In addition to these in-vitro tests, a future researcher should also carry out in-vivo testing to observe the bone healing effect of this biomaterial and to see if it can be used as a possible wound dressing in the future.

REFEENCES

- Adel A. and Mao J.J. (2004). Mesenchymal stem cells: Isolation and therapeutics. *Stem Cells and Development*. 13:436-448.
- Agrawal C.M., Ray R.B. (2001) Biodegradable polymeric scaffolds for musculoskeletal tissue engineering, *Journal of Biomedical Materials Research Part A*, 55 (2) : 141-150.
- Atala A., Mooney D., Vacanti J.P., Langer R. Synthetic biodegradable polymer scaffolds. Boston: Birkhauser. pg. 1.
- Balamurugan A., Kannan S., Rajeswari S. (2002) *Trends Biomater Artif.Organs*16(1)18.
- Barnes S.J. and Harris L. P., *Tissue Engineering: Roles, Materials and Applications*, Nova Publishers, May 1, 2008. ISBN 978-1-60456-293-4
- Bianco P., Riminucci M., Gronthos S., Robey P.G. Bone marrow stromal stem cells: nature, biology, and potential applications. *Stem Cells* 2001, **19**:180-192
- Blanc K.L. & Ringde O. (2007); Immunomodulation by mesenchymal stem cells and clinical experience; *Journal of Internal Medicine* ; 262; 509-525; doi: 10.1111/j.1365-2796.2007.01844.x
- Bos R., Henny C., Van der Mei, Busscher H. J. Physico-chemistry of initial microbial adhesive interactions—its mechanism and methods for study. *FEMS Microbiol* 1999; 23:179–230
- Bowers, G.N.Jr., McComb R.B., (1966) *Clinical Chemistry* 12:70
- Caplan A.I. : Adult mesenchymal stem cells for tissue engineering versus regenerative medicine. *J Cell Physiol* 2007, 213:341-347
- Caplan A.I. (1991). Mesenchymal stem cells. *Journal of Orthopaedic Research*. 9:641- 650.
- Chaignaud B.E, Langer R., Vacanti J.P. (1997). The history of tissue engineering using synthetic biodegradable polymer scaffolds and cells.

- Chen D. R., Bei J. Z. and Wang S. G.,(2000) *Polym. Degrad. Stab.*, 67, 455–459
- Chen L.B., Jiang X.B., Yang L. (2004). Differentiation of rat marrow mesenchymal stemcells into pancreatic islet beta-cells. *World Journal of Gastroenterology*. 10(20):3016-3020.
- Chong E.J., Phan T.T., Lim I.J. Zhang Y.Z., Bay B.H., Ramakrishna S., Lim C.T., Evaluation of electrospun PCL/gelatin nanofibrous scaffold for wound healing and layered dermal reconstitution. *Acta Biomaterialia* (2007), Volume 3, Issue 3, Pages 321–330
- Croft A.P. and Przyborski S.A. (2004). Generation of neuroprogenitor-like cells from adult mammalian bone marrow stromal cells in vitro. *Stem Cells And Development*. 13: 409-420.
- Cullity B. D.(1967), *Elements of X-Ray Diffraction*, Addison-Wesley, Reading, MA
- Davies J.E., Karp J.M., and Baksh D. (2002). Mesenchymal cell culture: Bone. Atala A., and Lanza R.P. *Methods of tissue engineering*. US: Academic press. pg. 333-344.
- Deligianni, D. D. Katsala N. D., Koutsoukos P.G. and Missirlis Y.F.. Effect of surface roughness of hydroxyapatite on human bone marrow cell adhesion, proliferation, differentiation and detachment strength. *Biomaterials*(2000), Volume 22,Issue 1,87-96.
- Dominici M., Le Blanc K, Mueller I, Slaper Cortenbach I, Marini F, Krause D, Deans R, Keating A, Prockop D, Horwitz E. Minimal Criteria for Defining Multipotent Mesenchymal Stromal Cells. the International Society for Cellular Therapy Position Statement. *Cytotherapy*. 2006;8:315–317
- Dutrow B. and Clark C.M.(2013), X-Ray Powder Diffraction-
http://serc.carleton.edu/research_education/geochemsheets/techniques/XRD.html
- Doshi, J., and Reneker, D.H. Electrospinning process and applications of electrospun fibres. *Electrostat*. 35, 151, 1995
- Ekaputra A. K., Zhou Y., Cool S. M., and Hutmacher D.W. Composite Electrospun Scaffolds for Engineering Tubular Bone Grafts. *Tissue Engineering. Part A* Volume 15, Number 12, 2009.

- Fidalgo T.K.S. , Barcelos R., Portela M. B. R, Soares R. M. A. S. , Gleiser R. and Filho F.C.S. (2010). Inhibitory activity of root canal irrigants against *Candida albicans*, *Enterococcus faecalis* and *Staphylococcus aureus*, *Braz Oral Res.* 24(4):406-12
- Friedenstein A. J. , Chailakhjan R. K. , and Lalykina K. S. (1970). The development of fibroblast colonies in monolayer cultures of guinea-pig bone marrow and spleen cells. *Cell and Tissue Kinetics.* 3:393-403.
- Friedenstein A. J, Piatetzky-Shapiro II, and Petrakova K. V. (1966). Osteogenesis in transplants of bone marrow cells. *Journal of Embryology and Experimental Morphology.* 16:381-390.
- Friedenstein A. J, Chailakhyan R. K, Gerasimov U. V. Bone marrow osteogenic stem cells: *in vitro* cultivation and transplantation in diffusion chambers. *Cell Tissue Kinetics* 1987, 20:263-272.
- Fujita, H. J. (1969) *Biochem.,(Japan)* 30:69
- Ghasemi-Mobarakeh L., Prabhakaran M.P., Morshed M., Nasr-Esfahani M.-H., Ramakrishna S.. Electrospun poly(ϵ -caprolactone)/gelatin nanofibrous scaffolds for nerve tissue engineering. *Biomaterials*, Volume 29, Issue 34, December 2008, Pages 4532–4539
- Gilbert, W. (1628) *De Magnete, Magneticisque Corporibus, et de Magno Magnete Tellure* (On the Magnet and Magnetic Bodies, and on That Great Magnet the Earth), London, Peter Short.
- Goupil D. (1996). Sutures. In: Ratner BD, Hoffman AS, Schoen FJ, Lemons JE. *Biomaterials science*. New York: Academic Press. Pg. 356-360
- Guptaa D., Venugopal J., Mitrac S., Giri Devd V.R., Ramakrishna S.. Nanostructured biocomposite substrates by electrospinning and electrospaying for the mineralization of osteoblasts. *Biomaterials* 30 (2009) 2085–2094
- Haynesworth S. E, Baber M, and Caplan A. I. (1992). Cell surface antigens on human marrow-derived mesenchymal cells are detected by monoclonal antibodies. *Bone.* 13:69-80
- Herliansyah M.K., Hamdi M., Ide-Ektessabi, A. Wildan M.W., Toque J.A. (2009) The influence of sintering temperature on the properties of compacted bovine hydroxyapatite. *Material Science and Engineering C* 29 1674-1680

- Herliansyah M.K., Toque J.A., Hamdi M., Ide-Ektessabi A., Wildan M.W. (2006). Fabrication of Bovine Bone Hydroxyapatite: effect of the material shapes and calcination temperature, *ISTECS Journal*, Vol. VIII 25-33
- Herliansyah M.K, Pujianto E., Hamdi M., Ide-Ektessabi A., Wildan M.W., Tontowi A.E. (2006) Preparation and characterisation of natural hydroxyapatite: study of X-ray diffraction result from bovine bone hydroxyapatite and natural gypsum hydroxyapatite, *Proceeding of International Conference on Product Design and Manufacture 2006*, Department of Mechanical Engineering, Faculty of Engineering, Gadjah Mada University, Yogyakarta, Indonesia
- Herliansyah M.K., Nasution D.A. Hamdi M., Ide-Ektessabi A., Wildan M.W., Tontowi A.E.(2007) *Materials Science Forum* 561–565 1441.
- Holmberg C., Matsumoto G., Kim S.. *Immunofluorescence Protocol* (2003)
- Ishuag-Riley S.L., Crane-Kruger G.M., Yaszemski M.J., Mikos A.G..Three-dimensional culture of rat calvarial osteoblasts in porous biodegradable polymers. *Biomaterials*:19 (1998) 1405-1412
- J. Peña, Corrales T., Izquierdo-Barba I., Doadrio A. L. and Vallet-Regí M.(2006), *Polym. Degrad. Stab.* 91, 1424–1432
- Johnson, B., & Christensen, L. (2010). *Educational Research: Quantitative, Qualitative and Mixed Approaches*. Thousand Oaks, CA: SAGE Publications Inc. Jolly C et al.(1997) *J Histochem Cytochem* 45, 1585-92
- Kallergi G., Papadaki M. A., Politaki E., Mavroudis D., Georgoulas V. and Agelaki S. (2011). Epithelial to mesenchymal transition markers expressed in circulating tumour cells of early and metastatic breast cancer patients. *Breast Cancer Research* 13 : R59
- Karlsson M. , Pålsgård E. , Wilshaw P.R, Di Silvio L. Initial in vitro interaction of osteoblasts with nano-porous alumina. *Biomaterials* (2003). Volume 24, Issue 18, Pages 3039–3046
- Kim S., Nollen E. A. A, Kitagawa K, Bindokas V. P, Morimoto R.I. Polyglutamine protein aggregates are dynamic. *Nat Cell Biol.* 2002 Oct ;4(10):826-31
- Kohn J., Langer R. Bioresorbible and bioerodible materials. (1996). In: Ratner B.D., Hoffman A.S., Schoen F.J., Lemons J.E. *Biomaterials science*. New York: Academic Press. Pg. 64-72

- Labet M. and Thielemans W. (2009), Synthesis of polycaprolactone: a review, *Chem. Soc. Rev.*,38, 3484–3504.
- Lam C. X. F., Teoh S. H. and. Hutmacher D. W (2007), *Polym. Int.*, 56, 718–728
- Langer R., Vacanti J.P. Tissue engineering. *Science* 1993; 260: 920–6
- Layrolle P., Ito A., Tateishi T.(1998) *J. Am. Ceram. Soc.* 81: 1421.
- LeGeros R. Z., Daculsi G. and. LeGeros J. P. *Bioactive Bioceramics, Orthopedic Biology and Medicine: Musculoskeletal Tissue Regeneration, Biological Materials and Methods*(2008). Edited by W. S. Pietrzak © Humana Press, Totowa, NJ Lewis O.G., Fabisial W. (1997) Sutures. In: Kirk-Othmer encyclopedia of chemical technology. 4th edition. New York: Wiley
- Li W.J., Laurencin C.T., Cateson E.J., Tuan R.S. and Ko F.K.. Electrospun nanofibrous structure : A novel scaffold for tissue engineering. *Journal of Biomedical Materials Research A* (2002). Volume 60, Issue 4, 613-621.
- Li W.J., Tuli R., Huang X., Lacquerriere P. and Tuan R.S. Multilineage differentiation of human mesenchymal stem cells in a three dimensional nanofibrous scaffold. *Biomaterials* 26 (2005) 5158-5166.
- Majubala I., Sivakumari M., Sampath Kumar T.S., Panduranga Rao K.(2000). Synthesis and characterisation of functional gradient materials using Indian corals, *Journal of Materials Science: Materials in Medecine II* 705-709.
- Maniatopoulos C., Sodek J., Melcher A.H. (1988). Bone formation in vitro by stromal cells obtained from bone marrow of young adult rats. *Cell Tissue Research.* 254:317-330
- Meijer G.J., de Bruijn J.D., Koole R., van Blitterswijk C.A. (2007) Cell-Based Bone Tissue Engineering. *PLoS Med* 4(2): e9.
- Min W. and Yu-Quan W. (2004). Concise Review: Development of respiratory stem cells and progenitor cells. *Stem Cells And Development.* 13: 607-613.
- Murugan R. , Rao K.P. (2006) *Trends Biomater. Artif. Organs* 16 (1) (2002) 43. 13

- Nitya G., Nair G.T., Mony U., Chennazhi K.P., Nair S.V. In vitro evaluation of electrospun PCL/nanoclay composite scaffold for bone tissue engineering. *Mater Sci Mater Med.* 2012 Jul;23(7):1749-61
- Ooi C.Y., Hamdi M., Ramesh S. (2007), *Ceram. Int.* 33 1171
- Orlic D., Kajstura J., Chimenti S., Jakoniuk I., Anderson S.M., Li B., Pickel J., McKay R., Nadal-Ginard B., Bodine D.M. (2001). Bone marrow cells regenerate infarcted myocardium. *Nature.* 410:701-705
- Petersen B.E., Bowen W.C., Patrene K.D., Mars W.M., Sullivan A.K., Murase N., Boggs S.S. (1999). Bone Marrow as a potential source of hepatic oval cells. *Science.* 284:1168-1170.
- Pham Q.P., Sharma U. and Mikos A.G.. Electrospinning of Polymeric Nanofibres for Tissue Engineering Applications: A Review. *Tissue Engineering.* Volume 12, Number 5, 2006
- Pittenger M.F., Mackay A.M., Beck S.C., Jaiswal R.K., Douglas R., Mosca J.D., Moorman M.A., Simonetti D.W., Craig S., Marshak D.R.: Multilineage potential of adult human mesenchymal stem cells. *Science* 1999, 284:143-147.
- Pittenger M.F., Mackay A.M., Beck S.C., Jaiswal R.K., Douglas R., Mosca J.D., Middleton JC, Tipton AJ. (2000). Synthetic biodegradable polymers as orthopedic devices. *Biomaterials.* 21:2335-2346
- Moorman M.A., Simonetti D.W., Craig S., and Marshak D.R. (1999). Multilineage potential of adult human mesenchymal stem cells. *Science.* 284:143-147
- Poulsom R., Alison M.R., Cook T., Jeffery R., Ryan E., Forbes S.J., Hunt T., Wyles S. and Wright N.A. (2003). Bone marrow stem cells contribute to healing of the kidney. *Journal of The American Society of Nephrology.* 14:48S-54S.
- Prabakaran K., Balamurugan A., Rajeswari S. (2005), *Bull. Mater. Sci.* 28 (2) :115.
- Pramanik S., Agarwaly A.K., Rai K.N. (2005) *Trends Biomater. Artif. Organs* 19 (1)
- Kivrak N., Tas A.C. (1998) *Journal of The American Ceramic Society* 81 2245.

- Qiua, H. Yanga J., Kodolib P., Kohb J., Ameer G.A. (2006). A citric acid-based hydroxyapatite composite for orthopedic implants. *Biomaterials* 27 : 5845–5854
- Qi X., Li H., Qiao B., Li W., Hao X., Wu J., Su B. and Jiang D. (2013). Development and characterisation of an injectable cement of nano-calcium deficient hydroxyapatite/multi(amino acid) copolymer/calcium sulfate hemihydrate for bone repair. *International Journal Nanomedicine* 8: 4441-4452
- Rocha J.H.G., Lemos A.F., Agathopoulos S., Valério P., Kannan S., Oktar F.N, Ferreira J.M.F(2005), *Bone* 37 850.
- Rocha J.H.G., Lemos A.F., Kannan S., Agathopoulos,J.M .F.Ferreira (2005),*J.Mater.Chem.*15: 5007.
- Rosenbaum A. J, Grande D. A, and Dines J. S. The use of mesenchymal stem cells in tissue engineering: A global assessment. *Organogenesis*. 2008 Jan-Mar; 4(1): 23–27.
- Ross M.H., Romrell L.J., Kaye G.I. (1995). *Histology: A text and atlas*. 3rd edition. USA: Williams & Wilkins. pg. 150-187.
- Ruksudjarit A. , Pengpat K., Rujijanagul G., Tunkasiri T.,(2007) *Curr. Appl. Phys.* 8 270
Sasikumar S., Vijayaraghavan R. (2006), *Biomater. Artif. Organs* 19 (2) :70.
- Saxena A.K., *Tissue engineering and regenerative medicine research perspectives for pediatric surgery*, *Pediatric Surgery International*, Springer,2010
- Scheiker M., Pautke C., Haasters F., Schieker J., Docheva D., Böcker W., Guelkan H., Neth P., Jochum M., Mutschler W., Human mesenchymal stem cells at the single-cell level: simultaneous seven-colour immunofluorescence. *Journal of Anatomy* (2007) 210(5):592-9.
- Schindler A., Jeffcoat R., Kimmel G.L., Pitt C.G., Wall M.E., Zwiedinger R. (1977) Biodegradable polymers for sustained drug delivery. *Contemporary Topics Polymer Science*. 2:251-289.
- Schnell E., Klinkhammer K., Balzer S., Brook G., Klee D., Dalton P..2007.Guidance of glial cell migration and axonal growth on electrospun nanofibres of poly-epsilon-caprolactone and a collagen/poly-epsilon-caprolactone blend, *Biomaterials*, 28 (19), pp. 3012–3025
- Seshi B., Kumar S. and Sellers D. (2000). Human bone marrow stromal cell: coexpression of markers specific for multiple mesenchymal cell lineages. *Blood Cells Molecules & Diseases*. 26:234-246.

- Shi D., Jaing G., Wen X. (2000) J. Biomed. Mater. Res. (Appl Biomater) 53 (5) : 457
- Shin M., Yoshimoto H. and Vacanti J.P. *In Vivo* Bone Tissue Engineering Using Mesenchymal Stem Cells on a Novel Electrospun Nanofibrous Scaffold. Tissue Engineering Volume 10, Number 1/2, 2004
- Shu S.N., Wei L., Wang J.H., Zhan Y.T., Chen H.S., Wang Y. (2004). Hepatic differentiation capability of rat bone marrow-derived mesenchymal stem cells and hematopoietic stem cells. World Journal of Gastroenterology. 10(19):2818-2822
- Sinha V. R., Bansal K., Kaushik R., Kumria R. and Trehan A.(2004), Int. J. Pharm., 278, 1–23
- Sill T.J., Recum H.A.V.. Electrospinning: Applications in drug delivery and tissue engineering. Biomaterials, Volume 29, Issue 13, May 2008, 1989-2006.
- Stevens M. Biomaterials for bone tissue engineering. Materials today, Volume 11, Issue 5, May 2008, 18-25.
- Stevens M.M and George J.H Stevens M.M and George J.H.. Exploring and Engineering the cell surface interface Science, 310(2005), 1135-1138.
- Suchanek W. Yoshimura M.(1998) J. Mater. Res. 13:94
- Sudo Sudo K., Kanno M., Miharada K., Ogawa S., Hiroyama T., Saijo K., Nakamura Y. Mesenchymal progenitors able to differentiate into osteogenic, chondrogenic, and/or adipogenic cells *in vitro* are present in most primary fibroblast-like cell populations. *Stem Cells* 2007, **25**:1610-1617.
- Sun H., Wu C., Dai K., Chiang J., Tang T. Proliferation and osteoblastic differentiation of human bone marrow derived stromal cells on akermite-bioactive ceramics. Biomaterials (2006). Volume 27, Issue 33, 5651-5657.
- Sun M., Ding B., Yu J., Sun Y-L. H·G. Self-assembled monolayer of 3-mercaptopropionic acid on electrospun polystyrene membranes for Cu²⁺ detection. Sensors and Actuators B: Chemical Volume 161, Issue 1, 3 January 2012, Pages 322–328
- Suon S., Hao J., Donaldson A.E., Caterson E.J., Tuan R.S., Deschenes G., Marshall C., and Iacovitti L. (2004). Transient differentiation of adult human bone marrow cells into neuro-like cells in culture: Development of morphological and biochemical traits is

mediated by different molecular mechanisms. *Stem Cells And Developmental*. 13:625-635.

Tan D.M.F., Miao, X. , Li J., Xiao Y. , Crawford R.. Characterisation of Calcium Phosphate Cement-Derived Hydroxyapatite Scaffolds with a PLGA-Bioactive Glass Composite Coating 2008, *Journal of Biomimetics, Biomaterials, and Tissue Engineering*, 1, 99-107

Tan L.L. Plugging bones the painless way. *Innovation*, 2004:4

Venugopal J. R., Low S., Choon A. T., Kumar A.B. and Ramakrishna S. (2008), Nanobioengineered Electrospun Composite Nanofibres and Osteoblasts for Bone Regeneration, *Artificial Organs* , 32(5):388–397

Warren B. E. (1969), *X-Ray Diffraction*, Addison-Wesley, Reading, MA

Webb K., Hlady V. and Tresco P.A., Relative importance of surface wettability and charged functional groups on NIH 3T3 fibroblast attachment, spreading, and cytoskeletal organization, *J Biomed Mater Res*, 41 (1998) 422–430

Wei G., Ma P.X., 2004. Structure and properties of nano-hydroxyapatite/polymer composite scaffolds for bone tissue engineering. *Biomaterials*. Volume 25, Issue 19, 4749-4757

Xin X., Hussein M. and Mao J.J. Continuing differentiation of human mesenchymal stem cells and induced chondrogenic and osteogenic lineages in electrospun PLGA nanofibrous scaffold. *Biomaterials* (2007), Volume 28, Issue 2, 316-325.

Yang X., Tare R.S., Partridge K.A., Roach H. I., Clarke N.M.P, Howdle S.M., Shakesheff K.M., Oreffo R.O.C. Induction of human Osteoprogenitor Chemotaxis, Proliferation, Differentiation and Bone formation by Osteoblast stimulating Factor-1/Pleiotropin: Osteoconductive Biomimetic Scaffolds for tissue engineering. *Journal of Bone and Mineral Research* (2003) Volume 16, Issue 1, 47-57

Yoshikawa H. and Myoui A.. Bone tissue engineering with porous hydroxyapatite ceramics. *Journal of Artificial Organs*, 131-136

Zhao G., Yin S., Liu G., Cen L., Sun J., Zhou H., Liu W., Cui L., Cao Y. (2009). In vitro engineering of fibrocartilage using CDMP1 induced dermal fibroblasts and polyglycolide, *Biomaterials* 30 3241–3250

Zhu N. and Chen X. (2013). *Biofabrication of Tissue Scaffolds*, *Advances in Biomaterials Science and Biomedical Applications*, Prof. Rosario Pignatello (Ed.), ISBN: 978-953-51-1051-4, InTech, DOI: 10.5772/54125.

Ziabicki, A. Fundamentals of fibre formation, John Wiley and Sons, London, 1976

Zong X., Bienc H., Chung C.-Y., Yinc L., Fangb D., Hsiaoa B. S., Chua B., Entcheva E.. Electrospun fine-textured scaffolds for heart tissue constructs. *Biomaterials* 26 (2005) 5330–5338

Zuk P.A., Zhu M., Mizuno H., Huang J., Futrell J.W., Katz A.J., Benhaim P., Lorenz H.P., Hedrick M.H. : Multilineage cells from human adipose tissue: implications for cell-based therapies. *Tissue Eng* 2001, **7**:211-228.

<http://www.biochem.northwestern.edu/morimoto/research/Protocols/II.%20Eukaryotes/H.%20Cell%20Imaging/1b.%20method.pdf>

<http://www.cf.ac.uk/biosi/staffinfo/kille/Methods/Cellculture/HAEMO.html>

The committee on enzymes of the Scandanavian Society of Clinical Chemistry and Clinical Physiology. *Scandanavian Journal of Clinical Lab Investigations* 32:291 (1974).

Miller-Keane Encyclopedia and Dictionary of Medicine, Nursing, and Allied Health, Seventh Edition. © 2003 by Saunders, an imprint of Elsevier, Inc